National Library
of Canada

Acquisitions and
Bibliographic Services Branch

395 Wellington Street
Ottawa, Ontario
K1A 0N4

Bibliothèque nationale
du Canada

Direction des acquisitions et
des services bibliographiques

395, rue Wellington
Ottawa (Ontario)
K1A 0N4

Your file Votre référence

Our file Notre référence

NOTICE

The quality of this microform is heavily dependent upon the quality of the original thesis submitted for microfilming. Every effort has been made to ensure the highest quality of reproduction possible.

If pages are missing, contact the university which granted the degree.

Some pages may have indistinct print especially if the original pages were typed with a poor typewriter ribbon or if the university sent us an inferior photocopy.

Reproduction in full or in part of this microform is governed by the Canadian Copyright Act, R.S.C. 1970, c. C-30, and subsequent amendments.

AVIS

La qualité de cette microforme dépend grandement de la qualité de la thèse soumise au microfilmage. Nous avons tout fait pour assurer une qualité supérieure de reproduction.

S'il manque des pages, veuillez communiquer avec l'université qui a conféré le grade.

La qualité d'impression de certaines pages peut laisser à désirer, surtout si les pages originales ont été dactylographiées à l'aide d'un ruban usé ou si l'université nous a fait parvenir une photocopie de qualité inférieure.

La reproduction, même partielle, de cette microforme est soumise à la Loi canadienne sur le droit d'auteur, SRC 1970, c. C-30, et ses amendements subséquents.

Canada

Preparation and Performance Testing of Sulfonated Poly(2,6-dimethyl-1,4-phenylene oxide) - Polyethersulfone Thin Film Composite Membranes

Ali Abdalla Hamza

A thesis submitted to the School of Graduate Studies and Research
in partial fulfillment of the requirement for the degree of
M. A. Sc. in Chemical Engineering
Department of Chemical Engineering
University of Ottawa
CANADA

January, 1995

ISBN 0-612-07819-1

UNIVERSITÉ D'OTTAWA
UNIVERSITY OF OTTAWA

Abstract

Thin film composite membranes were prepared by coating the surface of polyethersulfone ultrafiltration membranes with dilute solutions of sulfonated poly(2,6-dimethyl-1,4-phenylene oxide) polymer. Poly(2,6-dimethyl-1,4-phenylene oxide) was first sulfonated to different degrees, thus obtaining polymers of different ion exchange capacities, from which the coating solutions in methanol or methanol/chloroform mixtures were prepared. The reverse osmosis performance of the thin film composite membranes was studied using electrolyte solutes of different valences and ionic radii. The effect of the solvent used for the preparation of the polymer solution for surface coating was also investigated through testing the performance of the composite membranes in separating different electrolyte solutions as well as by micrographic techniques using a Scanning Electron Microscope and an Atomic Force Microscope. It was found that the preparation of thin film composite membranes with high selectivity and high flux was possible by adjusting properly the ion exchange capacity and the solvent used in making the coating solution. It was also found that the membrane performance was governed primarily by the ion exchange reaction between the solute cation and the proton in $-SO_3^- H^+$, as well as by the Donnan equilibrium. An attempt was also made to investigate the effect of changing the microporous substrate of the thin film composite membrane on the membrane permeation rate and selectivity. The porosity and the structure of the substrate play a significant role in determining the performance of the composite membrane.

Acknowledgement

The author is very thankful to the Secretariat of Scientific Research of Libya for their generous financial support throughout his studies and research.

The author would like to express his sincere appreciation of the supervision and support provided by Dr. Takeshi Matsuura. It has been a great opportunity and a pleasant experience studying under Dr. Matsuura's supervision at the Industrial Membrane Research Institute (IMRI). I would like to thank Honourable Dr. S. Sourirajan for encouraging and motivating me. Thanks are due to Osmonics Inc. and Mr. Brian Rudie for providing the HW17 and HW18 UF membranes and support. I would like to also express my thanks to Dr. Chowdhury, at IMRI, for her assistance throughout this project, to Dr. K.C. Khulbe and Mr B. Kruczek for their efforts with the AFM, to Mr. Y. Touhami and Mr. E. Bradateanu for their help with intrinsic viscosity measurement, as well as to all the staff at IMRI for their assistance and offering of a pleasant research environment. Thanks are due to Mr. Louis Tremblay and all the Technical Support staff, at the Department of Chemical Engineering, for their continuous support

Dedicated To My Dear Family.

Table Of Contents

List Of Tables

List Of Figures

Nomenclature

PWP	Pure water permeation rate, ($m^3/m^2.s$).
PR	Permeation rate when treating a feed solution, ($m^3/m^2.s$).
f	fractional solute separation.
C	Polymer solution concentration (intrinsic viscosity measurement), $g/100cm^3$.
t_o	Capillary flow time for pure solvent, (s).
t	Capillary flow time for polymer solution, (s).
PES	Polyethersulfone.
PPO	Poly(2,6-dimethyl-1,4-phenylene oxide).
SPPO	Sulfonated poly(2,6-dimethyl-1,4-phenylene oxide).
SPPOH	Hydrogen-form SPPO.
SPPONa	Sodium-form SPPO.
T_g	Glass transition temperature of polymer, (°C).

CHAPTER ONE

INTRODUCTION

Separation techniques have always been an integral part in the vast chemical and related industries. Over the last thirty five years, utilization of synthetic membranes has grown tremendously to cover a broad range of applications.

1.1 Membrane Separation Processes

The membrane separation process is a general and widely applicable technique for the separation, concentration, or fractionation of inorganic or organic substances in liquid or gaseous phase. Because of their lower energy requirements, since no heating or phase change is involved, the membrane separation processes are increasingly more competitive with conventional separation processes such as distillation, crystallization and extraction. Membranes can be designed to meet different separation objectives by having specific porosities and chemical functionalities. Membrane units are also compact and modular in design which enable them to be placed in existing plant designs and replaced with relative ease.

Figure 1.1 schematically represents the useful ranges of various separation processes. Both ultrafiltration and reverse osmosis are pressure-driven liquid-phase membrane separation processes. Ultrafiltration is mainly utilized for the separation of macromolecules and covers a wide range of solute size, as shown. Size exclusion can be the dominant mechanism of separation, although incorporation of certain functional groups on the surface of the skin layer can affect the membrane performance significantly. Reverse osmosis is capable of separating solutes of ionic radii, it is thus applicable in processes such as water desalination, for the production of potable water from sea water.. In reverse osmosis solute-membrane interactions, preferential sorption and diffusion dominate the separation mechanism.

At the heart of this separation technique is the membrane, which is a thin two-dimensional structure made mostly from polymeric materials. It is well-known that the first membrane of practical importance discovered by Loeb and Sourirajan in 1960 is asymmetric in structure, featuring a very thin skin layer, which controls the membrane performance, integrally on top of a much more porous support. The thinness of the skin layer is of a practical importance since it helps lower the hydrodynamic resistance to flow, while the porous substrate provides the membrane with mechanical strength. The chemical, thermal, and biological long-term stability of the membrane under its operating conditions has always been a driving force behind developing and fabricating new membranes.

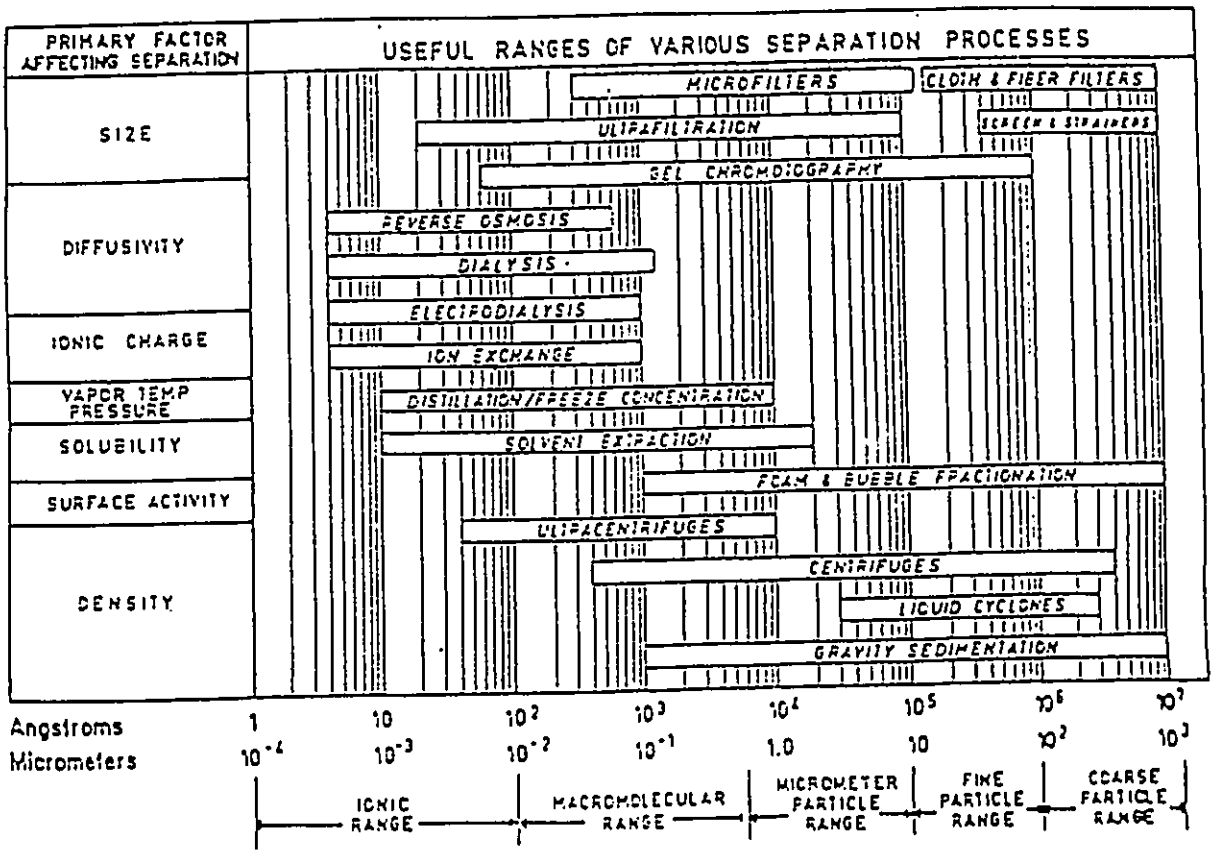

Figure 1.1 Useful ranges of various separation processes (Belfort, 1984).

1.2 Thin Film Composite Membranes

A composite reverse osmosis membrane is composed of a thin, dense polymer skin (barrier layer), formed over a microporous support film. A schematic diagram of a commercial composite membrane known as FT-30 is presented in Figure 1.2. Such membranes are direct descendants of the Loeb-Sourirajan asymmetric membrane developed in 1960. The skin (barrier) layer, which determines the membrane selectivity, sits on top of the significantly more porous substrate, often made of polysulfone or polyethersulfone. The microporous support is in turn cast on a woven or nonwoven backing material, usually made from polyester fibers. The Loeb-Sourirajan asymmetric membrane results from casting a single polymer solution in one step that produces a microporous film with a much thinner and much denser layer over one surface. Composite membranes, on the other hand, are formed in two steps -casting of the microporous support layer, followed by the deposition of the selective denser layer on top of it (Cadotte, 1985). Thus, in the case of composite membranes, the two different layers can be optimized separately to give the best overall membrane performance. Since its early stages, composite membrane development has focused to a large extent on non-cellulosic polymeric materials because of their improved long-term mechanical, thermal, chemical and biological stability.

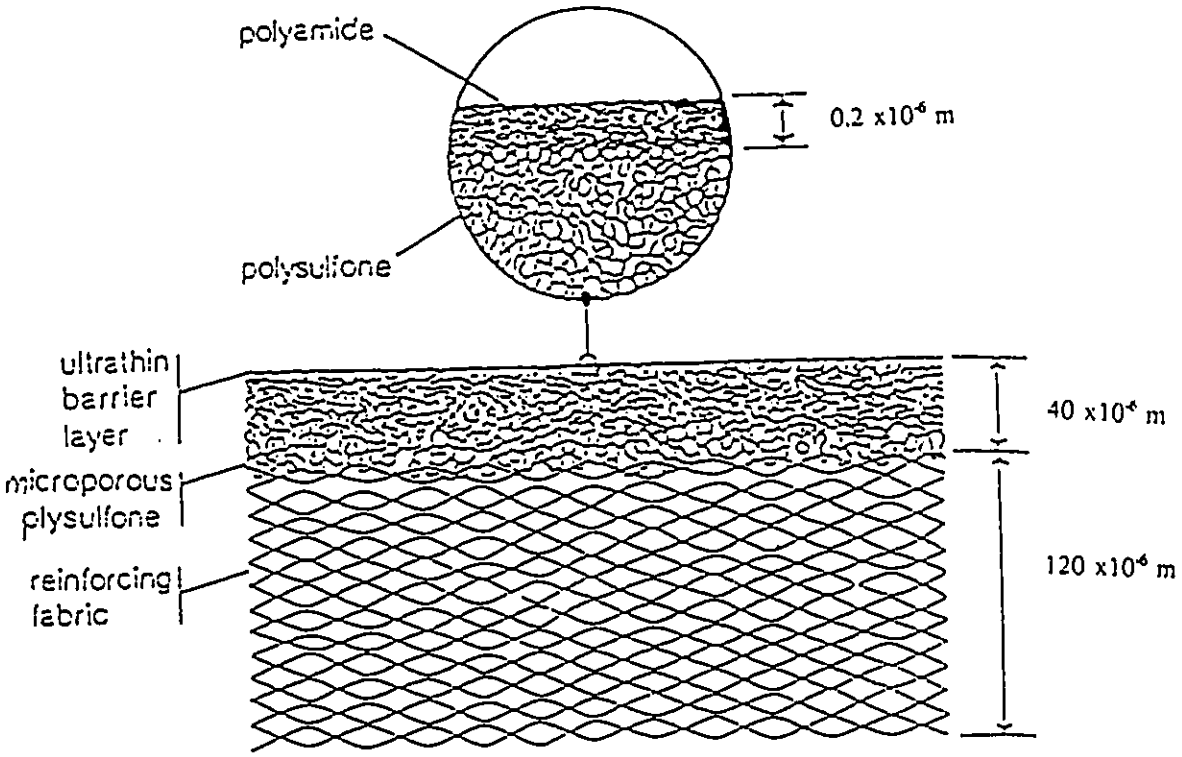

Figure 1.2 Schematic representation of the structure of FT-30 thin film composite membrane (Cadotte, 1985).

1.3 Charged Composite Membranes

In the recent years a number of charged thin film composite membranes have been developed. These membranes exhibit high water flux and are resistant to chlorine, high and low pH and high temperature (Agarwal et al., 1988, and Ikeda et al., 1988). The performance of these membranes is primarily controlled by the electric charge of the thin selective layer at the membrane surface. The ionic groups present at the surface layer of the composite membrane exert electric repulsion to solutes having the same charge as that of the surface layer. This repulsive force is effective over a range longer than the dielectric repulsive force working between the charged solute and the neutral surface. Therefore, a larger pore size is allowed at the surface of the charged membrane than the neutral membrane to maintain a given level of rejection of the charged solute. Together with the thinness of the selective surface layers, the charged thin film composite membrane is thus featured by a higher flux or a lower operating pressure than those of the neutral membranes (Kurihara et al., 1985). The above principle has been applied industrially for the development of nanofiltration membranes whose performance characteristics are between those of reverse osmosis and ultrafiltration membranes.

Studies on the performance of charged composite membranes have been reported by a number of authors (Allegrezza et al., 1987 and Kawada et al., 1987). Normally, the membranes are negatively charged, and electrolyte solutes with higher anionic charge densities and/or with lower cationic charge densities are rejected more effectively. On the other hand, the rejection of solutes without electric charge is less effective and, as a

result the charged thin film composite membrane can reject ions much smaller than the membrane pore radii but can not reject solute molecules, when the solutes do not carry any electric charge and their sizes are as small as ions (Nakao et al., 1988 and Jitsuhara and Kimura, 1983).

Polyphenylene oxide polymer has excellent chemical, physical and mechanical properties. Sulfonation of polyphenylene oxide enhances its hydrophilicity and produces a polymer having a charge functionality. A cation exchange membrane can be prepared by having sulfonated polyphenylene oxide as the material of the skin layer. The sulfonate group has an enormous affinity for water enabling the membrane to remain wetted even in the presence of hydrophobic colloids and particles.

Polyethersulfone is an outstanding membrane polymer used widely in making ultrafiltration membranes as well as substrate material for composite membranes. An amorphous glassy state, thermal and oxidative stability, excellent strength and flexibility and resistance to extremes of pH are some of its useful properties.

1.4 Scope of Research

Charged composite membranes are prepared by coating the surface of polyethersulfone ultrafiltration membranes with dilute solutions of sulfonated poly(2,6-dimethyl-1,4-phenylene oxide) polymer. Chlorosulfonic acid is used to sulfonate poly(2,6-dimethyl-1,4-phenylene oxide) polymer to various ion exchange capacities. The coating solutions are prepared by dissolving the hydrogen-form sulfonated poly(2,6-dimethyl-1,4-phenylene oxide) polymer in methanol or methanol/chloroform mixtures of different

compositions.

The reverse osmosis performance of the charged composite membranes is studied using electrolyte solutes of various valences and ionic radii. Effect of feed concentration on membrane performance is also investigated. The micrographic structure of these composite membranes is studied using a Scanning Electron Microscope and an Atomic Force Microscope. An attempt is also made to study the effect of the structure and porosity of the polyethersulfone substrate on the reverse osmosis performance of the composite membrane.

1.5 Objectives

The research objectives of preparing and studying Sulfonated poly(2,6-dimethyl-1,4-phenylene oxide) - Polyethersulfone composite membranes are to determine the effects of various membrane preparation and operating conditions, specifically:

1. Effect of the degree of sulfonation of polyphenylene oxide on the reverse osmosis performance of the composite membrane.

2. Effect of the solvent, used in making the coating solution, on the reverse osmosis performance of the membrane and on its microscopic structure.

3. Effect of the valence, ionic radii and concentration of the electrolyte solute on the reverse osmosis performance of the composite membrane.

4. Effect of changing the substrate polyethersulfone on the composite membrane performance.

CHAPTER TWO

LITERATURE SURVEY

A review is made on the preparation and evolution of synthetic composite membranes, followed by a brief discussion of membrane transport theories. Donnan exclusion and the selectivity of charged membranes are then discussed. A brief discussion of solvent power and its effects on polymer-polymer and polymer-solvent interactions is also presented. The chapter concludes with a survey of sulfonated polyphenylene oxide membrane development.

2.1 Preparation of Composite Membranes

The methods that have been widely used to form composite membranes may be grouped into the four general types listed in Table 2.1 (Cadotte and Peterson, 1981).

Table 2.1 : General Methods for Forming Composite Membranes

A. Casting of the barrier layer separately, followed by lamination to the support layer.

B. Dip-coating of the support film in a polymer solution and drying, or in a reaction monomer or prepolymer solution followed by curing with heat or radiation.

C. Gas-phase deposition of the barrier layer from a glow discharge plasma (Plasma Coating).

D. Interfacial polymerization of reactive monomers on the surface of the support film.

Barrier layers have been applied by all of the above mentioned methods on microporous support films with fibrous backing as well as on microporous hollow fibres (Cadotte, 1985). Normally, except for method C (gas-phase deposition), the support film is used in the wet "as cast" condition for applying the reagents to form the barrier layer. The final step of preparation. namely drying of the membrane, frequently aids in bonding the skin layer to the substrate.

Methods B, C, and D in Table 2.1 use *in-situ* formation methods in contrast to method A where the barrier layer is preformed and needs to be transported to the substrate. The *in-situ* methods are generally more practical for machine production of composite membranes.

2.2 Development of Composite Membranes

The first thin film composite membrane reported in the literature was made by Peter Francis at North Star Research Institute in 1964 (Francis, 1966). A liquid film of cellulose acetate solution in cyclohexane was float casted onto a water surface. The ultrathin polymer film (200-5000 $x10^{-10}$m) was then laminated to a microporous cellulose acetate support layer underneath .

In 1966, Cadotte developed a method of casting porous support films from polysulfone, polycarbonate, and polyethylene oxide plastics, of which polysulfone gave the best results. Among the properties which qualified polysulfone as an outstanding membrane polymer are a glass transition temperature (Tg) of 195 °C, an amorphous glassy state, thermal and oxidative stability, excellent strength and flexibility, and resistance to extremes of pH (Kesting, 1985). A closely related derivative which is totally devoid of aliphatic hydrocarbon groups is polyethersulfone. It has similar properties, with an even higher Tg of 230 °C. The chemical structures of polysulfone and polyethersulfone are shown in Figure 2.1. Since their early development, microporous polysulfone and polyethersulfone have been widely adopted as the material of choice for the support films in composite membranes.

A membrane designated as NS-200, was first developed by Cadotte in 1972. The membrane was made by dip-coating a polysulfone support film in a 2:2:1 solution of furfuryl alcohol : sulphuric acid : Carbowax 20M in 80:20 water:isopropanol. The excess coating solution was allowed to drain off. Oven drying at about 135 °C produced a black composite membrane having a sulfonated polyfurane layer, resulting in high salt rejection

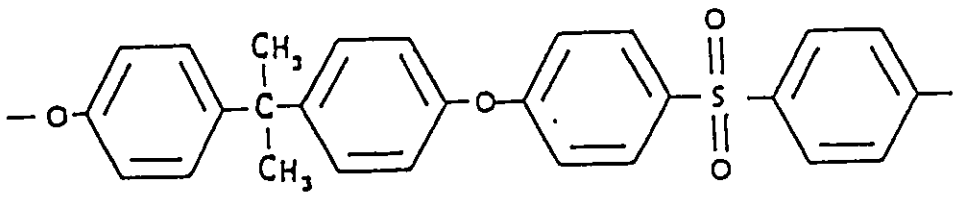

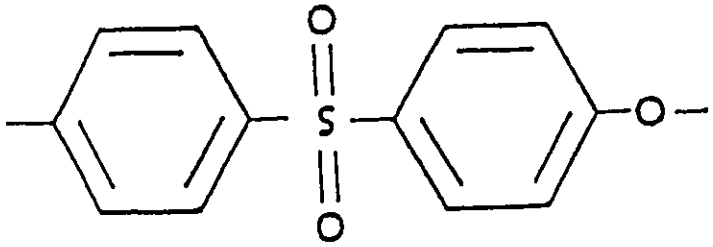

Figure 2.1 The chemical structure of the most commonly used substrate materials: (Top) Polysulfone, (Bottom) polyethersulfone.

performance. Decreasing the thickness of the barrier layer by means of thinner coating resulted in loss of flux. This behaviour was attributed to the loss of asymmetricity of coated layer upon thinness (Cadotte, 1985). Gradual loss of flux and the accompanying decrease in salt rejection were long-term stability problems of the NS-200 membrane. Irreversible swelling of the membrane, due to hydration of the sulfonic acid groups in salt solutions, was the potential cause of these problems.

Sulfonated polysulfone membranes, made by the dip-coating method, are of interest because of their high degree of chlorine resistance. The membrane was made by dip-coating of polysulfone supports (flat sheet or hollow fibres) in a water or water-alcohol solution of sulfonated polysulfone. Oven drying of the coated support film at 100 to 140 °C caused the formation of sulfone crosslinks that served to immobilize the sulfonated polysulfone barrier layer. In 5000-hour test using 3500 ppm-salt brackish water at 400 psi with addition of 100 ppm chlorine at pH 8, flux and salt rejection remained constant at 1 gallons/(ft^2.d) and 98%, respectively (Cadotte, 1985).

The NS-300 membrane was developed from an effort to form an interfacial poly(piperazine isophthalamide) membrane for its reported chlorine resistance. The initial efforts to develop interfacially formed piperazine isophthalamide and terephthalamide membrane were only partially successful. A variant of this membrane involved replacing the isophthaloyl chloride with its triacyl chloride analog, trimesoyl chloride. Thus the NS-300 membrane system comprised a family of membranes, with reverse osmosis properties determined by the isophthalic : trimesic ratio. NS-300 gave high water flux and high solute separation for dissolved salts involving polyvalent anions. Applications such as desalination of brackish sulfate ground waters and concentration of sucrose and

lactose in the food processing industry were candidates for such membranes (Matsuura, 1994).

In 1976 Riley and coworkers developed the reverse osmosis membranes known as PA-300 utilizing the method of interfacial polymerization (Riley et al., 1976). The membrane was prepared by depositing a thin layer of an aqueous solution of an epichlorohydrine ethylene diamine condensate on the finely porous surface of a polysulfone support membrane. Subsequent contact of the poly(ether/amine) layer with a water immiscible solution of isophthaloyl dichloride resulted in a film of cross-linked poly(ether/amide) copolymer. The membrane was further dried at an elevated temperature. The membrane was reported to have excellent characteristics including strong chemical resistance, wet-dry reversibility in addition to excellent reverse osmosis performance (Sourirajan and Matsuura, 1985).

Interfacial polymerization was also used in the development of FT-30 membranes by Film Tec Corporation in 1978. A schematic of this membrane was shown in section 1.2. FT-30 is a thin film (about 0.25 $x10^{-6}$ m) supported by a porous polysulfone coating (50 $x10^{-6}$m) on a polyester carrier web (125 $x10^{-6}$m). The material of the membrane was a proprietary crosslinked aromatic polyamide having some anionic functionality. Its thickness made it much more resistant to damage by mechanical stresses and oxidizing agents. FT-30 was stable over a wide range of pH, and could be cleaned with strong acid and base solutions. It showed more resistance to chlorine and other oxidizing agents than other commercially available polyamide membranes, though still not as good as cellulosic membranes in this regard. FT-30 came close to being the ideal membrane for sea water

desalination, in terms of productivity, chemical stability, and nonbiodegradability (Sourirajan and Matsuura, 1985).

Toray Industries of Japan developed a membrane from a thin film (300 $x10^{-10}$ m) crosslinked polyethers obtained by *in-situ* polymerization of two species of tri(hydroxyethyl)isocyanate and furfuryl alcohol in the presence of an acid catalyst on the surface of a porous polysulfone support membrane cast on a supporting fabric (Kurihara et al., 1980). This thin-film composite membrane was commercially known as PEC-3000. It was characterized by high salt rejection capacity, high rejection of a variety of organic compounds, and high operational stability at temperatures up to 40 °C, pressures up to 1000 psig and pH range 1 to 12.

The PA-300, FT-30 and PEC-1000 membranes described above represent major accomplishments in thin film composite membranes technology, and they are in the rise in the market place for a wide variety of reverse osmosis applications. Table 2.2 and Table 2.3 show the reverse osmosis performance and the chemical structures of the skin layer, respectively, for some advanced thin film composite membranes (Lang, 1993).

TABLE 2.2

Reverse Osmosis Performance of some Advanced Thin Film Composite Membranes (Lang, 1993) (Feed 3.5% NaCl Solution)[1]

Membrane trade name and its (Manufacturer)	Properties		pH range
	Separation (%)	Product rate ($l/m^2.d.atm$)	
NS-100 (NSRI)	99.4	7.1	0.5-13
NS-200 (NSRI)	>99	10.8-12	1.5-13
NS-300 (Film-Tec.)	99.6	11.1	1.5-13
PA-300 (UOP)	98.5-99.4	12-15	2-12
RC-100 (UOP)	99.4	9.7-11.2	2-12
FT-30 (Film-Tec.)	98.7	17.7	3-11
NTR-7250 (Nitto Electric)	99.5 *2	24.6	5-11
PEC-1000 (Toray Industries)	99.8	5.36	1-13
Solcon-P (Sumitomo Chemical)	98	9.6	1-10

[1]Feed 0.5% NaCl solution for *2.

TABLE 2.3

Chemical Structure of the Skin Layer of some Advanced Thin Film Composite Membranes (Lang, 1993)

Membrane trade name	Chemicals for skin layer	Skin layer structure
NS-100	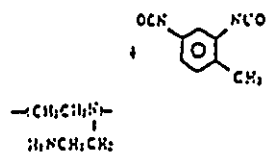	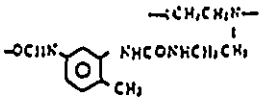
PA-100	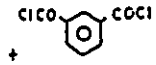	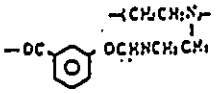
PA-300	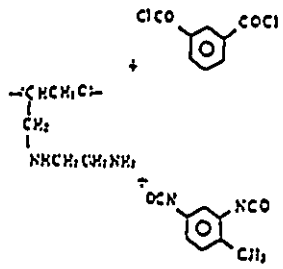	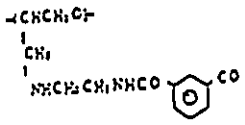
RC-100		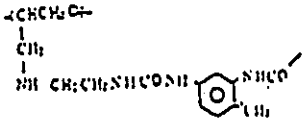
NS-200	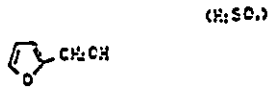	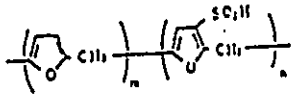
NS-300	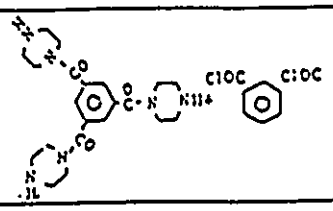	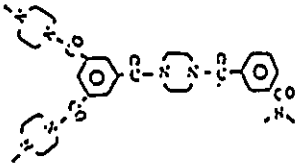
FT-30	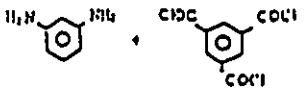	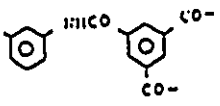
PEC-1000	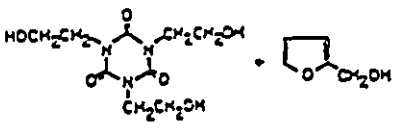	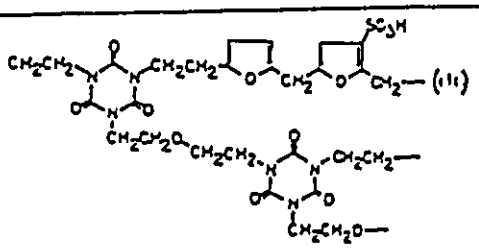

2.3 Membrane Transport Theories

Membranes differ widely in their preparation procedures as well as in their observed performance. A quantitative description of the membrane formation mechanism is nearly impossible (Strathmann, 1985). Consequently, transport through membranes is difficult to describe. In spite of all of these circumstances, membrane development and utilization have not suffered. Recently, a unified approach, in dealing with transport phenomena across membranes, has been developed (Mason and Lonsdale, 1990). It is based on fundamental statistical-mechanical principles, encompassing previous theories. Mason and Lonsdale state that there are basically two dominant theories that deal with transport phenomena across synthetic membranes. Irreversible thermodynamics theory was developed by Kedem and Katchalsky (1958) and Katchalsky and Kedem (1962) on the basis of Onsager's results. The second approach is the friction model theory which was initially developed by Spiegler (1958) and then by Kedem and Katchalsky (1961). Aside from these, there are some related or derivative approaches, such as ideal gas models, diffusion models, Nervst-Planck equations, and energy barrier models. Mason and Lonsdale further state that beyond these models, a host of special case derivative approaches attempt to postulate mechanisms on a molecular scale. Examples are the solution-diffusion model of Lonsdale, Merten and Riley (1965), and the preferential sorption-capillary flow model of Sourirajan (1977) and Sourirajan and Matsuura (1985).

2.3.1 Irreversible Thermodynamics

Transport across membranes may be described in a more general way by taking into account the possibility that water and salt fluxes may be interrelated (i.e., the fluxes are coupled). Irreversible thermodynamics assumes that fluxes are determined by all forces acting on the system, and if one is not too far from equilibrium, the relationship is linear. Therefore, with water and salt flow through a membrane, the fluxes are determined by the forces F :

$$J_w = L_{11} F_w + L_{12} F_s$$

$$J_s = L_{21} F_w + L_{22} F_s$$

where J_w and J_s are the water and salt fluxes, respectively, L_{ij} is the phenomenological coefficient, and F is the driving force (Vieth, 1991). The cross coefficients L_{12} and L_{21} are interdependent, specifically :

$$L_{12} = L_{21}$$

The second law of thermodynamics dictates the following :

$$L_{11} L_{22} - (L_{12})^2 > 0$$

Starting with the above equations, Kedem and Katchalsky (1963) derived the following equations:

$$J_v = L_p (\Delta P - \sigma \Delta \pi)$$

$$J_s = \omega \Delta \pi + (1 - \sigma) J_v C_{sB}$$

where: J_v = volume flux = water flux (m/s),

L_p = hydraulic permeability (m/Pa.s),

σ = reflection coefficient,

ω = solute permeability coefficient ($g/m^2.Pa.s$),

C_{sB} = log mean of solute concentration at either side of the membrane.(g/m^3).

Irreversible thermodynamics thus treats the membrane as a black box in which relatively slow processes are taking place near equilibrium. No information is needed on the mechanism of transport. The system is simply divided in small subsystems in which " local equilibrium" exists, therefore they are describable by thermodynamic parameters.

2.3.2 Solution-Diffusion Model

The concept that transport through membranes may be described by a solution-diffusion mechanism has been attributed back to L'Hermite in 1855. A model of this type assumes that each component is sorbed by the membrane at one interface, transported by diffusion across the membrane, and desorbed at the other interface. The surface layer of the membrane is expected to be homogenous and nonporous. The rate limiting step is taken to be diffusion across the membrane. The transport of solute and solvent is also assumed to be uncoupled, that is the flow of one component has no effect on the transport of the other (Vieth, 1991).

Lonsdale, Merten and Riley (1965) derived the following equation for water transport :

$$J_w = - \frac{D_W C_{WM} V_W}{R T} \left[\frac{\Delta P - \Delta \pi}{\Delta x}\right]$$

where J_w = water flux ($g/m^2.s$)

D_w = water diffusion coefficient (m^2/s)

C_{WM} = concentration of water in the membrane (g/m^3)

Δx = membrane thickness (m)

This equation was obtained by assuming: (1) Fick's law; (2) Henry's law; and (3) constancy of D_w and V_w with pressure. Some of these assumptions have been questioned (Hodges, 1964). The equation, however, appears to describe water transport in defect-free (non-porous) membranes fairly well, if salt rejections are high (Lonsdale et al., 1965).

Lonsdale et al. again assumed Fick's law and a constant diffusion coefficient to describe salt transport:

$$J_s = - D_s \left[\frac{\Delta C_{SM}}{\Delta x}\right]$$

where J_S = salt flux ($g/m^2.s$)

D_S = salt diffusion coefficient (m^2/s)

C_{SM} = salt concentration in the membrane (g/m^3)

A more convenient form of the salt transport equation is obtained by defining a molar distribution coefficient K:

$$K = (\text{g-salt/m}^3 \text{ membrane}) / (\text{g-salt/m}^3 \text{ solution})$$

and assuming K is constant over the concentration range of interest. The salt transport equation becomes:

$$J_s = D_s K \left[\frac{\Delta C_{SB}}{\Delta x}\right]$$

where C_{SB} is the salt concentration in the bulk solution.

The above equations have appeal both in their simplicity and direct relation of equilibrium sorption measurements to transport properties. Lonsdale et al. were able to correlate direct osmosis and salt immersion experiments with reverse osmosis results for cellulose acetate membranes with a good degree of success (Vieth, 1991).

For a perfectly selective membrane, (reflection coefficient (σ) = 1), irreversible thermodynamics equations reduce to the above-stated solution diffusion equations. The agreement is still good for reflection coefficient close to unity (Vieth, 1991).

2.3.3 Comparison of Transport Mechanisms

In practice, the simple solution-diffusion model has been found to match quite well observed membrane performance trends during reverse osmosis of solutions containing one ionic salt. However, the model has proved to be less adequate in dealing with organic solutions (Gutman, 1987). The rejection of organic solutes has been observed at times to decrease with increasing pressure, to the extent of being negative in some situations. Gutman has further stated that even the more sophisticated irreversible thermodynamics model, originally developed by Kedem and Katchalsky (1958), has also proved inadequate to explain the different types of behaviour observed during reverse osmosis of organic solutions.

Furthermore, according to Lonsdale's approach, the transport equations are applicable only to a perfectly dense membrane without any pores. The transport parameters in this case are considered intrinsic to the polymeric material. It is established, however, that different reverse osmosis membranes can be produced from a

given single polymeric material, depending on the size of the "pores" generated on the surface of the membrane (Matsuura, 1994). The solution-diffusion approach was established for the permeation of liquid and gas through the membrane before reverse osmosis membranes of practical usefulness were developed by the phase inversion technique. Dense membranes without asymmetricity were prepared from the polymeric materials, and their transport properties were measured, assuming that the membranes were defect-free and the transport parameters so produced were the values intrinsic to the material.

The membranes of practical usefulness are, on the other hand, prepared by the phase inversion technique, resulting in an asymmetric structure having a top selective layer. The microscopic structure of this thin layer depends on the conditions under which the membrane is prepared. Obviously, the numerical parameters associated with the membrane transport equations should depend on the microscopic structure of the membrane and also on the conditions under which the preparation is made (Matsuura, 1994). Elaborate models with numerous parameters covering the different interactions of the solute(s), solvent(s), and membrane material, and reflecting the microscopic structure of the membrane are needed in order to be able to predict the behaviour more accurately.

Such an approach has been adopted by Sourirajan, Matsuura and co-workers as reported by Sourirajan (1977) and Sourirajan and Matsuura (1985) in the form of "Preferential Sorption-Capillary Flow Mechanism". Kesting has explicitly stated that Sourirajan's model is much superior than the solution-diffusion model. Kesting has further recommended it as the most valid mechanism in representing reverse osmosis behaviour (Agarwal, 1991).

2.3.4 The Preferential Sorption-Capillary Flow Mechanism

The Gibb's equation relating interfacial tension of a solution σ and the surface excess of a solute at an interface Γ is given in the form:

$$\Gamma = - \frac{1}{RT} \frac{\delta\sigma}{\delta \ln a}$$

where R is the gas constant, T is the absolute temperature and a is the activity of the solute. This equation predicts the possible existence of a steep concentration gradient at the interface. For aqueous sodium chloride solution, there is a negative surface excess of solute resulting in a pure water layer at the air-solution interface.

The above ideas are embodied in the conceptual model shown in Figure 2.2 for recovering fresh water from aqueous salt solutions (Matsuura and Sourirajan, 1985). The solution is in contact with a solid material in the form of a porous membrane. With preferential water sorption or preferential repulsion for the solute, dictated by the chemical nature of the membrane, a multimolecular layer of preferentially sorbed pure water could exist at the membrane-solution interface. Continuous removal of this interfacial water is possible by forcing its flow under pressure through the capillaries of the membrane. The concept of a critical pore diameter for maximum separation and permeability arises: it is clearly twice the thickness of the interfacial pure water layer (t). If the pore diameter is larger, permeability will be higher but solute separation will be lower since the effective feed solution (concentrated boundary solution) will also flow through the pores. If the pore diameter is smaller, separation will be maximum but permeability will be reduced. In the absence of pores on the membrane surface, there can be no flow of the interfacial fluid across the membrane through capillaries and fluid permeability can be insignificantly

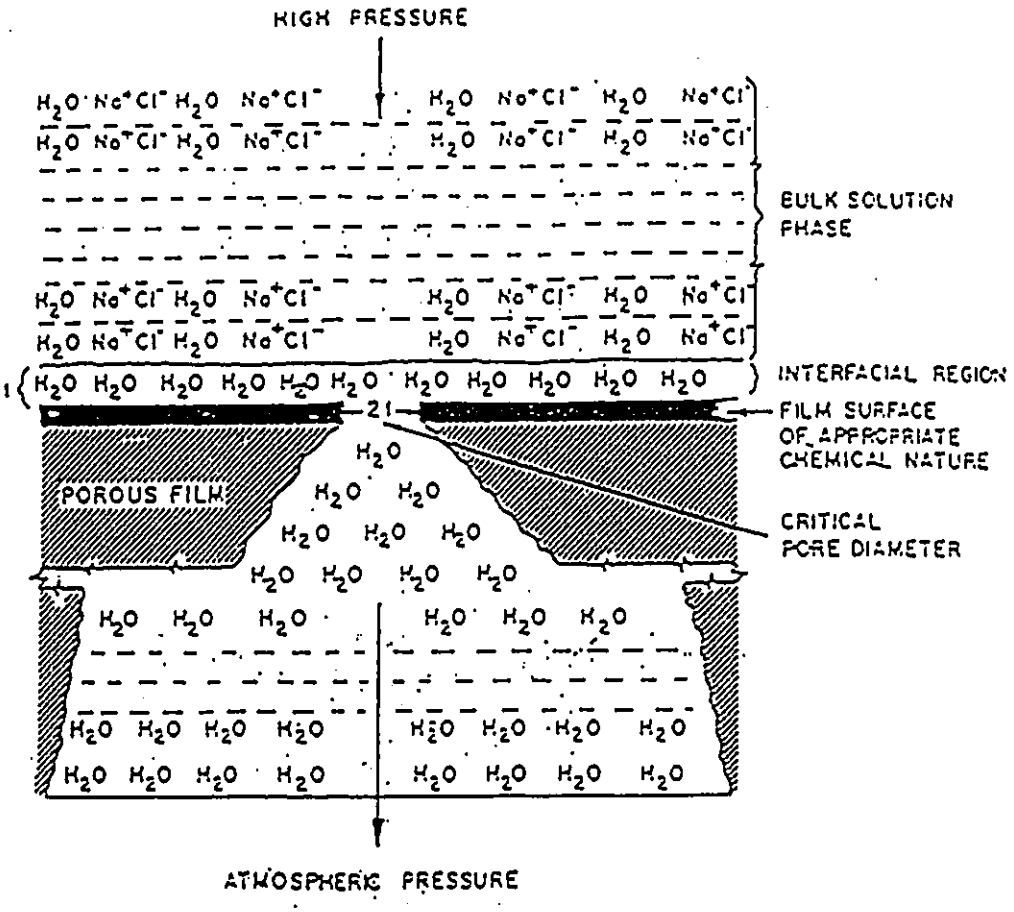

Figure 2.2 Schematic of preferential sorption-capillary flow mechanism for reverse osmosis separation of sodium chloride from aqueous solutions (Sourirajan, 1977).

small. For maximum separation and permeability it is necessary to maintain the pore size equal to 2t only on the surface layer of the membrane. The pores underneath the skin layer of the membrane could be, and should be, larger. This is important from a practical point of view so as to minimize the resistance to flow and thus minimize the pressure requirements for forcing and maintaining water flow through the membrane.

2.3.5 The Kimura-Sourirajan Transport Equations

The Kimura-Sourirajan (1967) analysis is based on a generalized capillary flow model involving viscous flow for water transport, pore diffusion for solute transport, and "film" theory for calculating an effective mass transfer coefficient applicable to the concentration polarization situation on the high pressure side of the membrane. This analysis is applicable to all levels of solute separation, and gives rise to the following basic equations relating the pure water permeability constant A, the solute transport parameter ($D_{AM}/K\delta$), and the mass transfer coefficient k on the high pressure side of the membrane at any point (position or time) in the system under operating conditions of constant temperature and pressure (Sourirajan and Matsuura, 1977),

$$A = PWP / (P \cdot S \cdot M_B \cdot 3600) \qquad (1)$$

$$N_B = A (P - \pi (X_{A2}) + \pi (X_{A3})) \qquad (2)$$

$$N_B = [D_{AM}/K\delta] [(1 - X_{A3}) / X_{A3}] [c_2X_{A2} - c_3X_{A3}] \qquad (3)$$

$$N_B = k c_1 (1 - X_{A3}) \ln [(X_{A2} - X_{A3}) / (X_{A1} - X_{A3})] \qquad (4)$$

In this analysis, the low pressure side of the membrane is assumed to be at atmospheric pressure, and the operating pressure P is given in gauge pressure.

Equation (1) defines the pure water permeability constant A, which is a fundamental quantity with respect to the membrane. A is a measure of the overall porosity of the membrane. It represents pure water transport in the absence of any concentration polarization in the high pressure side of the membrane. The magnitude of A is independent of any solute under consideration. Equation (2) is valid when the viscosity of the membrane permeated solution is essentially the same as that of pure water. Equation (2) enables the calculation of the boundary layer concentration X_{A2} on the high pressure side of the membrane. Equation (3) defines the quantity $[D_{AM}/K\delta]$ for the transport of solute through the membrane for any given solution system. This solute transport parameter is a fundamental one for any given membrane-solution system. It plays the role of a mass transfer coefficient with respect to solute transport through the membrane. Equation (4) enables the calculation of the mass transfer coefficient k on the high pressure side of the membrane. The magnitude of k is a function of the nature of solute, concentration of feed solution, feed flow rate, and the geometry of the apparatus used. For any reverse osmosis apparatus and membrane-solution-operating system, the relationship between feed flow rate and k is needed for process design.

Under steady-state operating conditions, a single set of experimental data on pure water permeation rate (PWP), membrane-permeated product rate (PR), and solute separation (f), enables the calculation of the quantities A, X_{A2}, k and $(D_{AM}/K\delta)$ at any

point using the Equations (1) to (4). Neither any one equation in the set of Equations (1) to (4), nor any part of this set of equations, is adequate representation of reverse osmosis transport, the latter is governed simultaneously by the entire set of Equations (1) to (4) (Matsuura and Sourirajan, 1977). These equations, furthermore, constitute the basis for predicting membrane performance regarding the separation of different solutes, based on experimental performance data of a single solute (Matsuura, 1994).

2.4 Donnan Exclusion

The characteristic which distinguishes ion-exchange membranes from other types is the presence of charges or ionic groups in their component polymer molecules. Mobile ions bearing a charge opposite to that born by the fixed ions are known as counter ions, those bearing the same charge as co-ions. Polymers containing negatively charged groups are polyanions. Because of the electroneutrality requirement they will have a stoichiometric amount of exchangeable cations in association with their fixed cations. Since such cations are mobile and can be exchanged for others in an external solution, polyanions are known as cation exchangers. For similar reasons polycations are termed anion exchangers.

The properties of ion-exchange polymers are exemplified by a cation-exchange membrane (containing no sorbed electrolyte) which is placed in a dilute solution of a strong electrolyte (Figure 2.3). The mobile-cation concentration is higher in the membrane (because the cations are attracted to its fixed negatively charged groups). The mobile-anion concentration, on the other hand, is higher in the solution than in the membrane. These concentration differences cannot be levelled out by diffusion because electroneutrality would then be disturbed, owing to the electric-charge-bearing properties of the mobile ions. The flux of cations into the solution and of anions into the membrane would result in an accumulation of positive charge in the solution and negative in the membrane. The first diffusing ions therefore result in a potential difference between the two phases. This *Donnan potential* effectively draws cations back into the membrane and

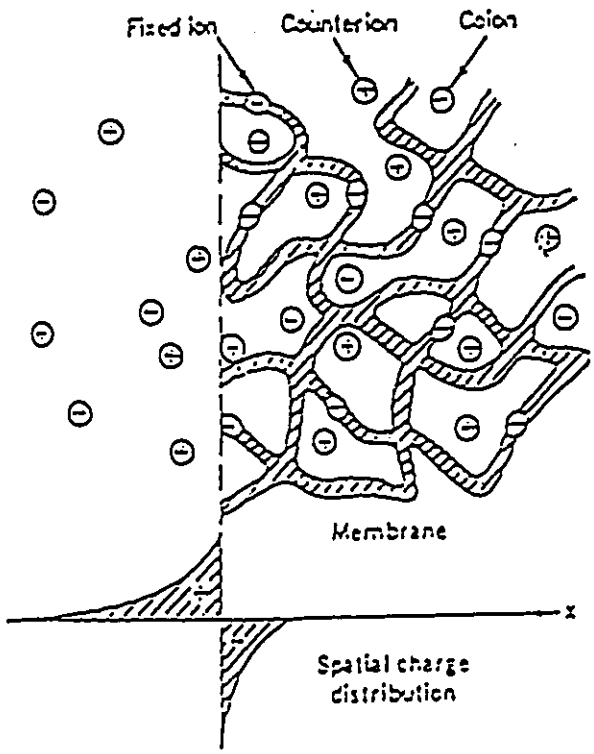

Figure 2.3 Schematic representation of the distribution of ions in the vicinity of the membrane-solution interface (Kesting, 1985).

anions back into the solution, with the eventual establishment of equilibrium between the electric field and the tendency of the ions to eliminate concentration differences by diffusion. For this reason counter-ion concentration in the membrane is higher, and co-ion concentration lower, than in the external solution. Since co-ions are repelled from the membrane, the electrolyte itself is too, because of the electroneutrality requirement. This exclusion of the electrolyte from the membrane is known as *Donnan Exclusion.*

Electrolyte exclusion increases with the magnitude of the Donnan potential. Therefore, this potential and its effects upon ions are of prime importance to understand the sorption and transport of ions by and through ion exchange and monomer membranes. Electrolyte sorption and transport depend chiefly upon the distribution of the co-ion since electrolyte and co-ion uptakes are stoichiometrically equivalent. Among the parameters which influence the magnitude of the Donnan potential are the ion exchange capacity of dry polymer (I.E.C.), the degree of swelling or its inverse, the crosslinking density, solution concentration, and ion charge density.

Capacity most often refers to the counter-ion content (in milliequivalents per gram) of anhydrous polymer before any electrolyte sorption has occurred. This definition is a characteristic of the membrane material and is independent of the experimental conditions. The concentration of fixed ionic groups is subject to change with such variables as degree of swelling and electrolyte solution concentration.

The volume concentration of fixed ionic groups determines the charge density of the membrane and hence its Donnan potential. Obviously, since swelling decreases this concentration, it must be minimized if a maximum Donnan potential is to be attained. The means most commonly employed to this end are the physical restriction of interchain

displacement by covalent crosslinks. Donnan potential, and hence electrolyte sorption, is inversely proportional to the degree of swelling and directly proportional to the crosslink density. Since Donnan equilibria are electric field phenomena which depend on the overall charge of both fixed and mobile groups, these values affect the magnitude of the Donnan potential.

The decreasing efficiency of electrolyte exclusion with increasing solution concentration is due to the increasing tendency of the ions to eliminate concentration differences by diffusion at a constant electric field. The electric field is constant because the concentration of fixed charges in the membrane is constant. The equilibrium between these opposing tendencies is therefore displaced, with the result that the Donnan potential and electrolyte exclusion decrease. Counter-ions of high charge density (small size and/or high valence) and co-ions of low charge density minimize electrolyte exclusion. This effect is due to maximum attraction and minimum repulsion by the membrane's fixed ionic groups of counter ions and co-ions, respectively. In addition to the effects upon interaction with, and repulsion by, the membrane, high counter-ion and low co-ion charge density inhibit the formation of ion pairs between mobile ions so that external forces, such as the electric field exerted by the membrane's fixed charges, have a correspondingly larger effect than would be if strong associations between the electrolyte's component ions were in effect. When, on the other hand, ion pairs or complexes are formed by counter-ions and co-ions, the combination can act as a unit with an effective charge density corresponding to the relative proportions of positive and negative charges. In such a case co-ion exclusion, and hence Donnan efficiency, may be diminished owing to the entry of the former as a disguised portion of a counter-ion complex (Kesting, 1985).

Likewise where association between fixed ionic groups and counter ions results in ion-pair formation, the effective charge density of the former, and with it the magnitude of the Donnan potential, is reduced. In extreme cases where multivalent counter-ions associate with the fixed ionic groups, the membrane can reverse its fixed charge.

An important characteristic of ion-exchange membranes is selectivity, that is, the sorption of one counter-ion in preference to another. Selectivity is influenced by the magnitude of membrane-solute and solute-solute interactions. Thus a membrane tends to prefer counter ions of high charge density (for electrostatic reasons) and small size (for steric reasons). It also tends to prefer those counter ions which are least encumbered by interactions with other mobile ions. Selectivity sequences for some of the more common cations are

$$Ba^{2+} > Pb^{2+} > Sr^{2+} > Ca^{2+} > Ni^{2+} > Cd^{2+} > Co^{2+} > Zn^{2+} > Mg^{2+} > UO_2^{2+}$$

$$Tl^{+} > Ag^{+} > Cs^{+} > Rb^{+} > K^{+} > NH_4^{+} > Na^{+} > Li^{+}$$

The corresponding anion-exchange sequence is

$$\text{citrate} > SO_4^{2-} > \text{oxalate} > I^{-} > NO_3^{-} > CrO_4^{2-}$$
$$> Br^{-} > SCN^{-} > Cl^{-} > \text{formate} > \text{acetate} > F^{-}$$

The position of H^{+} varies with the acid strength of the membrane. For strong

acids it usually lies between Na^+ and Li^+, whereas for weak acids it depends on the strength of the fixed anions. The position of OH^- also varies. For strong bases it usually lies between acetate and fluoride, and for weak bases it depends on the strength of the fixed cations.

In addition to the various fixed-ion and mobile-ion associations which occur for largely electrostatic reasons, ion-exchange membranes can also sorb weak electrolytes and nonelectrolytes from solution. Sorption of such solutes is generally, but not always, reversible and is governed by the same factors which govern solute sorption by nonionic membranes (Kesting, 1985).

2.5 Solvent Power

Relevant to membrane preparation, the polymer-solvent interactions in the coating solution may play a significant role in shaping the composite membrane and hence affecting its performance. Several measures of the strength of polymer-solvent interactions in macromolecular solutions are available. Among these is the solution viscosity. Solution viscosity increases with increasing polymer molecular mass because as the latter increases so does chain length, and with it the hydrodynamics volume which this coiled chain occupies and hence the resistance of its solutions to shear and flow. Polymer chains in solution can take the form of rods, spheres, or coils, with the lattermost being the most prevalent for polymers having high molecular mass. For a given chain length, the tightness of a coil and hence its size and viscosity can vary with the strength of competing Polymer-Polymer and Polymer-Solvent interactions. The viscosimetric behaviour of polymer solutions can therefore be utilized to deduce solvent power and sometimes even the role of other components within the solvent system. It is necessary, however, to distinguish between the behaviour of polymer coils in *dilute* solutions and their behaviour in *concentrated* solutions.

The most widely utilized measure of the dilute solution viscosity of a polymer is its intrinsic viscosity [η] (Kesting, 1985). Intrinsic viscosity of a polymer in a specific solvent or solvent mixture can be determined experimentally by utilizing the following relationship:

$$[\eta] = \lim_{C \to 0} \left(\eta_{sp}/C \right)$$

η_{sp} (specific viscosity of the polymer) is defined as $(t - t_o)/t_o$ where t_o and t are the times for the solvent and solution, respectively, to run through a capillary and C is the solution concentration in g/100cm^3. Because there is always competition between Polymer-Polymer and Polymer-Solvent interactions, it follows that in a good solvent, where Polymer-Solvent >> Polymer-Polymer, Polymer-Polymer interactions will be minimal. In other words, a polymer chain will tend to avoid any intramolecular contact. In so doing it will tend to stretch out to the maximum extent possible. For this reason, if the value of $[\eta]$ for solvent A is greater than that for solvent B, A is a stronger solvent than B; likewise if a third component is added to a binary solution of polymer and solvent and $[\eta]$ increases, then the third component is acting as a co-solvent and the solvent system is a stronger solvent than the pure solvent alone. Conversely, if $[\eta]$ is found to decrease with the addition of a third component to a binary solution, then the third component is acting as a nonsolvent and the advent system is a weaker solvent than the pure solvent by itself. Also $[\eta]$ may first increase and then, with increasing additive concentration, decrease. This implies that the additive is acting in a concentration-dependent manner, first as a cosolvent and then as a nonsolvent. Intrinsic viscosity measurements can thus be used as indicators in the study as well as in the design of specific Polymer-Solvent(s) systems.

2.6 Sulfonated Polyphenylene Oxide Membranes

In an original work, polyphenylene oxide was sulfonated and cast into homogeneous membranes aiming at reverse osmosis treatment of brackish water (Plummer et al., 1970). The work focused on casting 0.2 mil thickness membranes from solutions of sulfonated polyphenylene oxide (SPPO), of ion exchange capacity (I.E.C.) ranging from 2.0 to 2.6 meq/g, in methanol or methanol/chloroform mixtures. Lower I.E.C. values were avoided because the SPPO polymer required high chloroform content to dissolve, whereas I.E.C. higher than 2.6 meq/g showed excessive swelling when treated with water. One of the challenges faced was the variation in water content of the produced polymers cast under seemingly identical conditions and having the same I.E.C.. Higher relative humidity and higher drying temperature resulted in higher water content. Also, higher alcohol in MeOH/$CHCl_3$ solvent mixtures lead to the same effect. Moreover, the water content increased steadily with increase in degree of sulfonation or I.E.C. of the polymer. The flux increased with increase in I.E.C. of the polymer due to the increase in water content. Also, higher interstitial molality, or concentration of the sulfonate anionic group in the bound gel water, enhanced the rejection capability of the membrane (Plummer et al., 1970). Excessive increase in water content, consequently, causes rejection to decrease. The membranes were regarded to be suitable in treating brackish waters high in the sulfate ions, but gave poorer rejections when the feed waters contained monovalent ions such as Na^+ and Cl^-. It was recommended to investigate alternative ways of making thinner and composite membranes from SPPO.

Thin film composite membranes, in which the sodium form of sulfonated polyphenylene oxide, $SPPO^{-}Na^{+}$, served as the skin layer, were prepared by coating the surface of different substrates such as polysulfone (PS) and polypropylene (PP) (Huang and Kim, 1984). Porous polysulfone substrates were prepared. A solution containing 12.5 mass% PS and 12.5 mass% methyl cellosolve in dimethylformamide (DMF) was cast onto a clean glass plate to a thickness of 0.3 mm. The coated liquid film was immediately immersed into 15 mass% NaCl quenching bath. The PS film gelled quickly. It was then washed with water. Finally, it was put into deionized water for at least 24 hours and thoroughly dried before SPPO polymer solution casting. PP substrate, Celgard 2400, was obtained from Gelanese Fibres Co. The best results were those of composite membranes in which PS was the substrate (Huang and Kim, 1984). The water flux increased steadily with increase in the I.E.C. of SPPO, whereas rejection showed a maximum between I.E.C. of 2.0 and 2.3 meq/g. The effect of the solvent was not investigated as the coating solution was always 4 mass % SPPO polymer in methanol.

Membranes, prepared by under-lid coating of polysulfone with solutions of sulfonated polyphenylene oxide in methanol with isobutyl alcohol (IBA) as a nonsolvent and glycerin as a swelling agent, were proposed for bioseparation applications (Agarwal, 1991). Porous polysulfone was prepared by casting a solution containing 12.5 mass% PS and 12.5 mass% methyl cellosolve in DMF on a nonwoven polyester cloth held onto a glass plate, followed by immediate coagulation in 50 mass% DMF-water bath. As IBA was added to the coating solution, flux increased while separation decreased, due to thinner skin layer and increased porosity of substrate. Glycerin, on the other hand, acted as either a plasticizer (leading to lower flux) and pore former (resulting in higher flux),

depending on the SPPO polymer concentration (Agarwal, 1991).

It was revealed by the foregoing literature survey that little work was done to study the effect of variables involved in the formation of composite membranes on their performance. It was also found that the effect of solute-membrane interaction on the solute rejection and the permeation rate was not studied well enough with respect to the composite membranes with ionic charges.

The present research deals with preparing charged composite membranes by coating polyethersulfone substrate membranes with dilute solution of hydrogen-form sulfonated polyphenylene oxide (SPPOH). Methanol and methanol/chloroform mixtures are used as the solvents for making the coating solutions, thus SPPOH polymers having a wide range of ion exchange capacity are studied. The reverse osmosis performance of the composite membranes is investigated by using solutes of various valences and ionic radii, as well as various feed concentrations. The effect of the solvent, used in making the coating solution, is also studied through intrinsic viscosity measurements, reverse osmosis performance and by employing SEM and AFM microscopic methods. An attempt to indicate the role of the porosity and structure of the polyethersulfone substrate membrane is also made.

CHAPTER THREE

EXPERIMENTAL METHODS

This research involves preparing, testing and characterizing composite membranes using sulfonated poly(2,6-dimethyl-1,4-phenylene oxide) as the skin layer polymer and polyethersulfone ultrafiltration membranes as the substrate. The following sections describe the experimental methods employed.

3.1 Membrane Preparation

3.1.1 Materials

The flat sheet membranes used as the substrate for the composite membrane were ultrafiltration membranes HW17 and HW18 obtained from Osmonics Inc.. They were made, from polyethersulfone on polyester fibres as backing material, employing the phase inversion technique (Rudie, 1994). The molecular mass cut-off curves of these two membranes are shown in Figure 3.1 and Figure 3.2 respectively.

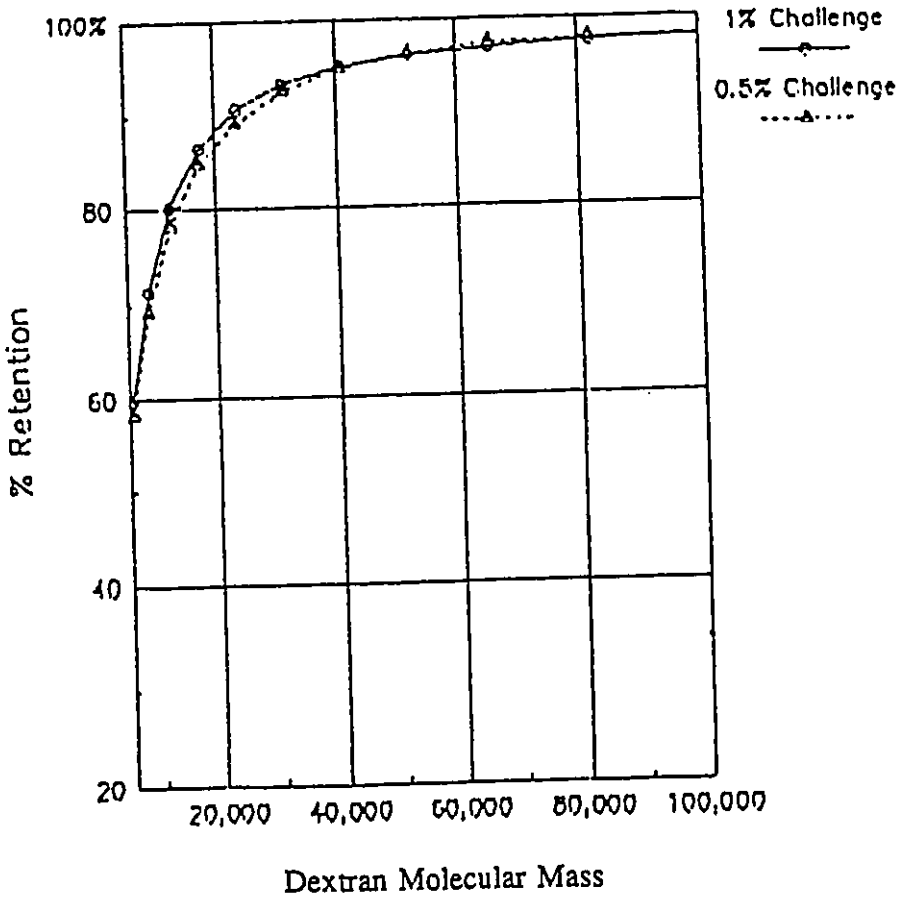

Figure 3.1 Molecular Mass cut-off curves of HW17 polyethersulfone ultrafiltration membrane using Dextran as the macromolecule (Rudie, 1994).

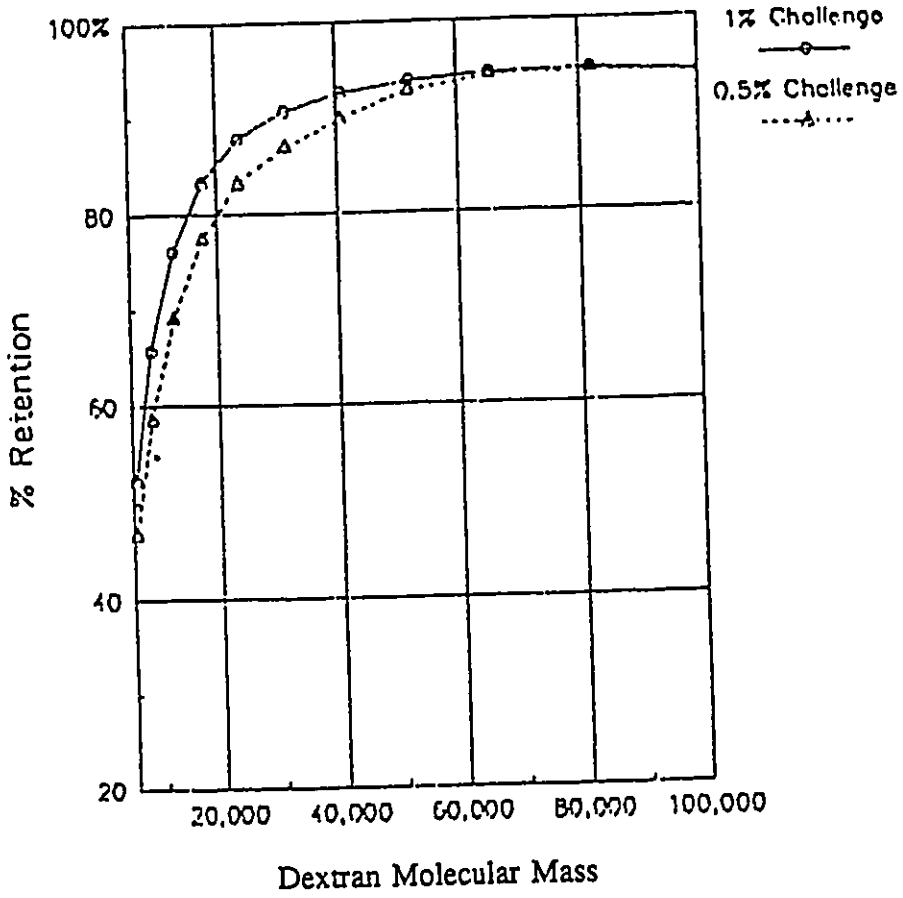

Figure 3.2 Molecular Mass cut-off curves of HW18 polyethersulfone ultrafiltration membrane using Dextran as the macromolecule (Rudie, 1994).

Scanning Electron Microscope micrographs of the substrate membrane cross-sections are shown in Figure 3.3, while Atomic Force Microscope micrographs are presented in Figure 3.4 and Figure 3.5, for HW17 and HW18, respectively. Polyphenylene oxide (poly(2,6-dimethyl-1,4-phenylene oxide) polymer, having an intrinsic viscosity in chloroform of 0.51 at 25 °C, was provided by General Electric Corporation. Chlorosulfonic acid ($Cl\text{-}SO_3H$) (General Reaction Grade), having a density 1.75 g/cm^3 at 20 °C and a minimum assay of 97%, was obtained from BDH Corporation. The organic solvents used were chloroform and methanol. Methyl alcohol (CH_3OH) BDH Assured had a density of 0.79 g/cm^3 and a minimum assay of 99.8%. Chloroform (CH_3Cl) OmniSolv, stabilized with a nonpolar hydrocarbon, had a density of 1.49 g/cm^3 and a minimum assay of 99.9%. Both chloroform and methanol were obtained from BDH Corporation.

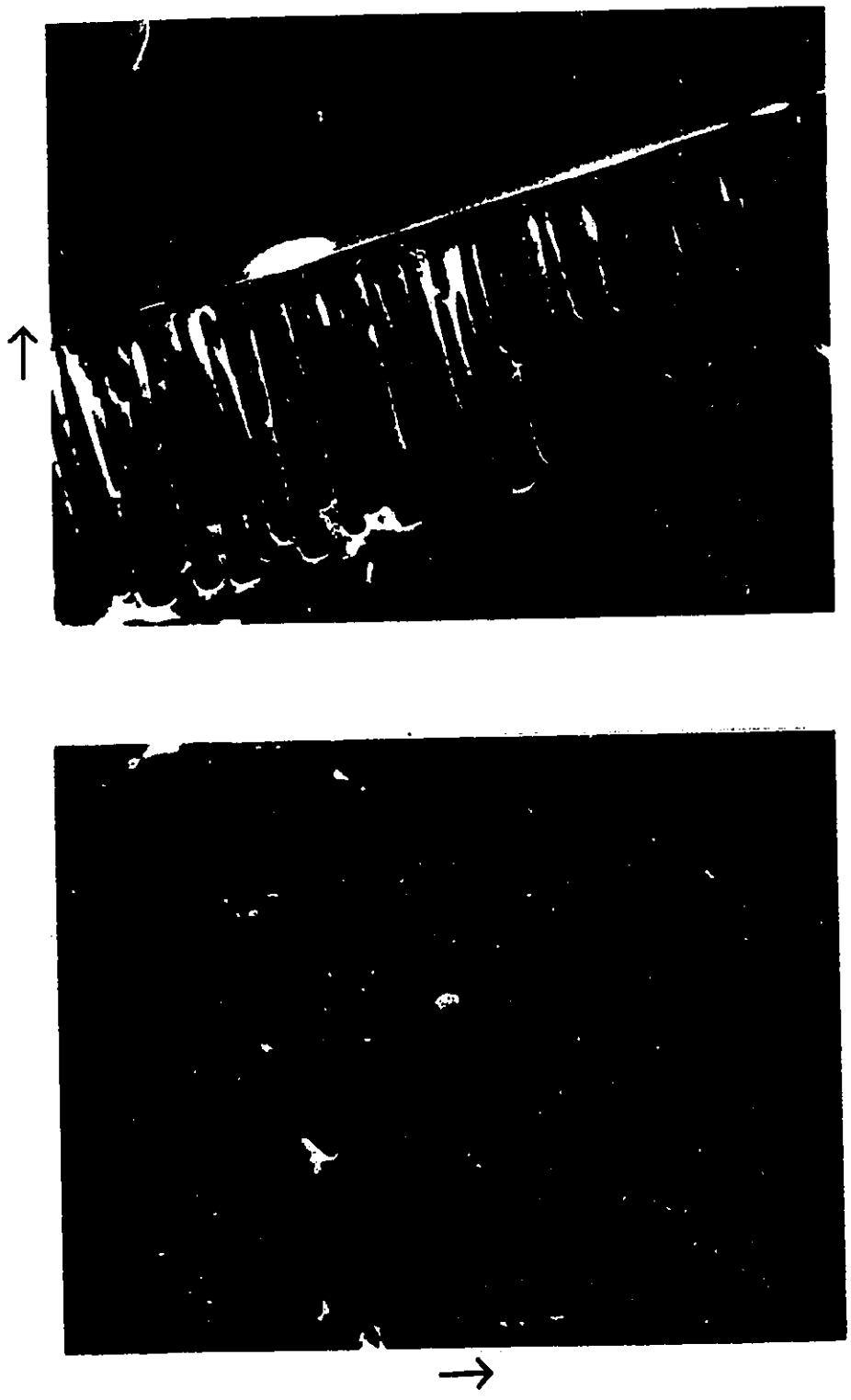

Figure 3.3 SEM micrographs of the cross-sections of polyethersulfone ultrafiltration membranes: (Top) HW17, (Bottom) HW18.

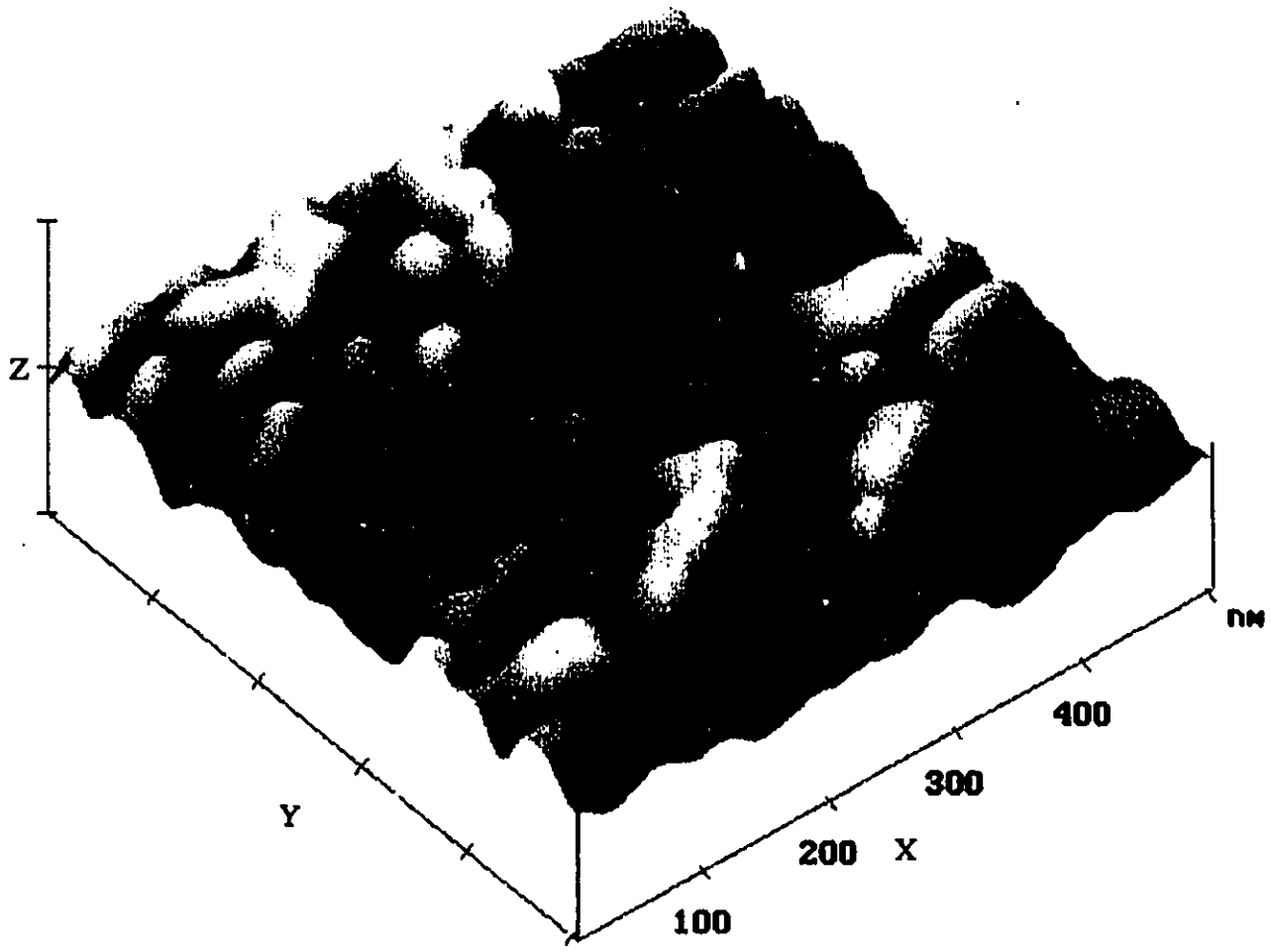

X and Y 100.000 nm / division

Z 15.000 nm / division

Figure 3.4 AFM micrograph of the skin layer of polyethersulfone ultrafiltration membrane HW17.

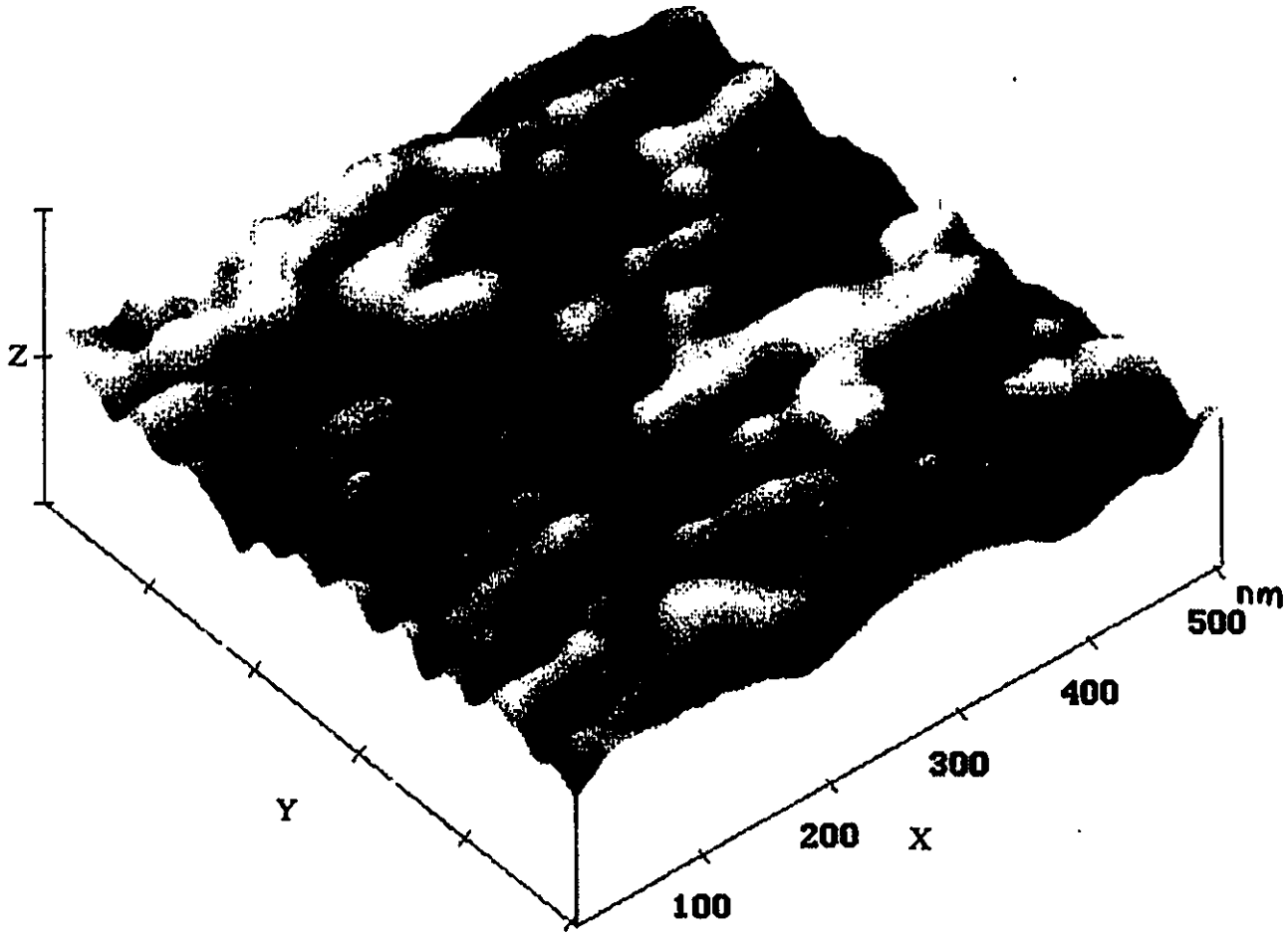

X and Y 100.000 nm / division

Z 15.000 nm / division

Figure 3.5 AFM micrograph of the skin layer of polyethersulfone ultrafiltration membrane HW18.

3.1.2 Preparation of Sulfonated Polyphenylene Oxide

Poly(2,6-dimethyl-1,4-phenylene oxide) (PPO) was sulfonated to various degrees using chlorosulfonic acid. The chemical structures of poly(2,6-dimethyl-1,4-phenylene oxide) and sulfonated poly(2,6-dimethyl-1,4-phenylene oxide) polymers are shown in Figure 3.6. PPO polymer was used without any further treatment. A 10 mass% PPO solution was prepared by dissolving PPO polymer in chloroform. Then, a stoichiometric quantity of chlorosulfonic acid was added dropwise to the above PPO solution, with vigorous stirring, according to the method reported originally by Plummer et al. (1970). The sulfonation of polyphenylene oxide was carried out according to the following chemical reaction:

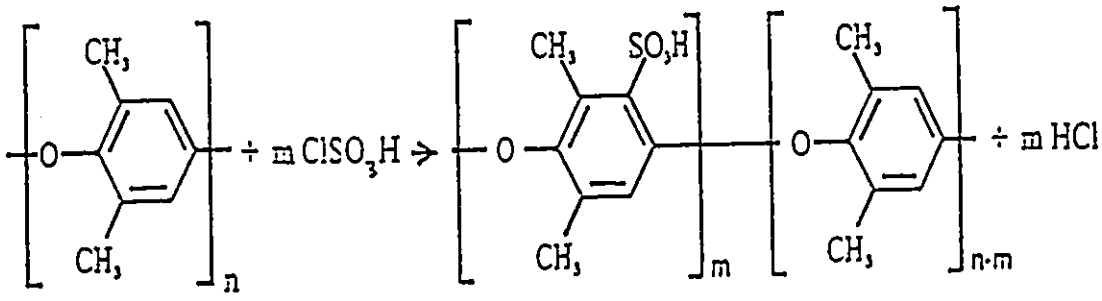

As sulfonation progressed, sulfonated polyphenylene oxide in the hydrogen-form (SPPOH) precipitated from the solution, since SPPOH is not soluble in chloroform. The precipitate was dissolved in methanol or a chloroform/methanol mixture and cast into a film 3-6 mm thick. The SPPOH film was then dried and cut into small pieces, which were further washed thoroughly with distilled water until the wash water showed a pH value higher than four. The precipitate was further dried for two days under vacuum at room temperature.

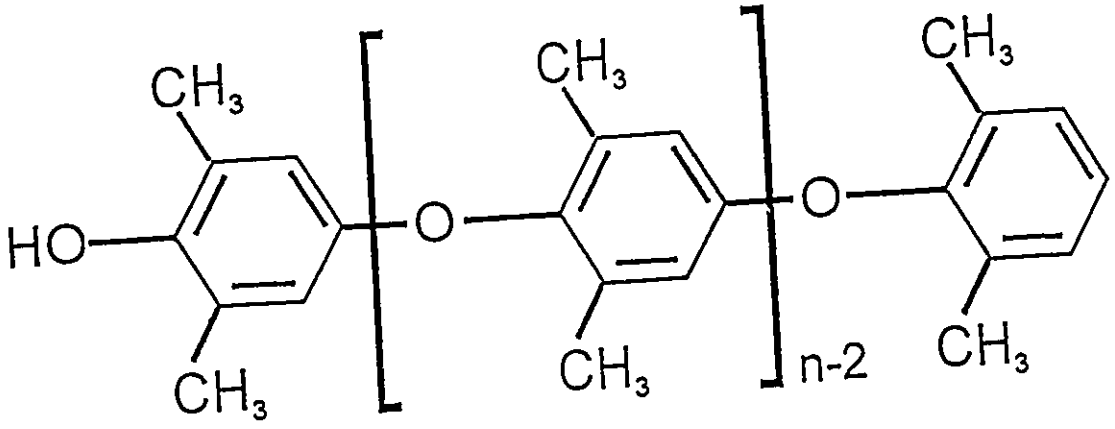

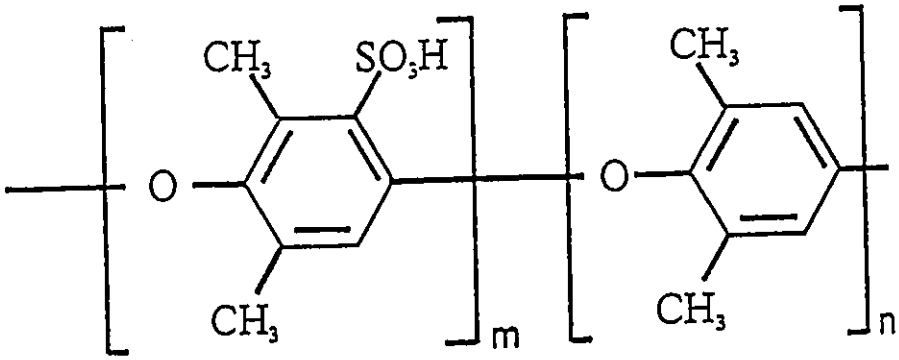

Figure 3.6 The chemical structure of : (Top) Poly(2,6-dimethyl-1,4-phenylene oxide) polymer, (Bottom) Sulfonated poly(2,6-dimethyl-1,4-phenylene oxide) polymer.

3.1.3 Determination of Ion Exchange Capacity of SPPOH

The ion exchange capacity (I.E.C.) of SPPOH polymer was measured by using the acid-base titration method. A weighed amount, 0.5 to 1 gram, of the vacuum dried SPPOH polymer was put in excess measured amount of 0.1 N NaOH solution for at least one day. The SPPOH exchanges the H^+ of the sulfonate group with Na^+ from the solution. The liberated H^+, consequently, consumes a stoichiometric quantity of OH^- ions. Titrating the excess NaOH with 0.1 N HCl then gives the meq of OH^- consumed per unit weight of dry polymer. This is the ion exchange capacity of the polymer. For each batch of SPPOH, three samples were used to eventually obtain an average I.E.C. of each batch of SPPOH. The I.E.C. values obtained range from 1.29 to 2.6 meq/gram dry polymer.

3.1.4 Preparation of Composite Membranes

The skin side of the substrate polyethersulfone ultrafiltration membrane was contacted with a 1.0 mass% SPPOH solution. The solvent used to prepare the SPPOH solution depended on the I.E.C. value of the SPPOH polymer, as indicated in the following:

For I.E.C. value of 1.29 meq/g, chloroform/methanol mixture (chloroform 47 mass%),
for I.E.C. value of 1.41 meq/g, chloroform/methanol mixture (chloroform 61 or 15 mass%),
for I.E.C. value of 1.93 meq/g, chloroform/methanol mixture (chloroform 66, 42, or 18 mass%) or methanol,

for I.E.C. value of 1.98 meq/g, chloroform/methanol mixture (chloroform 46 mass%) or methanol, and

for I.E.C. value of 2.21 and 2.60 meq/g, methanol.

The solution at the membrane surface was drained by holding the membrane vertically, leaving a thin layer of the SPPOH solution. The coated layer was then dried for half an hour at room temperature. This coating procedure was repeated three times and was followed by drying overnight under ambient conditions. The membranes so prepared were in hydrogen-form (SPPOH) and were stored in distilled water. The substrate, for all the composite membranes prepared in this work, was HW17 polyethersulfone ultrafiltration membranes except in the case of SPPOH having an I.E.C. value of 2.21 meq/g for which both HW17 and HW18 polyethersulfone ultrafiltration membranes were used.

3.2 Membrane Testing Procedure

3.2.1 Reverse Osmosis Apparatus

The reverse osmosis permeation cell, shown in Figure 3.7, was used in testing the performance of the thin film composite SPPOH-PES membranes. The cell was made of stainless steel 310 and consists of two detachable parts. The upper part was a high pressure chamber provided with inlet and outlet openings for the flow of the feed under pressure. The lower part was the membrane stand provided with an outlet opening for the collection and withdrawal of the permeating product. The membrane was supported by a stainless steel porous plate embedded in the lower part of the cell such that its active surface coated layer faced the feed solution under pressure. The two detachable parts of the testing cell were set in proper alignment with rubber O-ring contacts between the high pressure chamber and the membrane. The effective area of the membrane was 10.2 cm^2.

Six such cells were connected in series and thus six membranes could be tested simultaneously. The same feed concentration was assumed to enter each of the cells since the product permeating the membranes was significantly less than the feed circulation rate. A schematic flow diagram of the testing apparatus is illustrated in Figure 3.8, though only one cell is shown. All membranes were pressurized with pure water flow at 1723 kPa gauge (250 psig) until permeation rate became constant before any solute separation testing took place. A B.I.F. Model 1732 Propsuperb metering pump circulated the pressurized feed at a rate of 0.6 L/min.

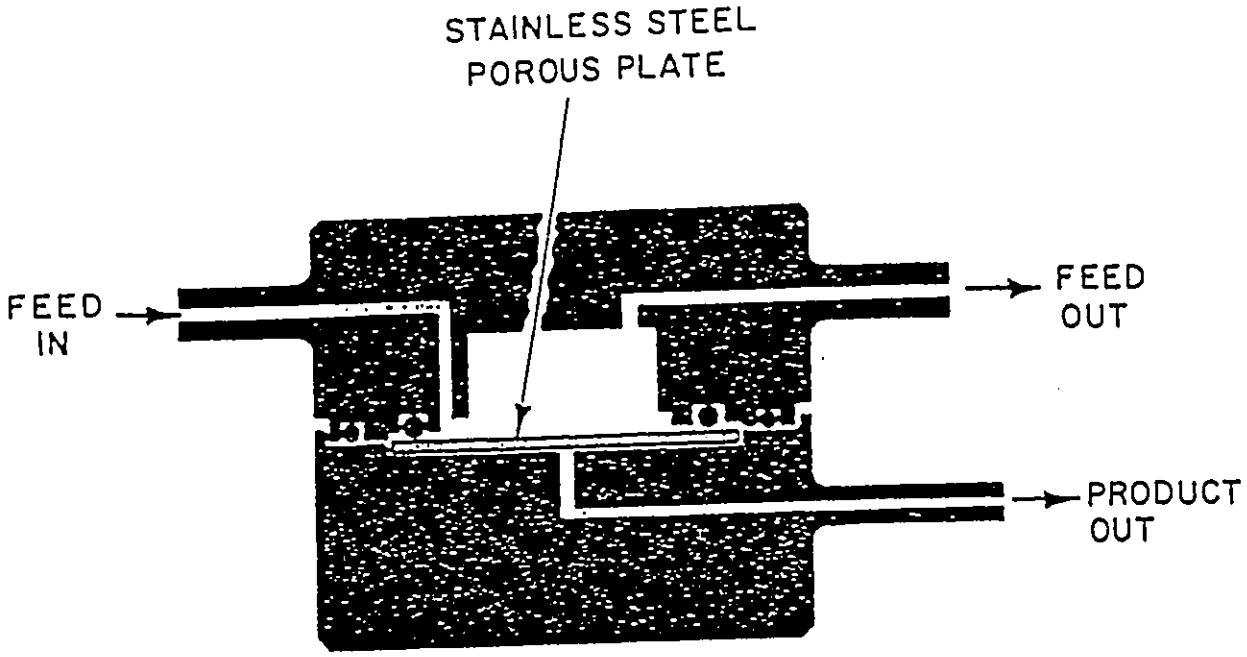

Figure 3.7 Schematic representation of the reverse osmosis test cell.

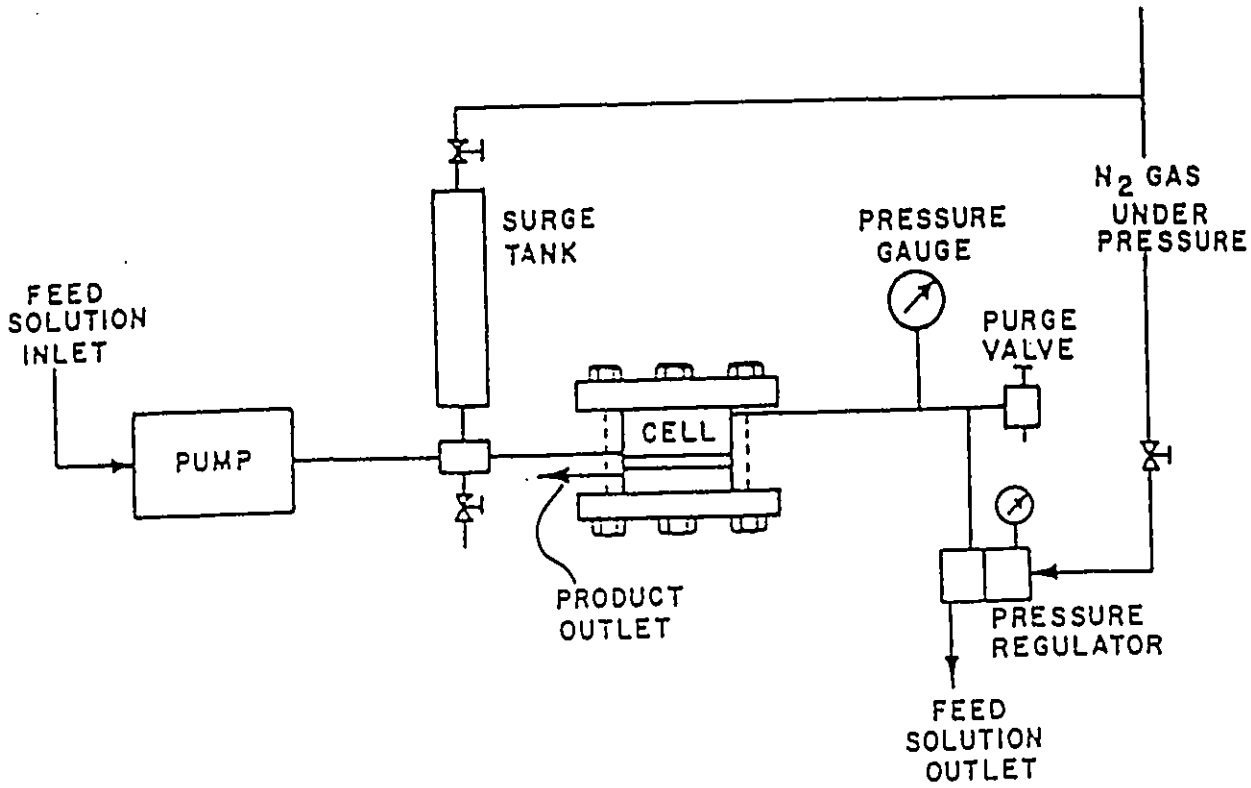

Figure 3.8 Schematic representation of the reverse osmosis test system.

3.2.2 Membrane Performance Measurement

The performance of the composite membranes was evaluated in terms of permeation rate across the membrane as well as membrane solute separation. The experiments were conducted at the operating pressure of 1379 kPa gauge (200 psig) and at room temperature. The solution concentration was 0.05 moles/L for all electrolyte solutes, and 200 ppm for nonelectrolyte organic solutes. For each experiment pure water permeation rate (PWP), the product permeation rate (PR) in the presence of the solute, both in ($m^3/m^2.s$), and the solute separation defined as

$$Separation = \left[\frac{Feed\ concentration - Permeate\ concentration}{Feed\ concentration}\right]$$

were determined. The permeation rate was converted to that at 25 °C by using the density and viscosity data of water. The following electrolytes, all of which were obtained from BDH Corporation, were used: LiCl, NaCl, KCl, NH_4Cl, $NaHCO_3$, Na_2CO_3, Na_2SO_4, K_2SO_4, $MgSO_4$, $MgCl_2$, $CaCl_2$, $AlCl_3$, $FeCl_3$ and $Al_2(SO_4)_3$. Polyethylene glycols, namely, PEG 1500, PEG 9000 and PEG 15000 were used as the nonelectrolyte macromolecules. The concentrations of the electrolyte solutes were determined using a Radiometer Copenhagen CDM 80 conductivity meter, whereas that of the macromolecules were measured using a DOHRMANN DC-190 TOC Analyzer obtained from Rosemount Inc.

3.3 Intrinsic Viscosity Measurement

The intrinsic viscosities of sulfonated polyphenylene oxide, having an I.E.C. value of 1.93 meq/gram dry polymer in different chloroform/methanol mixtures, were measured at 25 °C. A Cannon-Fenske Routine Viscometer of size 50 and a constant of 0.003635 centistokes/second, from International Research Glassware, was used for this purpose. The flow times (t) of 1.0, 0.5, and 0.25 mass% polymer in each solvent were measured as well as the flow time of the pure solvents (t_o). The solvents were methanol and chloroform/methanol mixtures of 18, 42, and 66 mass% chloroform content. A plot of $(t-t_o)/(t_o.C)$ versus C was then made, where C is the concentration of the polymer in the solvent in gram/100cm^3. The intrinsic viscosity of SPPOH of I.E.C. 1.93 meq/gram in each of these solvents was then obtained by linear extrapolation of $(t-t_o)/(t_o.C)$ to zero concentration.

3.4 Microscopic Structure of The Membranes

Micrographs of the cross-sections of composite membranes, coated using SPPOH having the I.E.C. value of 1.93 meq/g dissolved in different methanol/chloroform mixtures as well as of the uncoated substrates HW17 and HW18, were obtained using a Scanning Electron Microscope (SEM). An Atomic Force Microscope was used to obtain three-dimensional topographical micrographs of the skin layers of these membranes.

The Scanning Electron Microscope micrographs of these membranes were obtained using a Nanolab 7 SEM operating at 20 keV. The samples were prepared by immersing in liquid Nitrogen, then fracturing them. The fractured surfaces were then mounted for viewing the cross-sections (McCaffrey, 1994).

The three-dimensional surface topographical micrographs of the membranes were obtained using a Tapping-Mode AFM of a Digital Instruments's Multimode Scanning Probe Microscope (MMSPM). The membranes were readily used for the AFM without any preparatory treatment. A piezoelectric scanner performs a high resolution raster scan in the X-Y plane parallel to the surface of the membranes, while a sensing and feedback system operates in the Z direction reporting and controlling the variation in height across the skin layer. Calibration of the microscope, using standard samples, resulted in less than 2% deviation in the X-Y plane and less than 10% deviation in the Z direction. The AFM was equipped with NanoScope III system. Section Analysis, provided through the NanoScope III, were used to estimate the size of at least 15 SPPOH nodules in the skin layer of each of the composite membranes (Appendix D).

CHAPTER FOUR

RESULTS AND DISCUSSION

The results of the experiments are presented in this chapter, along with appropriate discussions.

4.1 Sulfonation of Poly(2,6-dimethyl-1,4-phenylene oxide)

Batches, each weighing 10 to 15 grams, of poly(2,6-dimethyl-1,4-phenylene oxide) were sulfonated to different ion exchange capacities using chlorosulfonic acid according to the chemical reaction given in section 3.1.2. The ion exchange capacity used in making the composite membranes ranged from 1.29 to 2.6 meq/gram dry polymer. I.E.C. values higher than 2.6 meq/g were not sought since the polymer was expected to swell excessively in water (Plummer et al., 1970). Lower ion exchange capacity SPPOH were not used because they required high chloroform content in chloroform/methanol mixtures for complete solvation. For example SPPOH of I.E.C. value of 1.19 meq/g required a

minimum of 66 mass% chloroform to dissolve and up to 92 mass% chloroform could be used. Such a high chloroform content appeared damaging to the polyethersulfone substrate as shall be shown in section 4.3. As the I.E.C. value of SPPOH increased, the amount of chloroform required to dissolve it decreased, though up to about 90 mass% chloroform could still dissolve even SPPOH having a high I.E.C. value of 2.21 meq/g. The I.E.C. values of SPPOH used in this work are shown in Table 4.1 along with the possible solvent(s). These I.E.C. values are averages of three determinations for each batch of SPPOH, and are shown in the Table 4.1 along with an estimated standard deviation in each case.

TABLE 4.1

Ion Exchange Capacity of SPPOH and Appropriate Solvents

Ion Exchange Capacity (meq/gram)		Soluble in MeOH	Soluble in MeOH/$CHCl_3$
1.29	± .037		X
1.41	± .045		X
1.93	± .024	X	X
1.98	± .086	X	X
2.21	± .070	X	X
2.60	± .115	X	X

4.2 Effect of I.E.C. value of SPPOH on Membrane Performance

Figure 4.1 and Figure 4.2 illustrate the change in the product rate and separation of sodium chloride with a change in the ion exchange capacity of the SPPOH-PES composite membrane, respectively. For each I.E.C. value, three membranes were prepared and tested except for I.E.C. value of 2.60 meq/g for which six membranes were used. The data points shown in the figures are the average values, with the bars indicating an estimated standard deviation for each I.E.C.. Regarding I.E.C. values of 1.29 and 1.41 meq/g, data correspond to membranes prepared with solvent mixtures containing 47 and 15 mass% chloroform, respectively. The membranes with I.E.C. value of 1.98 and 2.60 meq/g were prepared by using only methanol. Figure 4.2 indicates a continuous decrease in solute separation from I.E.C. value of 1.29 to 2.60 meq/g, although all separation data were found in a narrow range, namely 0.50 to 0.77. Correspondingly, the product rate data showed a steady increase with the I.E.C. of the membrane. The significant four fold change in the permeation rate when the I.E.C. value increased from 1.29 meq/g (product rate 4.28 $x10^{-6}$ $m^3/m^2.s$) to 2.60 meq/g (product rate 20.70 $x10^{-6}$ $m^3/m^2.s$) is attributable to increased hydrophilicity of the skin layer as the degree of sulfonation increased. The sulfonate group is known for its strong affinity for water, causing the swelling of the skin layer and hence increased permeation of water through the membrane. The separation is lowered, with increase of I.E.C. of the membrane, as a result of weaker Donnan potential due to lower sulfonate concentration in the gel water, which is the water bound to the swelled surface. These results indicate the possibility to prepare a membrane of higher productivity without much sacrifice in the separation by properly adjusting the ion exchange capacity of the skin layer.

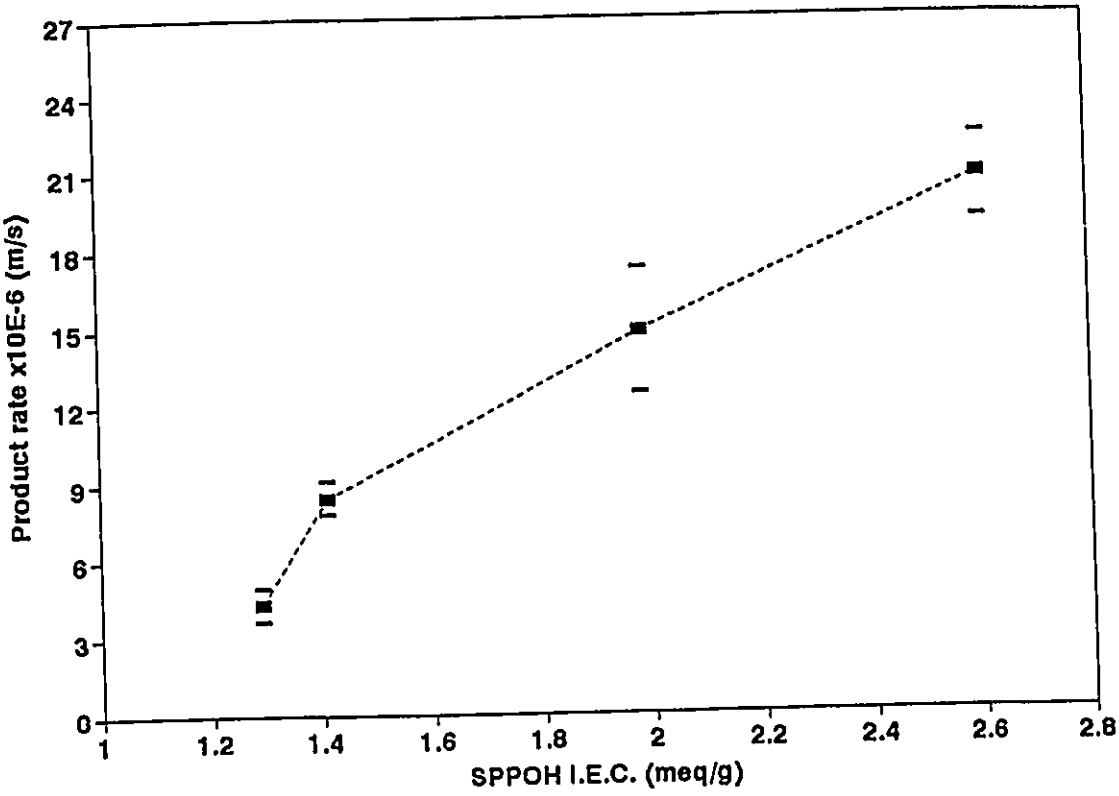

Figure 4.1 Effect of the I.E.C. value of SPPOH-PES membrane on the permeation rate of sodium chloride solution. Operating conditions: Pressure 1379 kPa gauge (200 psig), Temperature 25 °C.

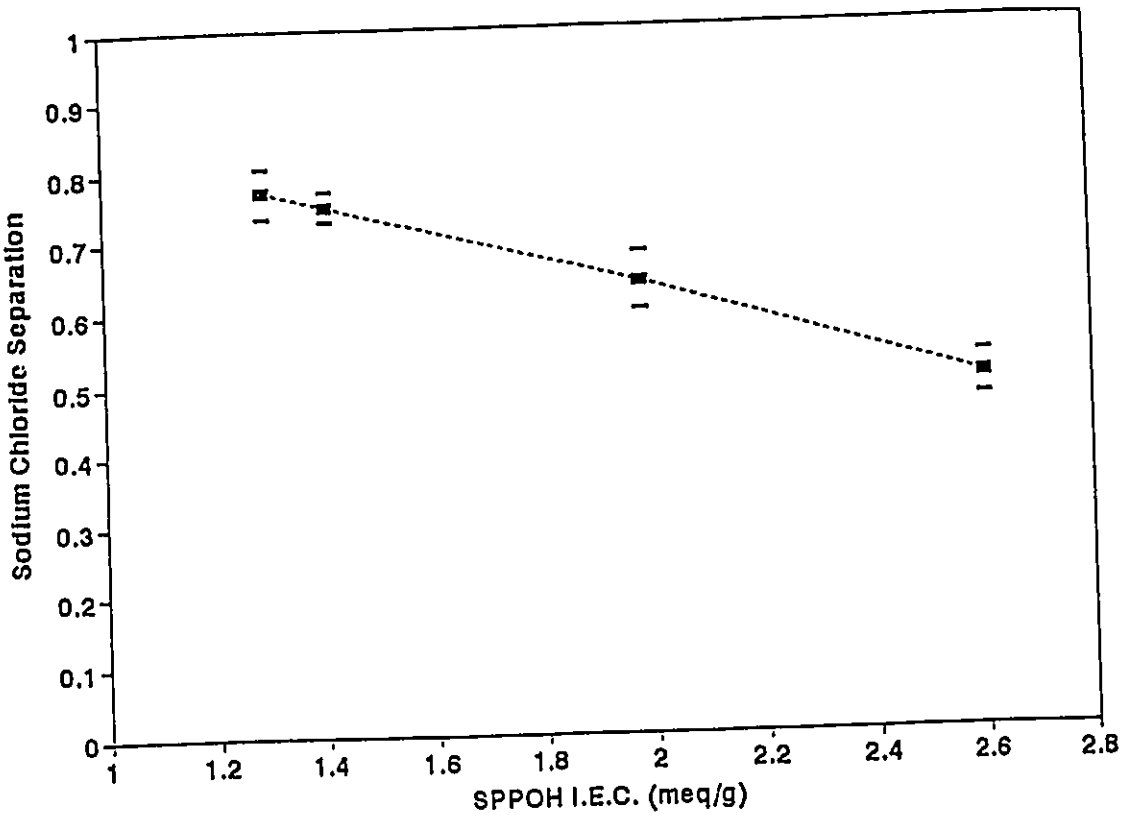

Figure 4.2 Effect of the I.E.C. value of SPPOH-PES membrane on the separation of sodium chloride. Operating conditions: Pressure 1379 kPa gauge (200 psig), Temperature 25 °C.

4.3 Effect of Solvent used in the Preparation of Casting Solutions.

As explained in the experimental section, the SPPOH of different I.E.C. values were dissolved in different solvents to prepare polymer solutions for coating. SPPOH with I.E.C. values of 1.29 and 1.41 meq/g are more hydrophobic and were dissolved in chloroform/methanol mixtures, whereas SPPOH with I.E.C. values of 1.98 and 2.60 are more hydrophillic and could be dissolved in methanol. Then, it is not entirely clear if we have observed in the above experiment the effect of the I.E.C. value alone or the effect of both the I.E.C. and the solvent, as far as the whole I.E.C range studied is concerned. In order to investigate the effect of the solvent, two membranes were prepared from the SPPOH polymer having an I.E.C. value of 1.41 meq/g using chloroform/methanol mixtures of 15 mass% chloroform and 61 mass% chloroform, and reverse osmosis performance of each membrane was examined. The solute separation and the permeation rate with respect to three alkali metal halide salts are summarized in Figure 4.3 and Figure 4.4, respectively. These figures indicate a slight decrease in the solute separation and an approximate 55% drop in the product rate with a change in chloroform content from 15 to 61 mass%. Similarly, SPPOH polymer with an I.E.C. value of 1.98 was dissolved in two different solvents; one methanol and the other chloroform/methanol mixture with 46 mass% chloroform, and reverse osmosis composite membranes were prepared. The performance of these reverse osmosis membranes are summarized in Figure 4.5 and Figure 4.6. These figures indicate a slight increase in the solute separation and an approximatet 50% drop in the product rate with a change in solvent from methanol to a chloroform/methanol mixture.

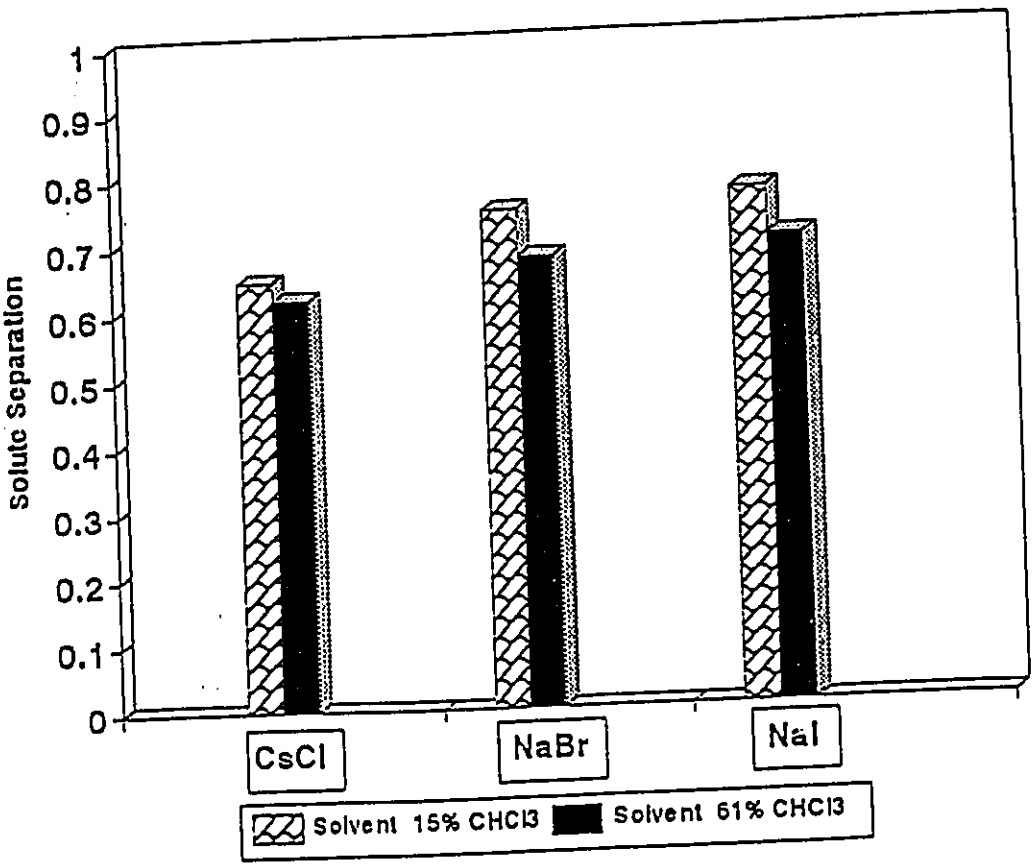

Figure 4.3 Effect of solvent in coating solutions on the separation of different electrolytes using SPPOH-PES membrane with an I.E.C. value of 1.41 meq/g. Operating conditions: Pressure 1379 kPa gauge (200 psig), Temperature 25 °C.

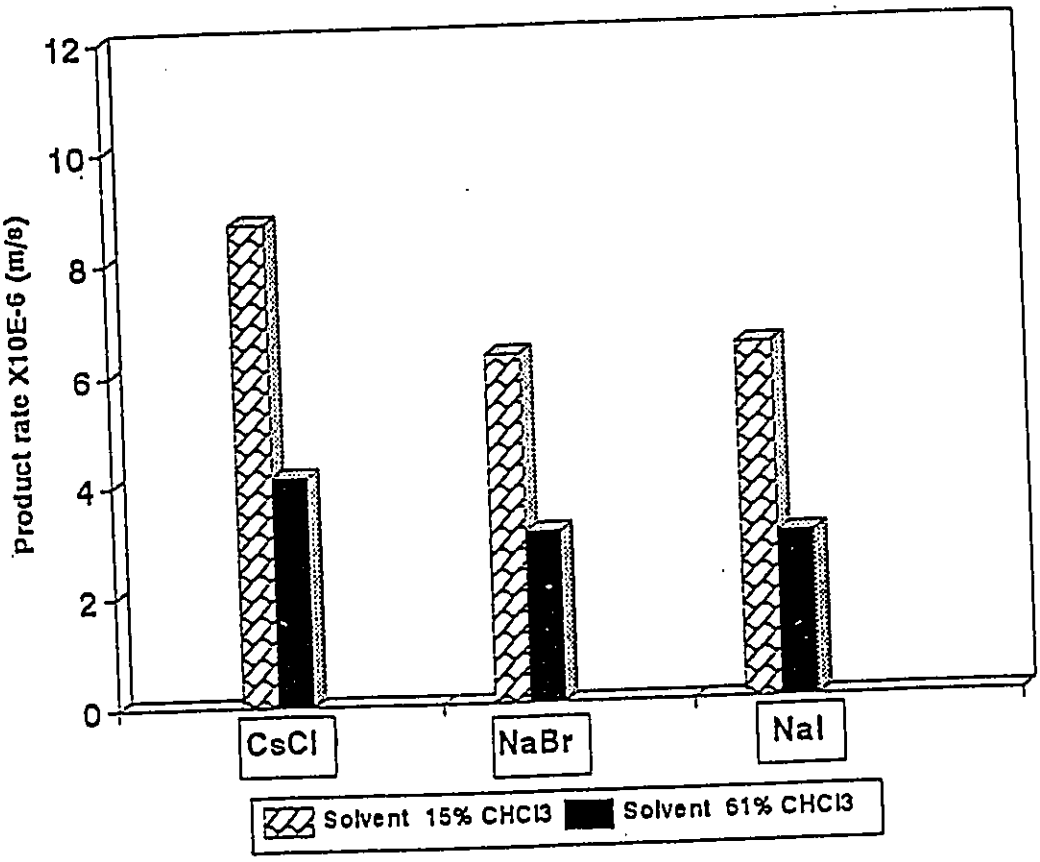

Figure 4.4 Effect of solvent in coating solutions on the permeation rate of different electrolyte solutions using SPPOH-PES membrane with an I.E.C. value of 1.41 meq/g. Operating conditions : pressure 1379 kPa gauge (200 psig), Temperature 25 °C.

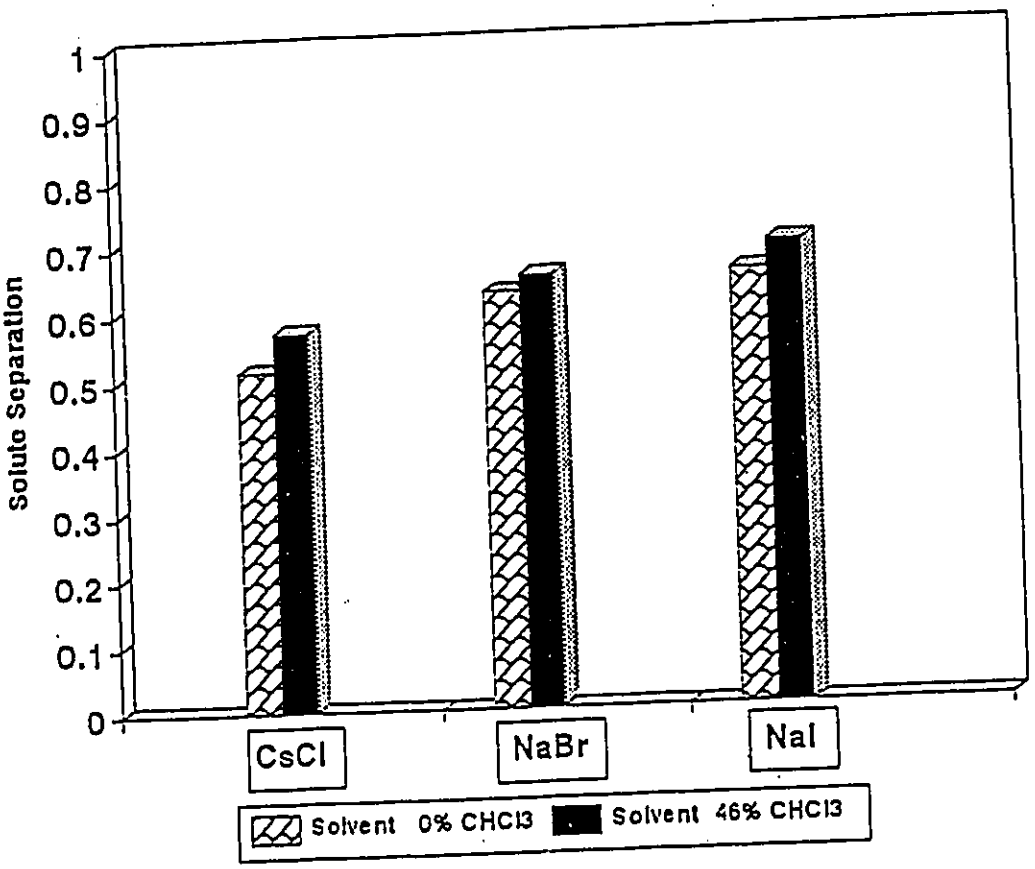

Figure 4.5 Effect of solvent in coating solutions on the separation of different electrolytes using SPPOH-PES membrane with an I.E.C. value of 1.98 meq/g. Operating conditions: Pressure 1379 kPa gauge (200 psig), Temperature 25 °C.

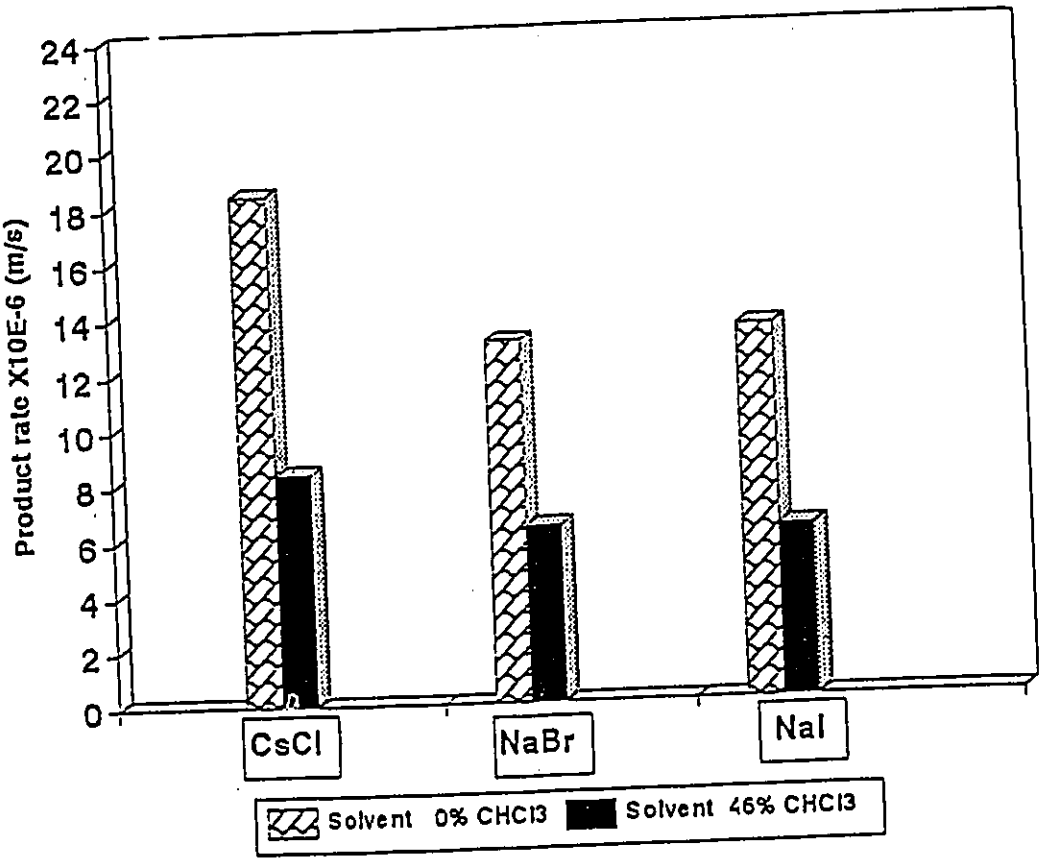

Figure 4.6 Effect of solvent in coating solutions on the permeation rate of different electrolyte solutions using SPPOH-PES membrane with an I.E.C. value of 1.98 meq/g. Operating conditions : pressure 1379 kPa gauge (200 psig), Temperature 25 °C.

Since the same polymer was used for the preparation of the coating layer, these marked results clearly indicate the effect of the morphological change of the coated polymer layer when different solvents were used to prepare the coating solutions.

Further experiments were done to study the effect of an incremental change in the composition of the solvent on the reverse osmosis performance as well as on the microscopic structure of the SPPOH-PES composite membrane. SPPOH having an I.E.C. value of 1.93 meq/g was dissolved in chloroform/methanol mixtures having 18, 42, and 66 mass% chloroform, as well as in methanol, and composite membranes were prepared. After Compaction for a day at 1724 kPa gauge (250 psig) under water, membranes were tested in separation of different alkali metal halides.

SEM micrographs of the cross-sections of the composite membranes are shown in Figure 4.7 and Figure 4.8. These micrographs indicate "similarity" between the structures of the membranes and show no adverse effect of the solvent composition on the substrate, at least in the micron range used. The coated layer of the composite membranes seems to be too thin to be visible on this scale. This can be deduced by comparing the SEM micrographs of the composite membranes with the SEM micrograph of the uncoated substrate which was shown in Figure 3.3.

The results for salt separation are shown in Figure 4.9, whereas those for product rate are displayed in Figure 4.10. It can be seen again that separation increases slightly with an increase in chloroform content with the exception of the membrane made from 66 mass% chloroform in the coating solvent. Product rate, on the other hand, shows a significant steady drop with the increase of chloroform in the solvent used for coating

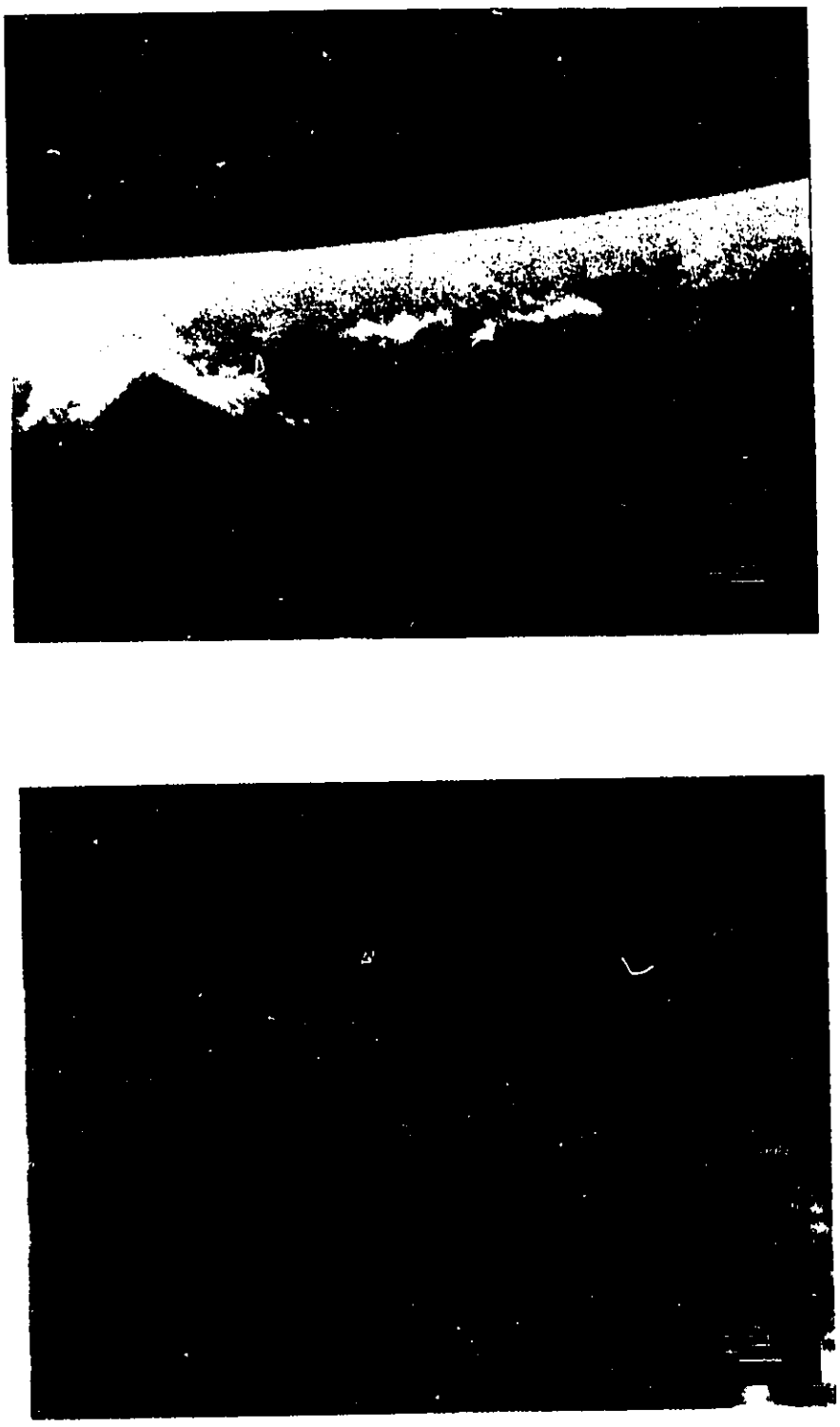

Figure 4.7 SEM micrographs of cross sections of SPPOH-PES composite membranes of I.E.C. 1.93 meq/g made using different solvents for coating solution: (Top) Methanol, (Bottom) 18 mass% Chloroform and 82 mass% Methanol.

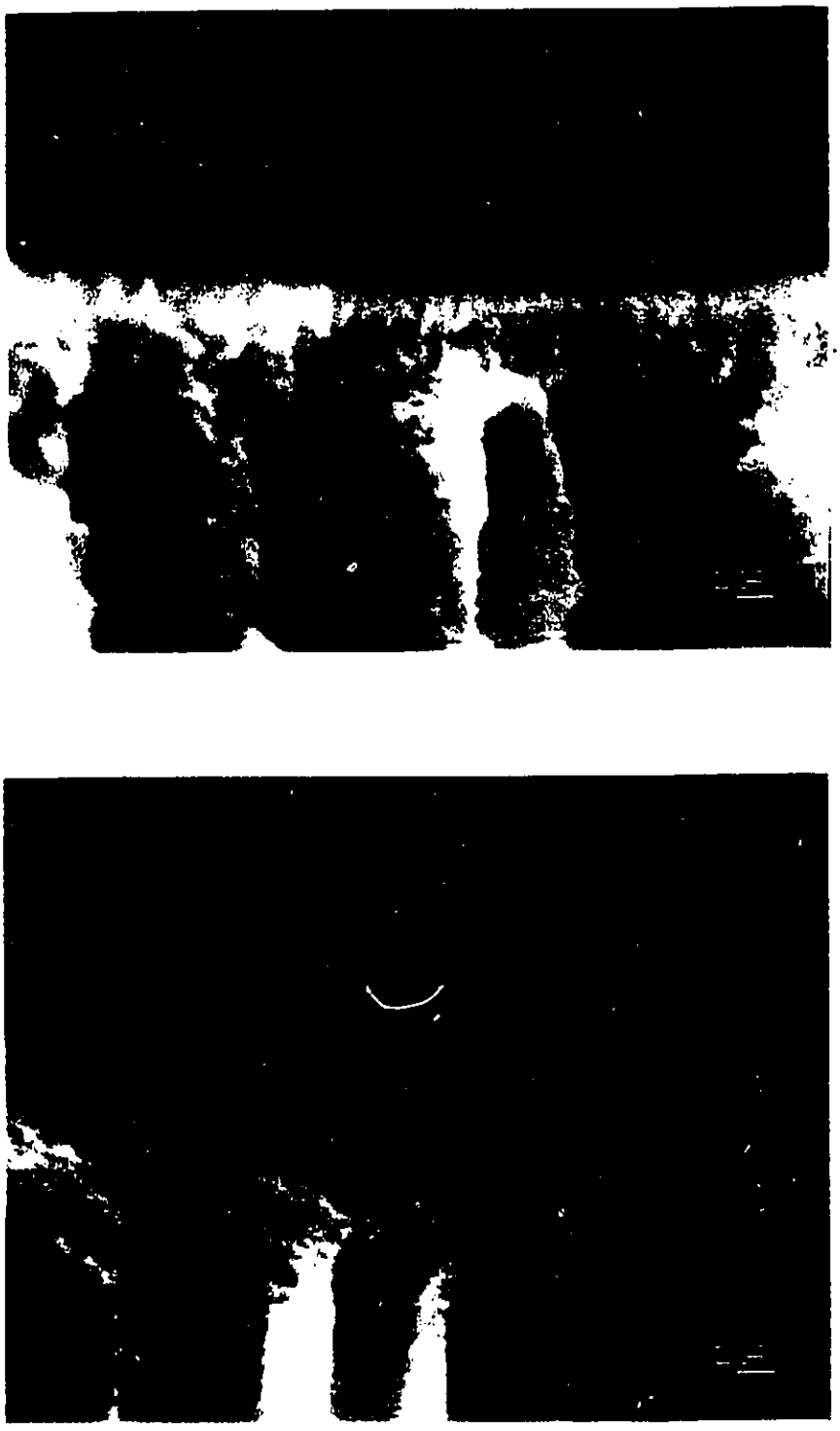

Figure 4.8 SEM micrographs of cross sections of SPPOH-PES composite membranes of I.E.C. 1.93 meq/g made using different solvents for coating solution: (Top) 42 mass% Chloroform, 58 mass% MeOH, (Bottom) 66 mass% Chloroform and 34 mass% MeOH.

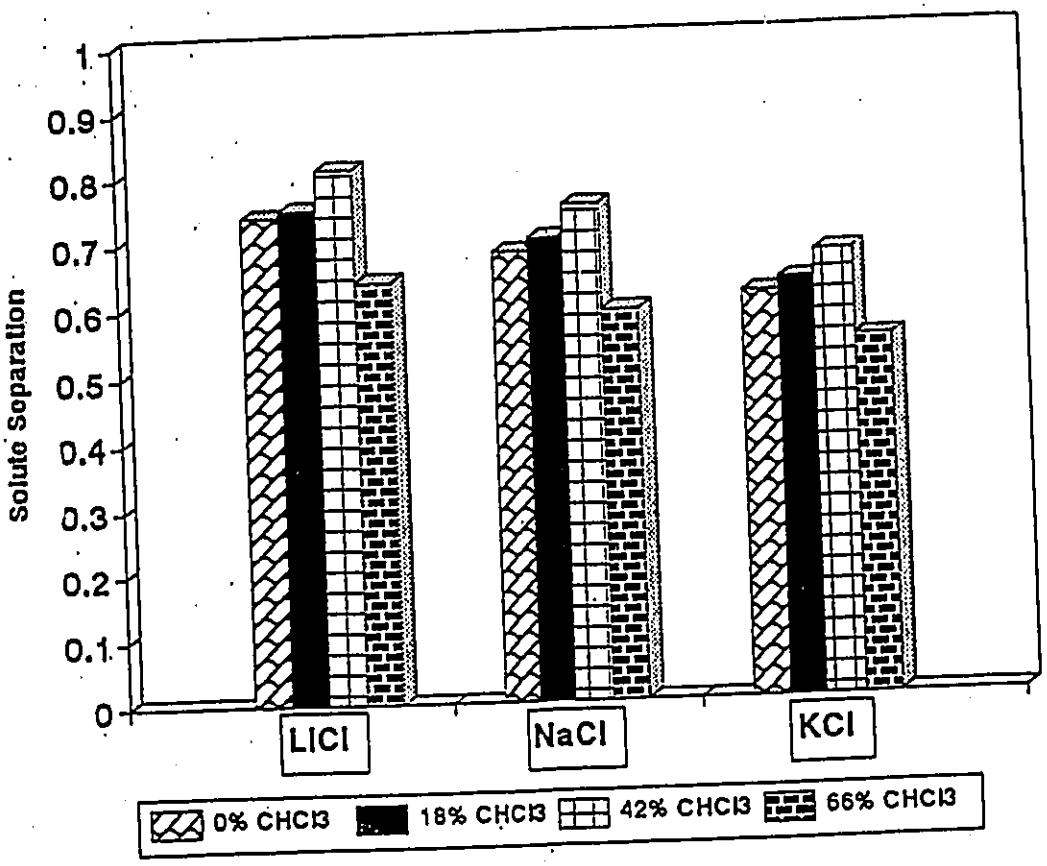

Figure 4.9 Effect of solvent in coating solutions on the separation of different electrolytes using SPPOH-PES membrane with an I.E.C. value of 1.93 meq/g. Operating conditions: Pressure, 1379 kPa gauge (200 psig), Temperature 25 °C.

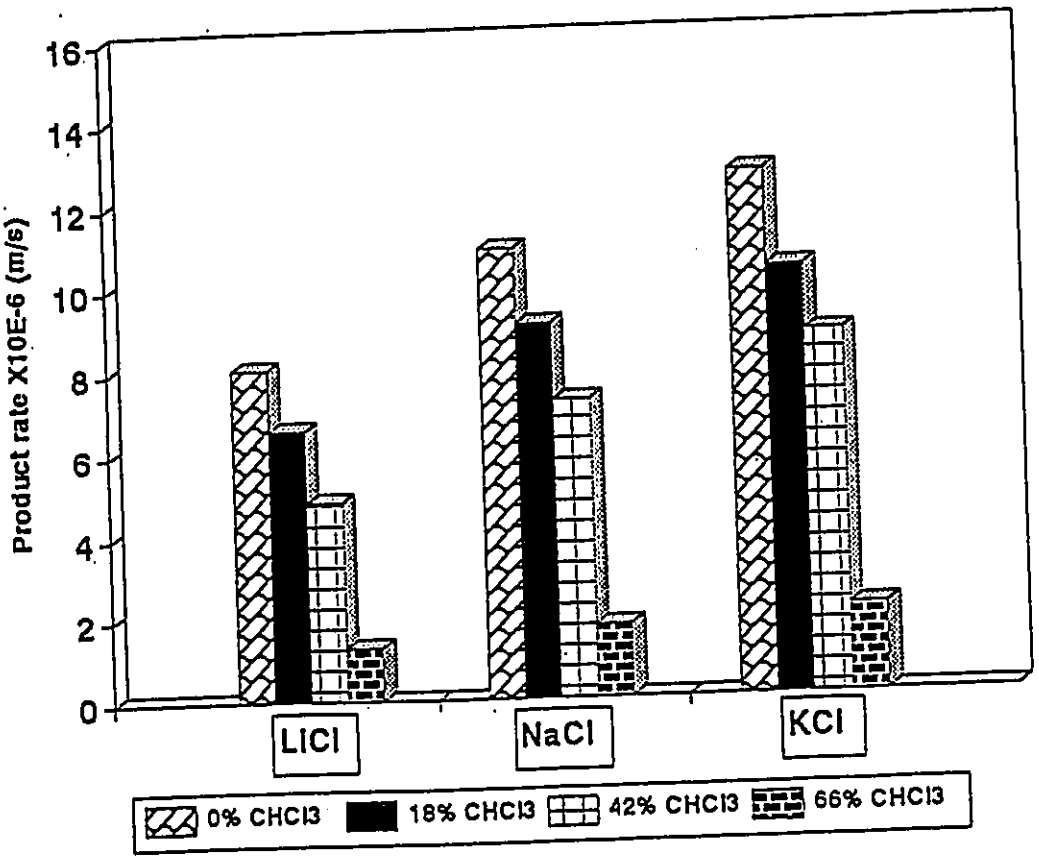

Figure 4.10 Effect of solvent in coating solutions on the permeation rate of different electrolyte solutions using SPPOH-PES membrane with an I.E.C. value of 1.93 meq/g. Operating conditions : Pressure, 1379 kPa gauge (200 psig), Temperature 25 °C.

Four substrate ultrafiltration membranes which were the same as the one used for the preparation of the composite membranes, were contacted with methanol and chloroform/methanol mixtures of 18, 42, 66 mass% chloroform, separately, and dried after draining the solvent from the membrane surface. The contacting with the solvent and the drying was done in a way similar to that of SPPOH-PES composite membrane preparation. Then, pure water permeation rate (PWP) was determined for each membrane after one hour of compaction at 2069 kPa gauge (300 psig) under water. PWP measurements at 1379 kPa gauge were 18.9, 17.1, 18.2, and 12.5 x 10^{-6} $m^3/m^2.s$, respectively, for the first, second, third and fourth membrane. These results indicate that the permeability of the substrate membrane does not significantly change for the different solvents used except for the mixture of 66 mass% chloroform which appears to affect the substrate. This latter effect might be the cause of trend change in the separation results of the composite membranes at solvent chloroform content of 66 mass%, which was shown in Figure 4.9. The permeability of the SPPOH coated membranes, on the other hand, decreases steadily with the increase in the chloroform content in the solvent. Therefore, the effect of the solvent on the performance of the SPPOH coated membranes is not due totally to the change of the substrate membrane.

The significant differences in membrane performance, shown in Figure 4.9 and Figure 4.10, are due to the morphological change of the coated SPPOH layer. Apparently, the use of a more hydrophilic solvent with a higher methanol content created a more open structure in the charged polymer and such an open structure was retained even after drying and subsequent contact of the coated layer with the feed aqueous

solution. Interestingly, this open structure affected the membrane product rate more substantially than the solute separation. Intrinsic viscosities in the different polymer solutions were measured in order to quantify the polymer-polymer interactions in the different solvent mixtures. Table 4.2 shows the values of intrinsic viscosity of SPPOH, having an I.E.C. value of 1.93 meq/g, in the different chloroform/methanol mixtures. The values indicate that the polymer-polymer interaction increases with increase in chloroform content, seen in the form of lower measured intrinsic viscosity, thus resulting in tighter and more closed structure in the skin layer. This is in accordance on the discussion of section 2.5 dealing with solvent power and intrinsic viscosity.

Three-dimensional topographic AFM micrographs of the skin layers of the composite membranes are shown in Figure 4.11 to Figure 4.14, noting the difference in the scales used. Section Analysis, provided through the NanoScope III software, was used to estimate the size-range of the nodules on the surface of the four composite membranes. Sizes of nodules for these skin layers are estimated as follows :

solvent methanol, skin layer nodule size ranges from 85 to 125 nm

solvent 82% methanol 18% chloroform, nodule size ranges from 54 to 70 nm

solvent 58% methanol 42% chloroform, nodule size ranges from 37 to 51 nm

solvent 34% methanol 66% chloroform, nodule size ranges from 20 to 32 nm

TABLE 4.2

Intrinsic Viscosity of SPPOH Polymer of I.E.C. value 1.93 meq/g in Solvents of Various Chloroform : Methanol Proportions

Solvent Composition (mass%)	Intrinsic Viscosity at 25 °C [η]
Methanol	1.99 ± 0.12
18 % $CHCl_3$: 82 % MeOH	1.51 ± 0.07
42 % $CHCl_3$: 58 % MeOH	1.27 ± 0.06
66 % $CHCl_3$: 34 % MeOH	0.92 ± 0.07

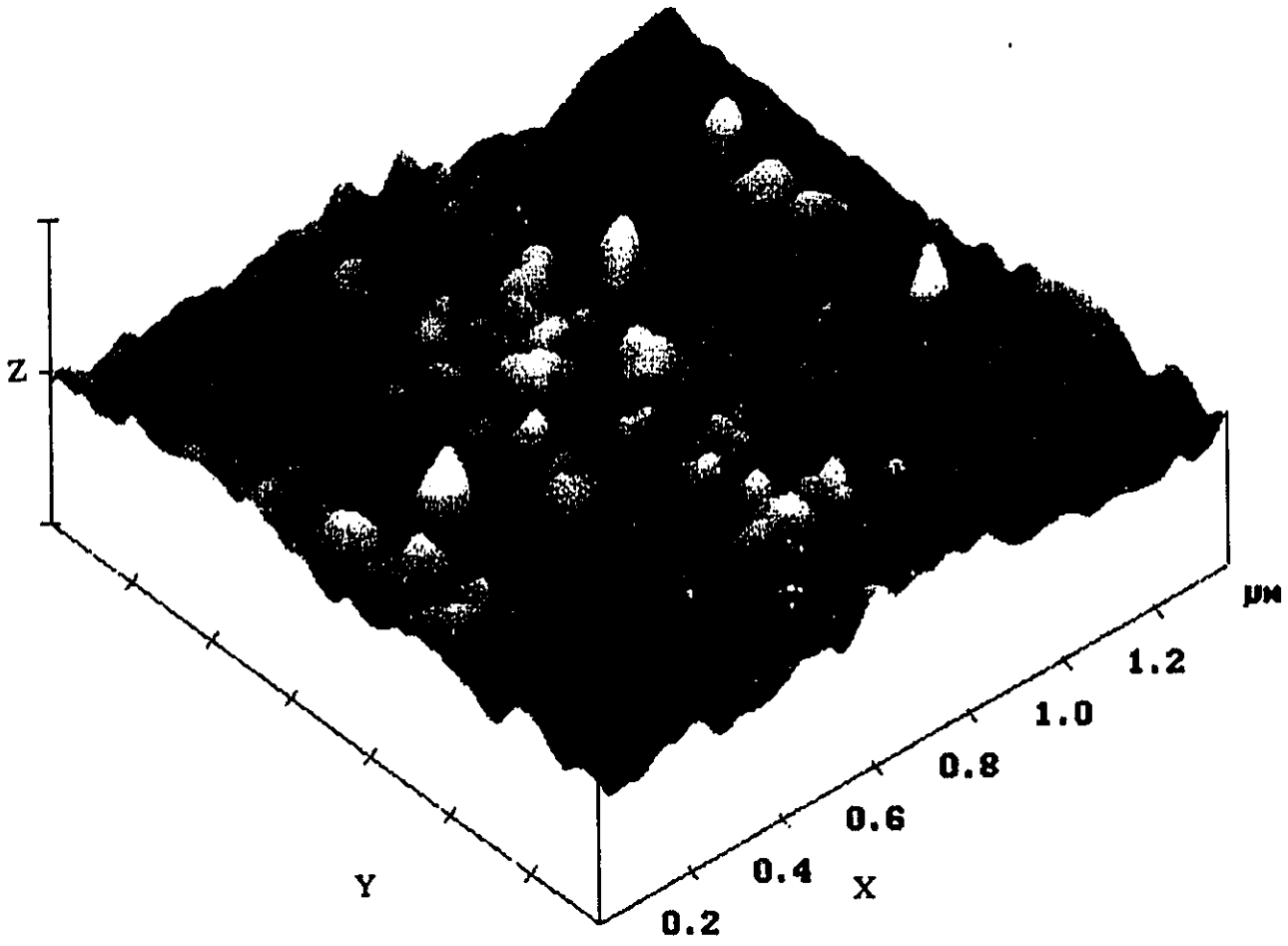

X and Y 200.000 nm / division

Z 15.000 nm / division

Figure 4.11 AFM micrograph of the skin layer of SPPOH-PES composite membrane made using SPPOH of I.E.C. value 1.93 meq/g and Methanol as the solvent for coating solution.

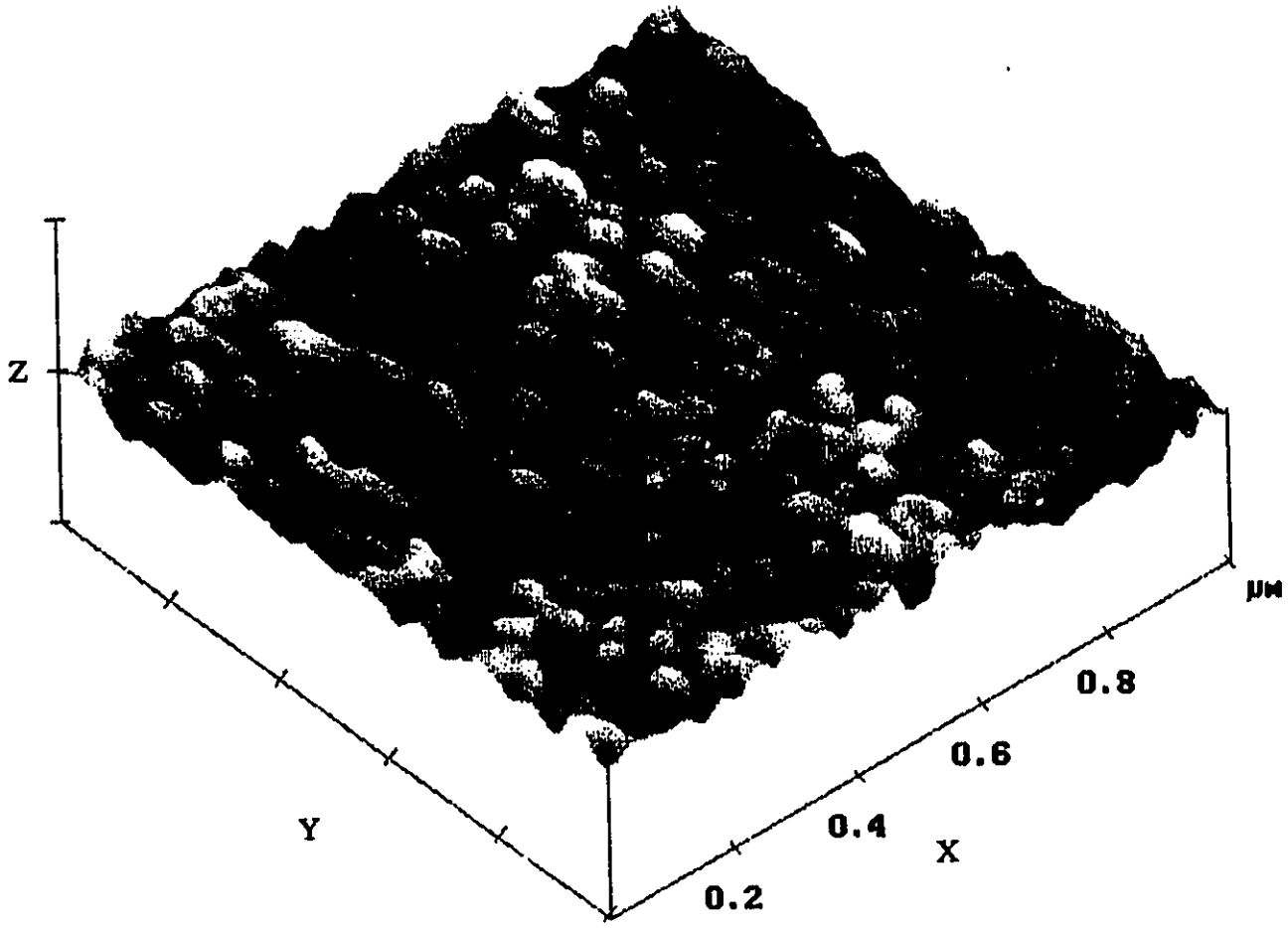

X and Y 200.000 nm / division

Z 7.500 nm / division

Figure 4.12 AFM micrograph of the skin layer of SPPOH-PES composite membrane made using SPPOH of I.E.C. value 1.93 meq/g and (82 mass% Methanol 18 mass% chloroform) as the solvent for coating solution.

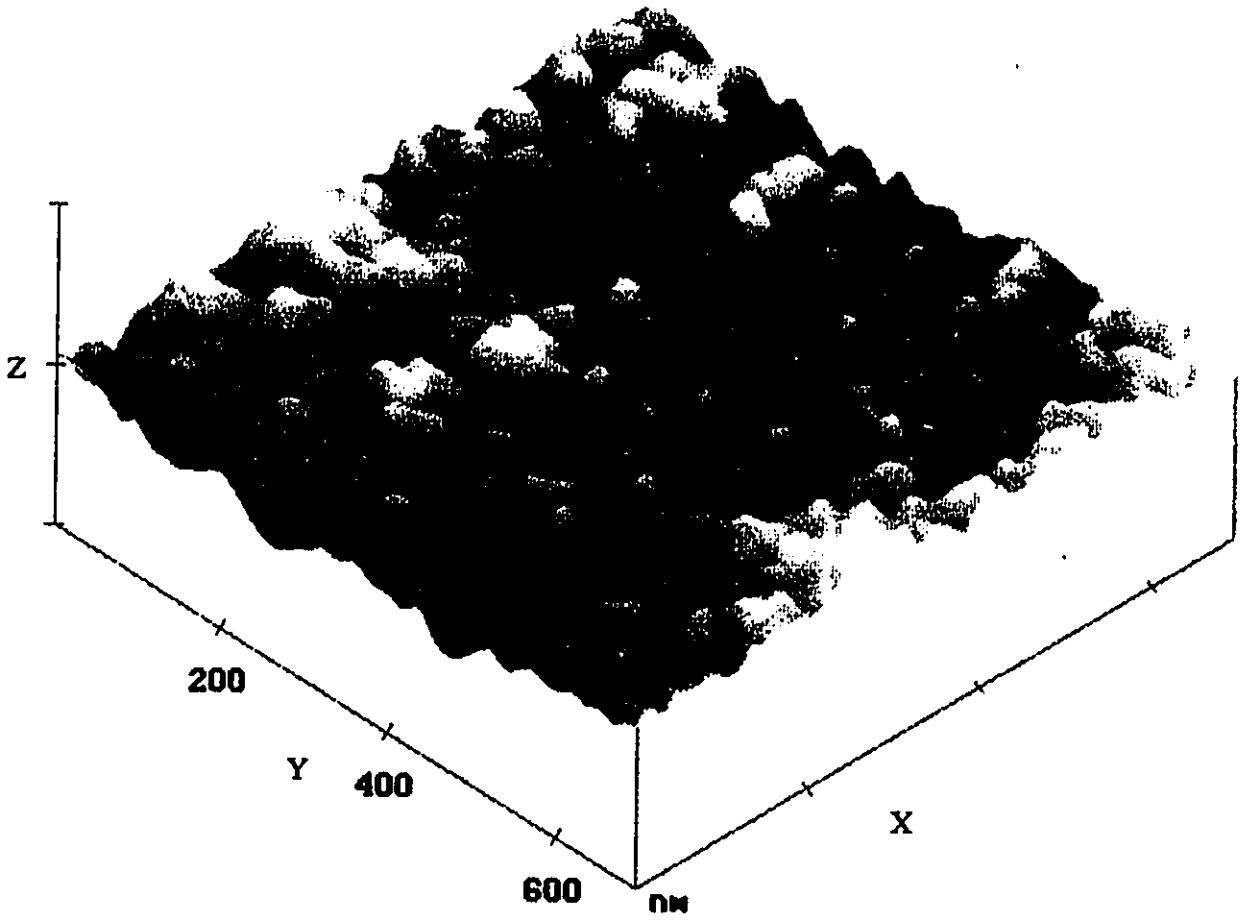

X and Y 200.000 nm / division

Z 7.500 nm / division

Figure 4.13 AFM micrograph of the skin layer of SPPOH-PES composite membrane made using SPPOH of I.E.C. value 1.93 meq/g and (58 mass% Methanol 42 mass% chloroform) as the solvent for coating solution.

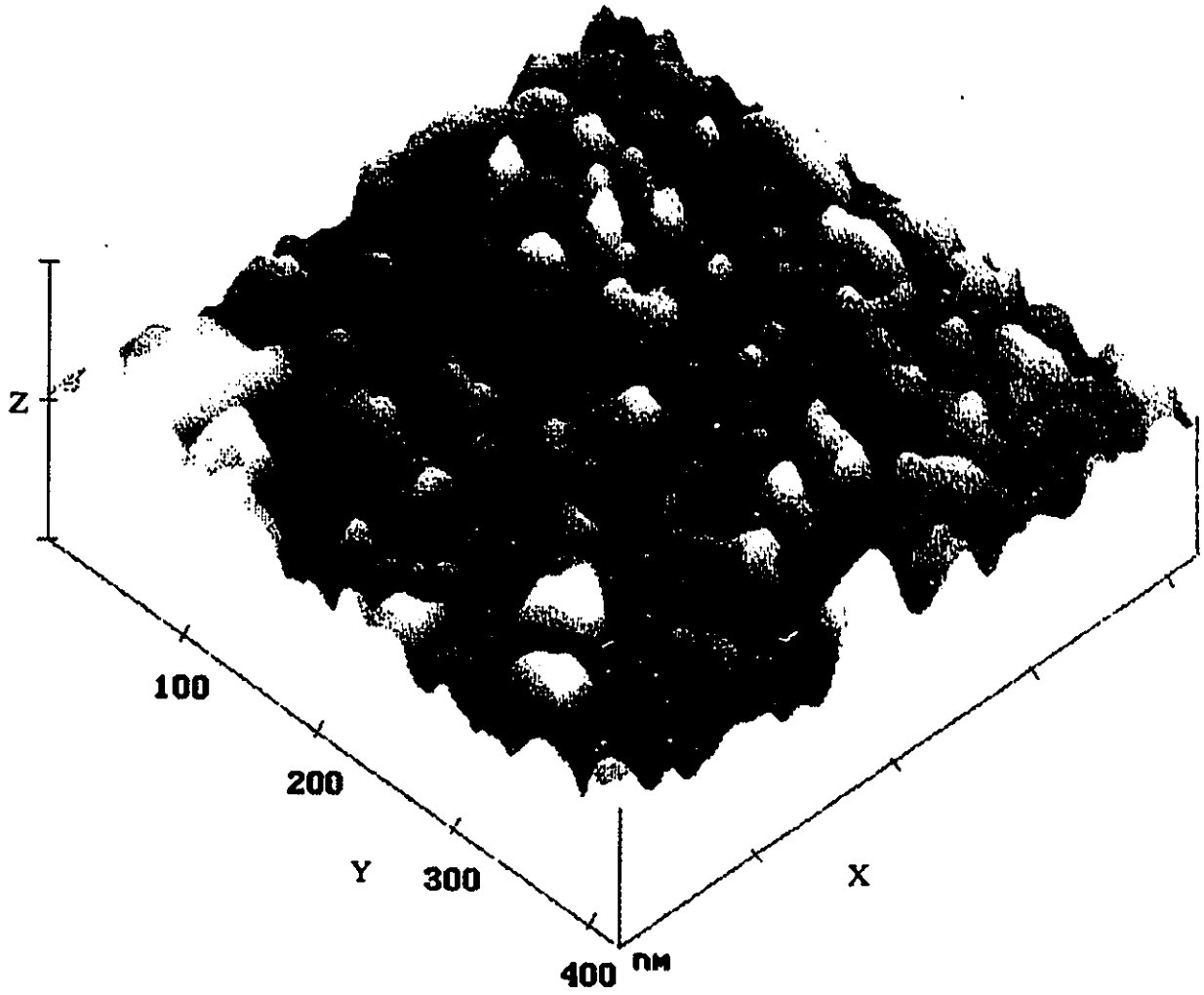

X and Y 100.000 nm / division

Z 15.000 nm / division

Figure 4.14 AFM micrograph of the skin layer of SPPOH-PES composite membrane made using SPPOH of I.E.C. value 1.93 meq/g and (34 mass% Methanol 66 mass% chloroform) as the solvent for coating solution.

These remarkable results demonstrate the effect of the solvent composition on the microscopic morphological structure of the skin layers of the membranes. As more chloroform is added to the coating solution, the polymer-polymer interactions increase leading eventually to smaller nodule sizes. These results are consistent with the intrinsic viscosity measurements. These resultant morphologies contribute significantly to the reverse osmosis performance of the composite membranes, especially the permeation rate.

It can be concluded, therefore that the effect of I.E.C. values shown in Figures 4.1 and 4.2 is in fact a result of the superimposition of two different effects, one is the effect of the I.E.C. value and the other is the effect of the solvent. As the I.E.C. value increases from 1.29 meq/g to 1.98 meq/g, the chloroform content in the solvent mixture should be decreased (or the methanol content should be increased), and as a result the product rate increases without much sacrifice in the solute separation. A further increase in I.E.C. value from 1.98 meq/g to 2.60 meq/g leads to a further increase in the product rate accompanied by a separation decrease, as a result of the increased hydrophilicity and swelling of the skin layer of the composite membrane.

These observations are very important in the design of composite reverse osmosis membranes with a SPPOH coated layer. They indicate that the I.E.C. value of SPPOH should be properly adjusted and the solvent(s) should be properly chosen for the preparation of the coating solution.

4.4 Effect of Solute Cations on Membrane Performance When the Anion is Chloride.

Reverse osmosis separation of various metal chlorides were investigated and the results are summarized in Table 4.3. The ionic radii of the cations are also included in the table. The precision of these results for the various salts is comparable to that of sodium chloride which was shown in Figure 4.1 and Figure 4.2. There are two effects involved in this table. One is the effect of the ionic radius and the other is the effect of the ionic valence.

Regarding the effect of the ionic radius, the following tendency can be observed for ions of the same valence :

1) The product rate (PR) can become greater than pure water permeation rate (PWP) and increases with an increase in the ionic radius, as shown in going from LiCl to KCl.

2) Comparing the monovalent cations, the solute separation markedly decreases with the increase in the ionic radius.

Small cations such as Li^+ and Na^+ are present in water in hydrated-form. They are surrounded by layers of water less mobile than the bulk water, thus these cations are called structure-making ions. They permeate less readily than structure-breaking ions whose surrounding water is more mobile than bulk water (Kesting, 1985). The more hydrated the cation is, as in the case of Li^+, the less accessible it becomes to interactions with other ions. Anions, on the other hand, are more free for interactions with other ions and thus their role is more dominant (Luck, 1984). Large monovalent cations, such as

TABLE 4.3

REVERSE OSMOSIS PERFORMANCE OF SPPOH-PES MEMBRANES[1]
Solutions of Various Chlorides

SOLUTE	IONIC RADIUS OF CATION $X10^{10}$ m		I.E.C. 1.29	I.E.C. 1.41	I.E.C. 1.98	I.E.C. 2.60
		PWP	3.36	6.54	11.48	18.63
LiCl	0.60	PR	3.12	6.14	10.68	17.75
		Separation f	0.80	0.79	0.69	0.57
NaCl	0.95	PR	4.28	8.44	14.84	20.70
		Separation f	0.77	0.75	0.64	0.50
KCl	1.33	PR	5.05	9.78	17.27	26.47
		Separation f	0.73	0.71	0.59	0.45
NH_4Cl	1.43	PR	4.84	9.05	16.46	25.59
		Separation f	0.71	0.69	0.58	0.42
$MgCl_2$	0.65	PR	2.81	5.07	10.64	17.15
		Separation f	0.37	0.33	0.25	0.19
$CaCl_2$	0.99	PR	2.90	5.39	11.15	19.40
		Separation f	0.40	0.37	0.31	0.22
$AlCl_3$	0.51	PR	1.53	2.59	6.22	10.04
		Separation f	0.58	0.60	0.37	0.20
$FeCl_3$	0.64	PR	1.52	2.56	5.55	10.31
		Separation f	0.48	0.45	0.38	0.19

[1] PWP and PR $x10^6$ ($m^3/m^2.s$)

K^+, are capable of orienting water molecules only in the layer immediately adjoining the ion. Water molecules other than those in the layer adjacent to the ion have a higher mobility in the presence of such ions than in the bulk (Kesting, 1985). This phenomenon causes the separation to be highest for LiCl and lowest for KCl as shown in Table 4.3, opposing that expected by considering the Donnan Equilibrium. Lower charge density counter-ion (K^+) would have been expected to be more effectively separated by the anionic membrane than higher charge density counter-ions such as (Li^+) and (Na^+), as was discussed in section 2.4.

Exactly the same tendency was observed in recent work on the reverse osmosis performance of SPPO membranes with respect to alkali metal chloride solutes (Chowdhury et al., 1994). The above observation was explained by the change in the free energy of the following exchange reaction:

$$-SO_3H + Me^+ hy \rightleftarrows -SO_3^- Me^+ + H^+ hy \quad (1)$$

The free energy of the above exchange reaction decreases as the ionic radius of Me^+ cation increases (Jencks, 1969), favoring the right side of the equation (Marcus and Howery, 1975). The number of species in the membrane increases from one to two for each conversion of $-SO_3H$ to $-SO_3^- Me^+$. Consequently, more water flows into the membrane phase due to an increase in the osmotic pressure effect. As a result, the product rate increases with an increase in the ionic radius and simultaneously the solute separation decreases. The same explanation may be applicable for ions of other valences.

Considering the case of membranes prepared from SPPOH of I.E.C. value 1.98 meq/g, the pure water permeation rate (PWP) was found to be 11.48 $x10^{-6}$ $m^3/m^2.s$ whereas the permeation rate (PR) in the presence of KCl was 17.27 $x10^{-6}$ $m^3/m^2.s$, which is more than 50% greater than PWP. Referring to the Kimura-Sourirajan transport model presented in section 2.3.5, the first two equations were:

$$A = PWP / (P \cdot S \cdot M_B \cdot 3600)$$

$$N_B = A (P - \pi (X_{A2}) + \pi (X_{A3}))$$

The concentrations involved in the present experiments are low as far as osmotic pressure effects are concerned, as will be shown in section 4.7. This model assumes a constant water permeability (A) given by the first equation. As seen from the second equation, the permeation rate in the presence of a solute can never exceed the pure water permeation rate. The experimental results obtained in this work indicate otherwise. The inability of this model to predict such a significant increase in the permeation rate in the presence of the solute, over that of pure water, may be attributed to the assumption of invariability of the membrane water permeability (A). For charged membranes, such as those made from SPPOH polymer, the membrane permeability seems to be a variable changing with the electrolyte solute. The swelling or intake of water by the active skin layer is affected by the ionic species present in the solution.

Regarding the effect of the valence, the following tendency is observed in Table 4.3. Comparing Li^+, Mg^{2+} and Fe^{3+}, whose ionic radii are close to each other (Li^+ (0.60), Mg^{2+} (0.65) and Fe^{3+} (0.64) $x10^{-10}$m), the product rate decreases only slightly from Li^+ to Mg^{2+} and decreases significantly from Mg^{2+} to Fe^{3+}. The solute separation, on the other hand, has a minimum at Mg^{2+}.

Considering the following exchange reaction

$$n(-SO_3H) + Me^{n+}(hy)_n \rightleftarrows (-SO_3^-)_nMe^{n+} + nH^+hy \qquad (2)$$

the free energy of reaction becomes smaller as the valence of cation, n, increases from 1 to 2, as in going from Li^+ to Mg^{2+}, due to an increase in the electrostatic force between ($-SO_3^-$) and Me^{n+}, which is consistent with the Donnan potential theory. Therefore, the intake of electrolyte into the membrane phase is enhanced, resulting in the lower solute separation. The change in the number of species at the conversion of $2(-SO_3H)$ to $(-SO_3^-)_2Me^{2+}$, is from 2 to 3 when $(-SO_3^-)_2Me^{2+}$ is completely dissociated, whereas it is from 2 to 1 when $(-SO_3^-)_2Me^{2+}$ is completely associated. Therefore, the osmotic pressure effect may increase or decrease as a result of the exchange reaction, depending on the degree of association. Consequently, the product rate is found to remain the same or decrease from the pure water permeation rate, depending on the extent of association and dissociation.

When the cationic valence, n, increases further to 3, the metal cation is very strongly bound to the sulfonate anion, causing the cross-linking of SPPOH polymer. The

polymeric coating layer becomes denser, resulting in the lower product rate and higher solute separation than n = 2. The densification of the polymer is permanent and the initial pure water permeation rate can no longer be recovered. In fact the membrane can even be changed from cation-exchange membrane to anion-exchange membrane as a result of such strong electrostatic attraction forces (Kesting, 1985).

4.5 Effect of Solute Cations on Membrane Performance when Anion is Sulfate.

Table 4.4 summarizes the effect of cations on the membrane performance when the anion is sulfate. Exactly the same tendency is observed as in the case of chloride anion. The solute separation decreases and the product rate increases when the cation changes from sodium to potassium. The separation of such solutes, however, is much more effective than in the case of chloride anion due to the stronger electrostatic repulsive force between the sulfonate of the membrane skin layer and the divalent larger sulfate anion in the solution. This is expected from the Donnan exclusion mechanism. This performance indicates the suitability of these composite membranes for treating feed streams that contain similar anionic groups.

Both solute separation and product rate decrease when the cation changes from Na^+ to Mg^{2+}. There is only a small change in solute separation but the product rate decreases significantly when the cation changes from Mg^{2+} to Al^{3+}, again due to stronger attraction between Al^{3+} in the solution and $-SO_3^-$ of the membrane.

TABLE 4.4

REVERSE OSMOSIS PERFORMANCE OF SPPOH-PES MEMBRANES
Solutions of Various Sulfates

SOLUTE		I.E.C. 1.29	I.E.C. 1.41	I.E.C. 1.98	I.E.C. 2.60
Na_2SO_4	PR x10^6 ($m^3/m^2.s$)	3.44	6.41	11.86	18.27
	Separation f	0.95	0.94	0.84	0.72
K_2SO_4	PR x10^6 ($m^3/m^2.s$)	4.31	7.86	14.52	23.31
	Separation f	0.93	0.92	0.78	0.66
$MgSO_4$	PR x10^6 ($m^3/m^2.s$)	2.74	4.92	10.38	17.18
	Separation f	0.65	0.63	0.43	0.22
$Al_2(SO_4)_3$	PR x10^6 ($m^3/m^2.s$)	1.73	2.99	6.25	12.61
	Separation f	0.61	0.61	0.39	0.14

4.6 Effect of Solute Anions on Membrane Performance when the Cation is Sodium.

Table 4.5 summarizes the effect of anions on the membrane performance when the cation is sodium. It is obvious that the separation increases whereas the product rate decreases slightly as the valence of the anion increases. This can be difficult to explain by considering the exchange reactions (1) and (2) alone, since the above equations do not include anions. When considering the Donnan equilibrium expressed by:

$$K = ((Na^+)_{mem}((-SO_3^-)_{mem} + (X^{n-})_{mem})) / ((Na^+)(X^{n-})) \qquad (3)$$

where ( ) and ( )$_{mem}$ indicate the concentration in the solution phase and in the membrane phase, respectively, the equilibrium constant K should decrease as the anionic valence n increases because of the stronger electrostatic repulsion between ($-SO_3^-$) and X^{n-} for larger n. The intake of the electrolyte solute $(Na^+)_nX^{n-}$ into the membrane phase, therefore, should decrease in order to maintain electroneutrality. Thus, the solute separation increases as anionic valence increases.

TABLE 4.5

REVERSE OSMOSIS PERFORMANCE OF SPPOH-PES MEMBRANES
Various Sodium Solutions

SOLUTE		I.E.C. 1.29	I.E.C. 1.41	I.E.C. 1.98	I.E.C. 2.60
NaCl	PR x10^6 ($m^3/m^2.s$)	4.28	8.44	14.85	20.70
	Separation f	0.77	0.75	0.64	0.50
$NaHCO_3$	PR x10^6 ($m^3/m^2.s$)	3.76	7.19	12.91	19.60
	Separation f	0.85	0.83	0.71	0.58
Na_2CO_3	PR x10^6 ($m^3/m^2.s$)	3.32	6.35	11.29	17.77
	Separation f	0.93	0.91	0.81	0.72

4.7 Effect of Solute Concentration on Membrane Performance.

Figure 4.15 to Figure 4.20 illustrate the effect of feed sodium chloride concentration on the solute separation and product rate. The bars shown are estimates of the standard deviation based on testing two membranes. These figures indicate that the solute separation decreases significantly with an increase in sodium chloride concentration. For example, with respect to the membrane made from SPPOH of I.E.C. value of 1.98 meq/g and solvent methanol, the solute separation shown in Figure 4.17 changed from 88% to 57% when the concentration of the feed NaCl solution changed from 0.006 to 0.081 molar. This is in contrast to the membranes without electric charge such as cellulose acetate membranes for which the solute separation depends only little on sodium chloride concentration. The strong dependency of the solute separation on the concentration of electrolyte solutes is a well known phenomena for charged reverse osmosis membranes and explained by the fact that the intake of electrolyte solutes to the membrane phase is more favoured at a higher electrolyte concentration according to the Donnan equilibrium (Heyde et al., 1975). The observed decreasing efficiency of NaCl exclusion with increasing solution concentration is due to the tendency of the ions to eliminate concentration differences (between the membrane phase and the solution phase) by diffusion at a constant electric field. The electric field is constant because the concentration of fixed sulphonate charge is constant. The equilibrium between these opposing tendencies is therefore displaced, with the result that the Donnan potential and NaCl exclusion decrease when the sodium chloride concentration increases (Kesting, 1985).

Figure 4.16, Figure 4.18 and Figure 4.20 indicate that the permeation rate through the SPPOH composite membranes is little affected by sodium chloride concentration. This is also reasonable since the sodium chloride concentrations involved in this study are low enough that the effect of osmotic pressure on the product rate is not very significant. The osmotic pressure of sodium chloride solutions, in the concentration range studied, can be approximated by the following relationship :

$$\pi (x_A) = B\ x_A$$

where $B = 2.5645 \times 10^5$ (kPa per mole fraction) is the coefficient for osmotic pressure (Matsuura, 1994) and x_A is the mole fraction of sodium chloride is solution. Considering the membrane made from I.E.C. value of 1.98 meq/g in methanol for which the reverse osmosis performance is shown in Figure 4.17 and Figure 4.18: At feed concentration of 0.043 mol/L the NaCl separation is 70%. The feed mole fraction is 0.00077 which gives a feed side osmotic pressure of 197 kPa, whereas the permeate NaCl mole fraction of 0.00023 results in permeate-side osmotic pressure of 60 kPa. Thus the effective osmotic pressure difference across the membrane equals 138 kPa. Higher feed concentration such as 0.081 molar is accompanied by lower NaCl separation namely 57%. Thus the feed side osmotic pressure equals 374 kPa, while the permeate side osmotic pressure is 176, resulting in osmotic pressure difference, across the membrane, of 198 kPa. Thus, little difference in permeation rates is observed when the concentration changes under the operating pressure of 1379 kPa gauge.

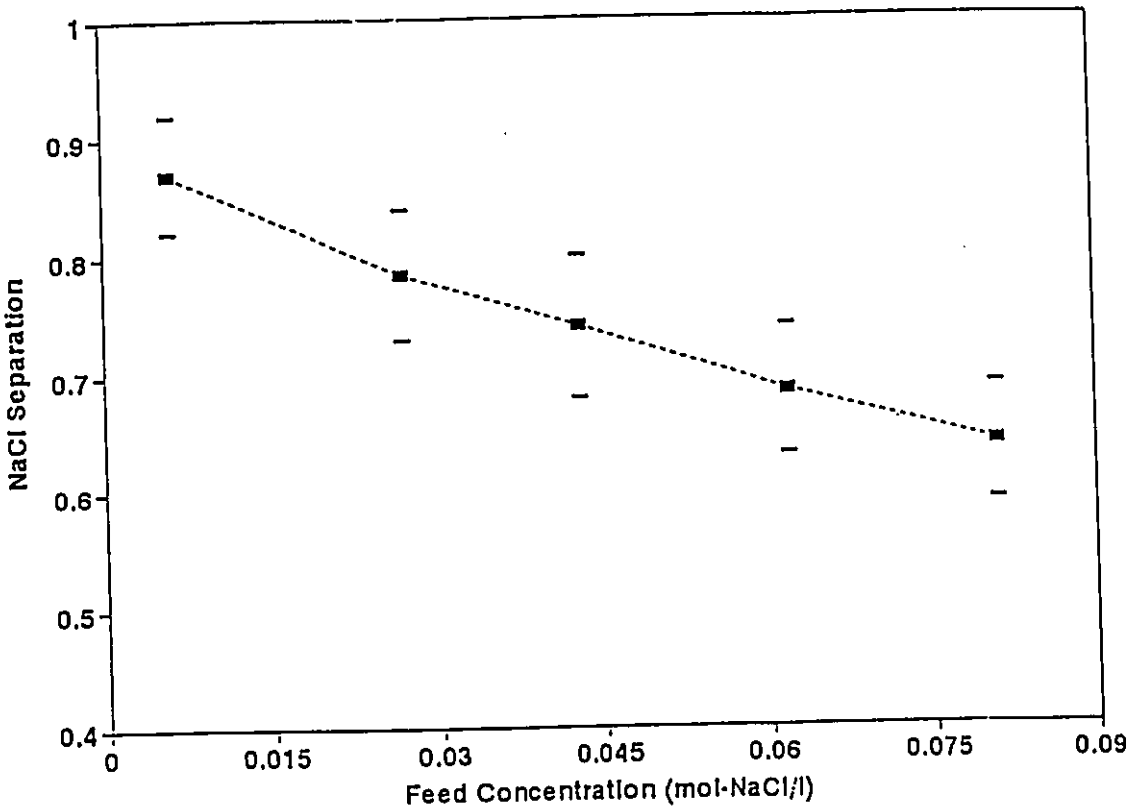

Figure 4.15 Effect of feed sodium chloride concentration on the separation using SPPOH-PES membrane with I.E.C. value of 1.29 meq/g. Operating conditions: Pressure 1379 kPa gauge (200 psig), Temperature 25 °C.

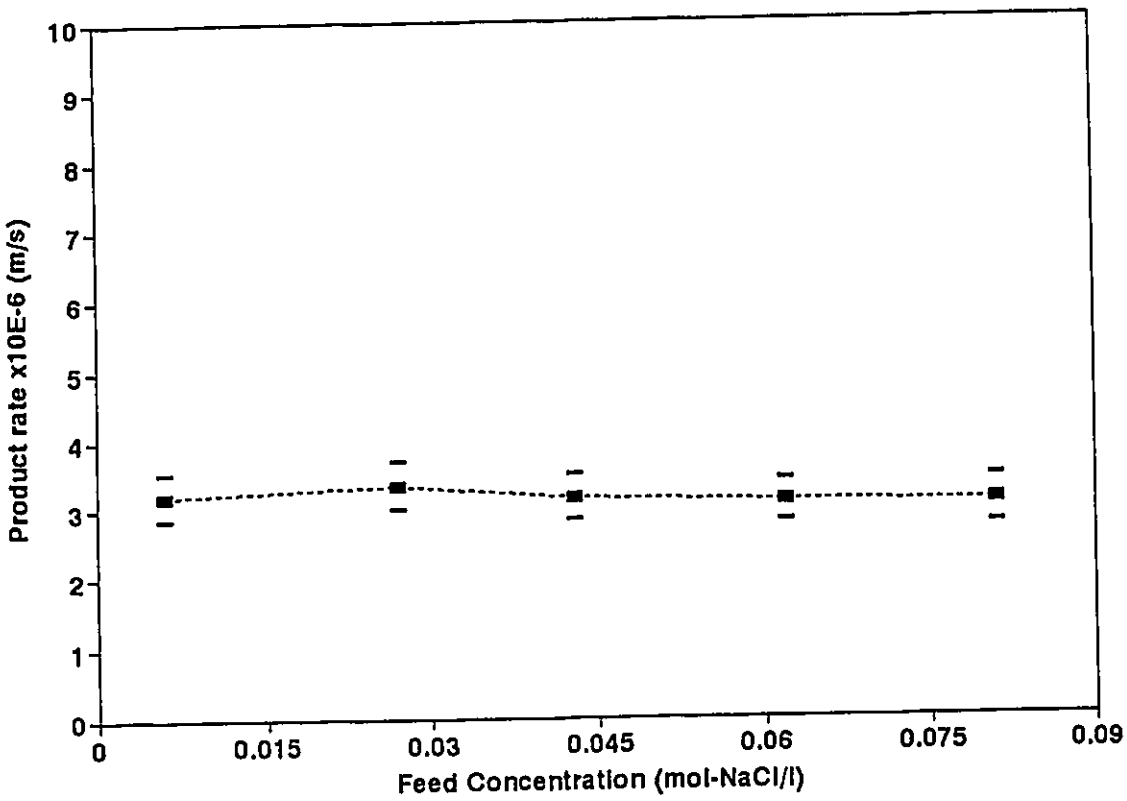

Figure 4.16 Effect of feed sodium chloride concentration on the permeation rate using SPPOH-PES membrane with I.E.C. value of 1.29 meq/g. Operating conditions: Pressure 1379 kPa gauge (200 psig), Temperature 25 °C.

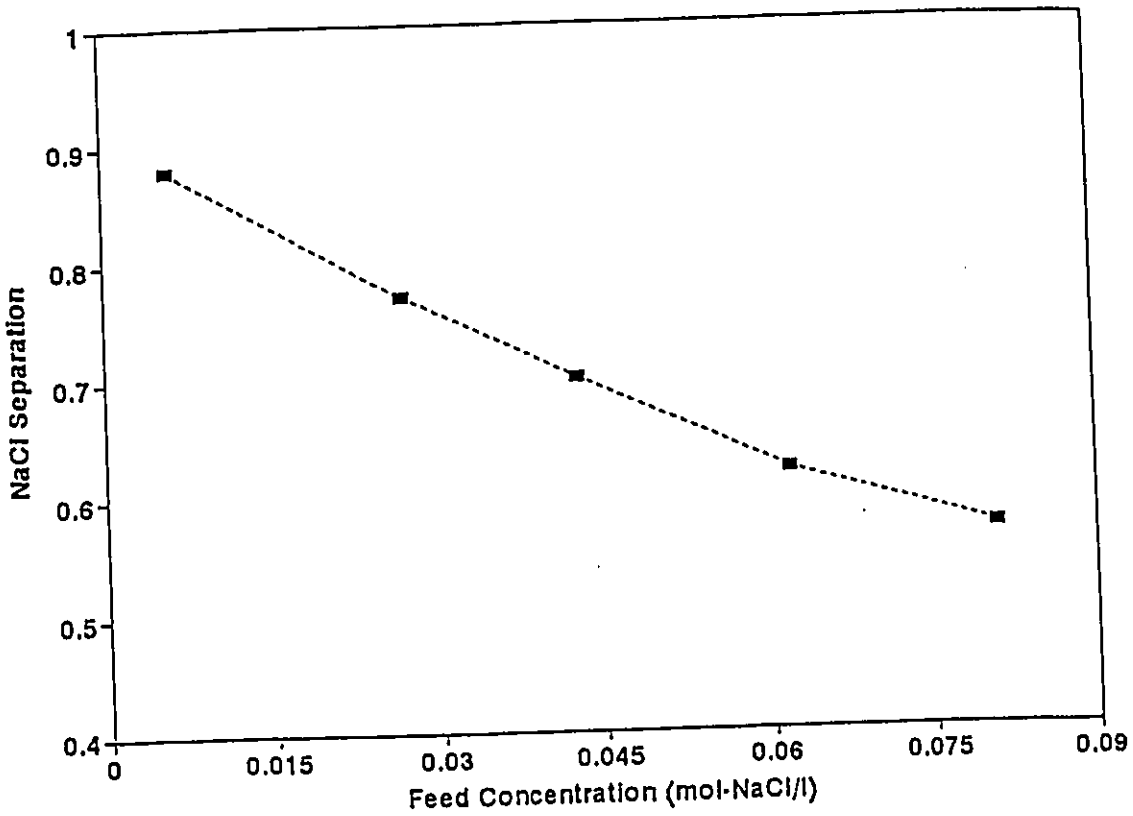

Figure 4.17 Effect of feed sodium chloride concentration on the separation using SPPOH-PES membrane with I.E.C. value of 1.98 meq/g and methanol as the coating solution solvent. Operating conditions: Pressure 1379 kPa gauge (200 psig), Temperature 25 °C.

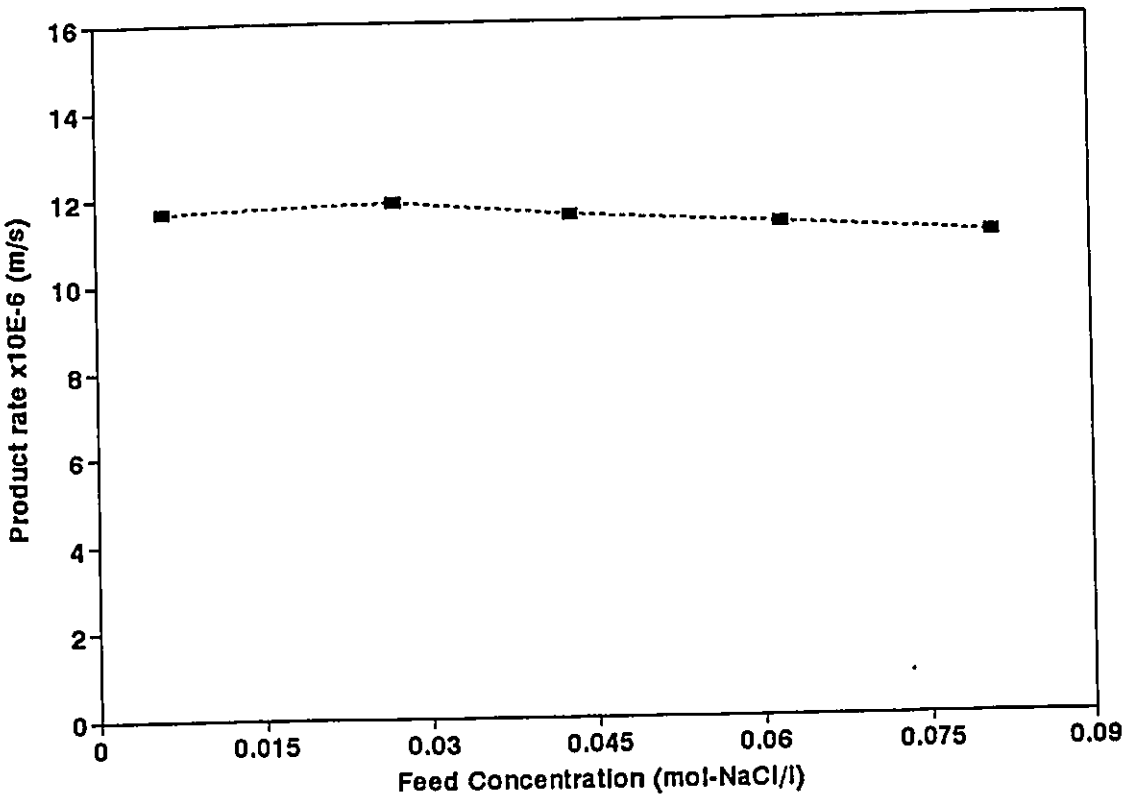

Figure 4.18 Effect of feed sodium chloride concentration on the permeation rate using SPPOH-PES membrane with I.E.C. value of 1.98 meq/g and methanol as the coating solution solvent. Operating conditions: Pressure 1379 kPa gauge (200 psig), Temperature 25 °C.

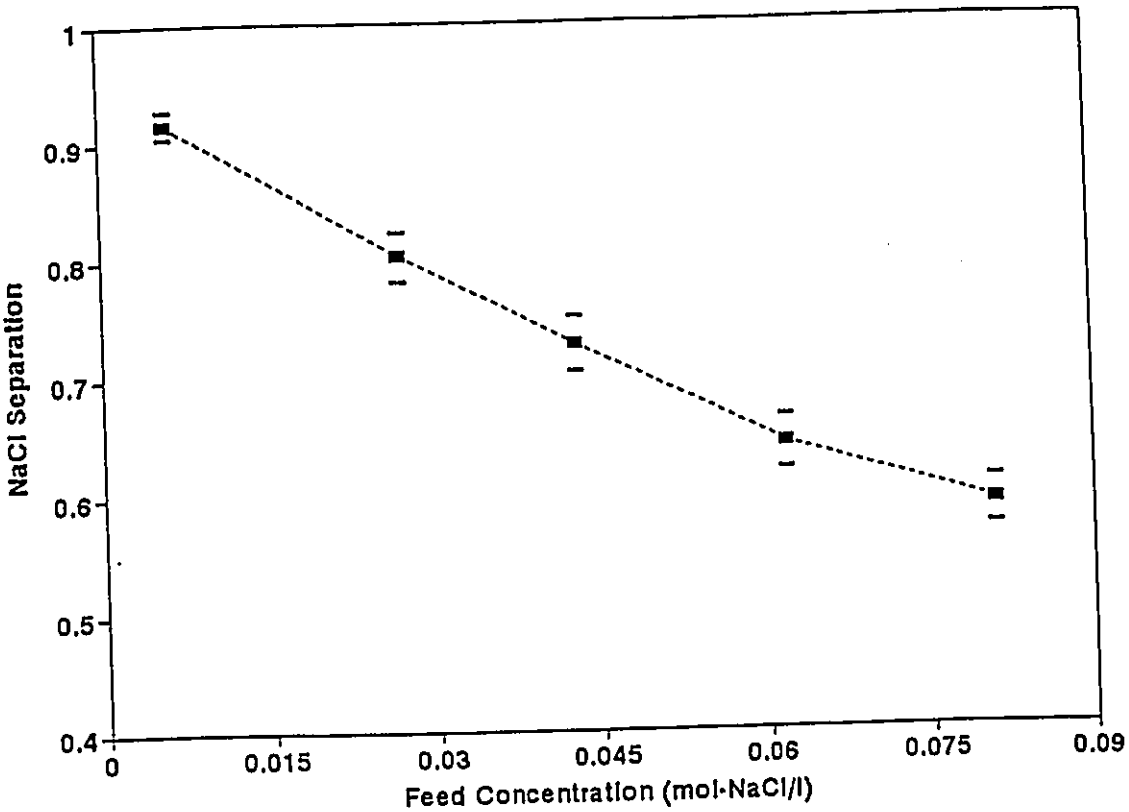

Figure 4.19 Effect of feed sodium chloride concentration on the separation using SPPOH-PES membrane with I.E.C. value of 1.98 meq/g and 56:44 mass% chloroform: methanol as the coating solution solvent. Operating conditions: Pressure 1379 kPa gauge (200 psig), Temperature 25 °C.

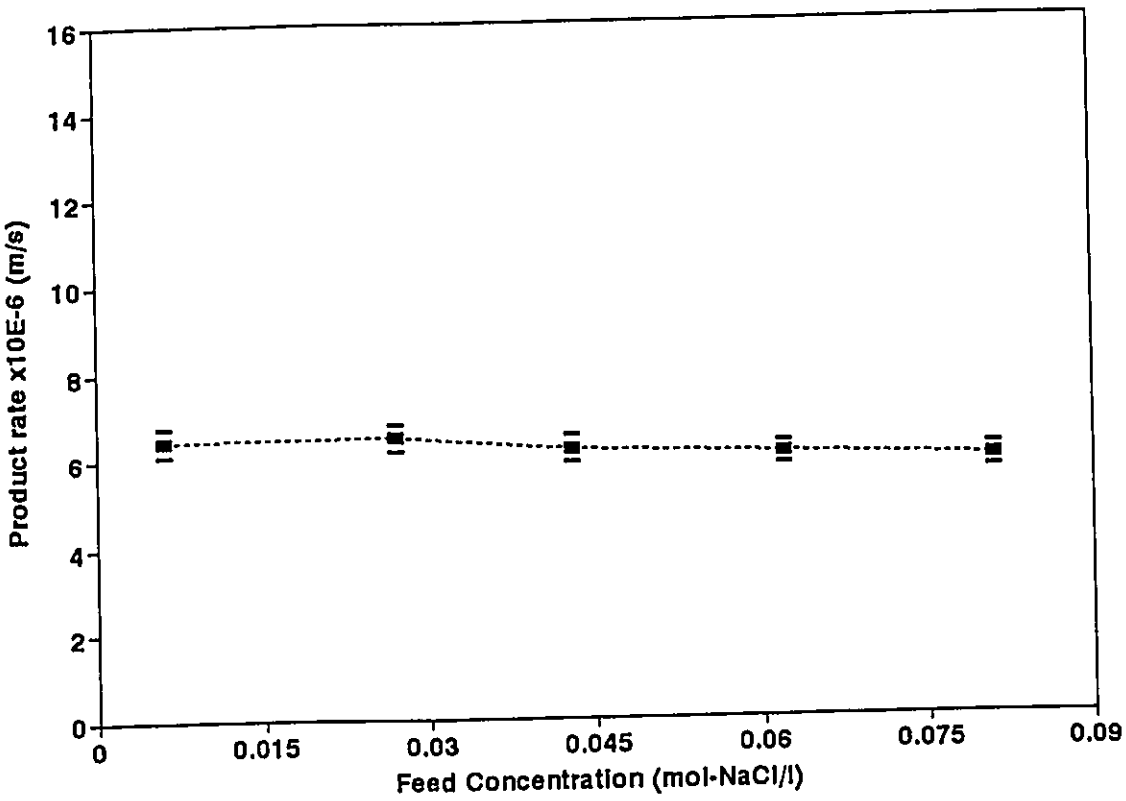

Figure 4.20 Effect of feed sodium chloride concentration on the permeation rate using SPPOH-PES membrane with I.E.C. value of 1.98 meq/g and 56:44 mass% chloroform: methanol as the coating solution solvent. Operating conditions: Pressure 1379 kPa gauge (200 psig), Temperature 25 °C.

4.8 Effect Of Microporous Support

SPPOH of ion exchange capacity 2.20 meq/g was used in making thin film composite membranes with two different microporous substrates. Two types of polyethersulfone ultrafiltration membranes, designated as HW17 and HW18 by Osmonics Incorporated, were coated with 1 mass% SPPOH in methanol. HW17 and HW18 show little visible difference as far as their molecular mass cut-off curves are concerned, as were shown in Figure 3.1 and Figure 3.2, respectively, with HW18 being "slightly" more porous (Rudie, 1994). PWP measurements, after one day of compaction at 2069 kPa gauge (300 psig), were 11.1 $x10^{-6}$ and 39.4 $x10^{-6}$ $m^3/m^2.s$ for HW17 and HW18 respectively. SEM micrographs, already shown in Figure 3.3, reveal that HW17 has a finger-like structure whereas HW18 is spongy.

The reverse osmosis performance of the resultant thin film composite SPPOH-PES membranes is shown in Table 4.6. It is evident from the table that the performance of the composite SPPOH-PES is significantly affected by the substrate used, with the permeation rate being more than two times greater in the case of HW18 substrates. SPPOH-PES with HW18 as the substrate still maintains some salt rejection especially in the case of electrolytes of large anionic groups such as the sulfate, SO_4^{2-}. These results clearly indicate the importance of the porosity and structure of the substrate membrane in determining the performance of the composite membrane. The substrate is not merely a mechanical support for the skin layer posing no resistance to flow. It does play a significant role in shaping the pores and hence determining the performance of the composite membrane.

TABLE 4.6

REVERSE OSMOSIS PERFORMANCE OF SPPOH-PES MEMBRANES
Using Two Different Polyethersulfone Substrates
Coated With SPPOH of I.E.C. 2.21 meq/g

Solute (MW)		PES HW17	PES HW18
	PWP $m^3/m^2.s$ (gfd) 1379 kPa gauge	17.3×10^{-6} (36.7)	36.4×10^{-6} (77.2)
NaCl (58)	Separation	0.48	0.29
Na_2SO_4 (142)	Separation	0.78	0.67
PEG (1500)	Separation	0.61	0.05
PEG (9000)	Separation	0.92	0.35
PEG (15000)	Separation	–	0.87

Table 4.6, moreover, shows that the molecular mass cut-off for the composite membrane employing HW17 to be approximately 9000, based on PEG, whereas for the composite membrane employing HW18 to be slightly more than 15000. The charged nature of these composite membranes is clearly manifested. Solute separation for ionic NaCl, using HW18 substrate, is 29% and still only 35% for neutral PEG 9000, though the molecular masses of these two solutes are drastically different.

CHAPTER FIVE

CONCLUSIONS

The following conclusions can be drawn from the experimental results and discussions :

1. Thin film composite membranes of high selectivity and high flux can be prepared from SPPOH polymer by properly adjusting the ion exchange capacity of the polymer and the solvent used for the preparation of the polymer solution for surface coating.

2. The solvent system used in making the coating solution must be properly selected since it controls the polymer-polymer interactions therein. The final microscopic structure of the coated selective layer of the membrane and its reverse osmosis performance are consequently determined.

3. When the anion of the electrolyte solute is fixed, the membrane performance is a rather complicated function of the cationic valence and radius. In particular, the separation of alkali metal chloride solutes decreases with an increase in the radius of, or

the decrease in the charge density of, the alkali metal cation. These results are unexpected considering the electrostatic interaction between a solute cation and a membrane surface charged anionically by $-SO_3^-$. These results, however, can be interpreted by considering the ion exchange reaction between the solute cation and the proton in $-SO_3^- H^+$.

4. When the cation of the solute electrolyte is sodium, the solute separation increases whereas the product rate decreases as the valence of the anion increases. This phenomena can be interpreted by the Donnan equilibrium.

5. The solute separation decreases with an increase in the electrolyte concentration. This also can be explained by the Donnan equilibrium. The permeation rate remains fairly constant because the osmotic pressure across the membrane is insignificant due mainly to low electrolyte concentrations.

6. The porosity of the substrate membrane and its structure play a significant role in determining the performance of the charged thin film composite membrane

CHAPTER SIX

RECOMMENDATIONS

After performing this experimental work on preparing thin film composite membranes from sulfonated polyphenylene oxide on polyethersulfone and studying their performance and structure, the following three recommendations are expected to be helpful in reaching further improvements :

1. Crosslinking of Sulfonated Poly(2,6-dimethyl-1,4-phenylene oxide)

As poly(2,6-dimethyl-1,4-phenylene oxide) is sulfonated to higher degrees, thus obtaining higher ion exchange capacity, its hydrophilicity is improved significantly. The improved hydrophilicity is desirable as the permeation rate of water through the membrane is enhanced. However, selectivity of the membrane declines. This is due to not being able to increase or maintain the anionic sulfonate concentration in the swelled polymer once subjected to the aqueous feed. Crosslinking SPPOH and restricting its excessive swelling is likely to enable maintaining high rejection while improving on permeation rate through higher degrees of sulfonation.

2. Choice of the Appropriate Solvent

This work focused only on using methanol/chloroform mixtures or methanol as the solvent(s) for the coating solution. Based on the importance of the polymer-polymer and polymer-solvent interactions, using intrinsic viscosity as an indicator, there seems to exist an appropriate solvent or solvent mixture for the polymer of the skin layer, in this case SPPOH of a specific I.E.C.. Such an appropriate solvent or solvent mixture may be different from those explored in this work. Further investigation can be beneficial.

3. Optimization of the Composite Membrane for a Specific Application

Charged thin film composite membranes such as those prepared from SPPOH polymer should be optimized for the specific application for which they are intended. Important factors that should be considered in order to optimize the final performance of the membrane include: I.E.C. of polymer and possible crosslinking, solvent(s) for the coating solution and its concentration, addition of swelling agents or nonsolvent(s), type and porosity of substrate, method of drying after coating (ambient conditions, under lid, or under air flow), in addition to the nature of the stream(s) to be treated and the solute(s) therein. This statement is made to emphasize that such an optimization was not the subject of this work.

REFERENCES

Agarwal, A. K., "Development and Transport Properties of Novel Sulfonated Poly(Phenylene Oxide) Thin-Film Composite Charged Ultrafiltration Membranes for Bioseparations", Ph. D. Thesis, Chemical Engineering, University of Waterloo (1991).

Agrawal, A. K. and Huang, R. Y. M., Angew. Makromol. Chem. 163, 1 (1988).

Allegrezza, A. E., Jr., B. S. Parekh, P. L. Parise, E. J. Swiniarski and J. L. White, "Chlorine Resistant Polysulfone Reverse Osmosis Modules", Desalination 64, 285-304 (1987).

Belfort, G., "Membrane Methods in Water and Wastewater Treatment: An Overview" in "Synthetic Membrane Processes: Fundamentals and Water Applications", G. Belfort, Ed., Academic Press, Inc. (1984), pp. 1-19.

Cadotte, J. E., "Evaluation of Composite Reverse Osmosis Membranes", in "Materials Science of Synthetic Membranes", D. R. Lloyd Ed., ACS Symposium Series 269, American Chemical Society, Washington, DC (1985), pp. 273-294.

Cadotte, J. E. and R .J. Peterson in "Synthetic Membranes: Volume I Desalination", A. F. Turbak Ed., ACS Symposium Series 153, (1981).

Francis, P. S., "Fabrication and Evaluation of New Ultrathin Reverse Osmosis Membranes", National Technical Information Service, Springfield, VA, Report No. PB177083 (1966).

Chowdhury, G., T. Matsuura and S. Sourirajan, "A Study of Reverse Osmosis Separation and Permeation Rate for Sulfonated Poly(2,6-dimethyl-1,4-phenylene oxide) Membranes in Different Cationic Forms", J. Appl. Poly. Sci. 51, 1071-1075 (1994).

Gutman, R.G., Membrane Filtration, Adam Hilger, Bristol (1987).

Heyde, M. E., C. R. Peters and J. E. Anderson, J. Col. Interf. Sci. 50, 467 (1975).

Hodges, R. M. Jr., Ph. D. Thesis in Chemical Engineering, Massachusetts Institute of Technology (1964).

Huang, R. Y. M. and J. J. Kim, "Synthesis and Transport Properties of Thin-Film Composite Membranes, I Synthesis of Poly(phenylene Oxide) Polymer and Its Sulfonation", J. Appl. Poly. Sci. 29, 4017-4027 (1984).

Huang, R. Y. M. and J. J. Kim, "Synthesis and Transport Properties of Thin-Film Composite Membranes, II. Preparation of Sulfonated Poly(phenylene Oxide) Thin Film Composite Membranes for the Purification of Alberta Tar Sands Waste Waters", J. Appl. Poly. Sci. 29, 4029-4035 (1984).

Ikeda, K., T. Nakano, H. Ito, T. Kubota and S. Yamamoto, "New Composite Charged Reverse Osmosis Membrane", Desalination 68, 109-119 (1988).

Jencks, W. P., "Catalysis in Chemistry and Enzymology", McGraw Hill, New York (1969).

Jitsuhara, I. and S. Kimura, "Structure and Properties of Charged Ultrafiltration Membrane made of Sulfonated Polysulfone", J. Chem. Eng. Jpn, 16, 389-393 (1983).

Jitsuhara, I. and S. Kimura, "Rejection of Inorganic Salts by Charged Ultrafiltration Membranes made of Sulfonated Polysulfone", J..Chem. Eng. Jpn, **16**, 394-399 (1983).

Katchalsky, A. and O. Kedem, "Thermodynamics of Flow Processes in Biological Systems", Biophys. J., 2:Suppl. 53, (1962).

Kawada, I., K. Inoue, Y. Kazuse, H. Itch, T. Shintani and Y. Kamiyama, Desalination 64, 387 (1987).

Kedem, O. and A. Katchalsky, "Thermodynamic Analysis of the Permeability of Biological Membranes to Non-electrolytes", Biochimica et Biophysica Acta. 27, 229, (1958).

Kedem, O. and A. Katchalsky, "A Physical Interpretation of the Phenomenological Coefficients of Membrane Permeability", J. Gen. Physio. 45, 143 (1961).

Kedem, O. and A. Katchalsky, Trans. Farady Soc. 59, 1921 (1963).

Kesting R. E., "Synthetic Polymeric Membranes: A Structural Perspective", second edition, A Wiley-Interscience Publication (1985).

Kimura, S. and S. Sourirajan, "Analysis of Data in Reverse Osmosis with Porous Cellulose Acetate Membranes Used", AIChE J. 13, 497-503 (1967).

Kurihara, M., T. Uemura, N. Nakagawa and T. Tonomura, Desalination 54, 75 (1985).

Lang, Kangmin, "Synthesis and Properties of Thin-Film Polyvinyl Alcohol Composite Membranes", M.A.Sc.Thesis in Chemical Engineering, University of Ottawa (1993).

Lonsdale, H. K., U. Merten and R. L. Riley, "Transport Properties of Cellulose Acetate Osmotic Membranes", J. Appl. poly. Sci. 9, 1341-1362 (1965).

Luck, W. A. P., "Structure of Water and Aqueous Systems", in "Synthetic Membrane Processes", G. Belfort, Ed., Academic Press, Inc. (1984), pp. 21-72.

Mason, E. A. and H. K. Lonsdale, "Statistical-Mechanical Theory of Membrane Transport", J. Membrane Sci. **51**, 1-81 (1990).

Marcus, Y. and D. G. Howery, "Ion Exchange Equilibrium Constants", Butterworths, London (1975).

Matsuura, T., "Synthetic Membranes and Membrane Separation Processes", CRC Press, Inc. (1994).

Matsuura, T. and S. Sourirajan, "Theory and Practice of Reverse Osmosis", International Desalination Association (1985).

McCaffrey, J. P., National Research Council of Canada, Private Communications (1994).

Nakao, S., H. Osaka, H. Kurata, T. Tsuru and S. Kimura, Desalination 70, 191 (1988).

Plummer, C. W., G. Kimura and A. B. La Conti, "Development of Sulfonated Polyphenylene Oxide Membrane for Reverse Osmosis", Research and Development Progress Report # **551**, Office of Saline Water, United States Department of Interior (1970).

Riley, R. L., R. L. Fox, C. R. Lyons, C. E. Milstead, M. W. Seroy and M. Tagami, "Spiral-Wound Poly(ether/amide) Thin-Film Composite Membrane Systems", Desalination 19, 113-126 (1976).

Rudie, B., Membrane Development Supervisor, Osmonics Inc., 5951 Clearwater Drive, Minnetonka, MN., 55343, U.S.A., Private Communications (1994).

Sourirajan, S., "Reverse Osmosis and Synthetic Membranes: Theory-Technology-Engineering", NRC Canada (1977).

Sourirajan, S. and T. Matsuura, 'Reverse Osmosis/Ultrafiltration Process Principles", National Research Council of Canada (1985).

Sourirajan, S., "Reverse Osmosis: A General Separation Technique" In "Reverse Osmosis and Synthetic Membranes", National Research Council Canada, Ottawa (1977).

Spiegler, K. S., "Transport Processes in Ionic Membranes", Trans. Farady Soc. 54, 1408 (1958).

Strathmann, H., "Production of Microporous Media by Phase Inversion Processes", in "Material Science of Synthetic Membranes", D. R. Lloyd, Ed., ACS Symposium Series 269, American Chemical Society, Washington DC (1985), pp. 165-195.

Vieth, W. R., "Diffusion In and Through Polymers: Principles and Applications", Hanser Publishers (1991), pp. 111-141.

APPENDIX A Sample Calculations of Permeation Rate (PR) and Solute Separation (f) of SPPOH-PES Composite Membranes.

Using raw data for SPPOH-PES Composite Membrane of I.E.C. 1.29 (meq/g), prepared from Coating Solution of 1 mass% SPPOH, with Sodium Chloride Feed Solution (Appendix B, page 112).

The permeation rate is calculated as follows:

$$PR = \left(\frac{V}{A \cdot t}\right) \cdot (T_c)$$

where V is the volume permeating the membrane of area A in time t and T_c is the temperature correcting factor (from temperature T °C to temperature 25 °C.) estimated based on pure water properties as:

$$T_c = \left(\frac{\mu_{T°C}}{\mu_{25°C}}\right)\left(\frac{\rho_{25°C}}{\rho_{T°C}}\right)$$

The water density and viscosity values were taken from "Lange's Handbook of Chemistry", J. A. Dean Ed., McGraw-Hill Book Company, Thirteenth Edition (1985).

Operating temperature was 27 °C. Water properties are:

$$\mu_{25°C} = 0.890x10^{-3}\ N.s/m^2 \qquad \mu_{27°C} = 0.851x10^{-3}\ N.s/m^2$$

$$\rho_{25°C} = 997.0\ kg/m^3 \qquad \rho_{27°C} = 996.5\ kg/m^3$$

Thus, the temperature correction factor is

$$T_c = 0.957$$

From the table, the volumes permeating membrane 1, membrane 2 and membrane 3 are 21.4, 25.7 and 17.8, respectively, resulting in an average of $V = 21.6\ cm^3$ in time $t = 79$ minutes. Each membrane area $A = 10.2\ cm^3$.

Thus the average permeation rate is

$$PR = 4.3 \text{ X}10^{-6} \text{ m}^3/\text{m}^2.\text{s}$$

In the range of salt concentrations studied, the relationship between the solution concentration and its conductivity is linear enabling direct calculations of solute separation from conductivity measurements.

The Solute Separation is calculated as follows:

$$f = 1 - \frac{P_c}{F_c}$$

where P_c is the permeate conductivity and F_c is the feed conductivity.

Feed conductivity changed from initial value of 6.00 mS/cm to a final value of 6.23 mS/cm, during the experiment, giving an average F_c = 6.12 mS/cm, whereas the permeate conductivities through the three membranes were 1.22, 1.53 and 1.49 mS/cm resulting in an average of P_c 1.41 mS/cm

Thus, the average fractional sodium chloride separation is

$$f = 1 - \frac{1.41}{6.12}$$

$$f = 0.77 \quad (77\%)$$

APPENDIX B Experimental Reverse Osmosis Performance Raw Data at 1379 kPa gauge Using SPPOH-PES Composite Membranes Prepared from 1 mass% Coating Solutions (in Methanol or Methanol/Chloroform Mixtures with Minimum Chloroform) and Various Electrolyte Solutes.

Reverse Osmosis Performance Of SPPOH-PES
Composite Membranes Using Different Electrolytes
I.E.C. 1.29 (meq/g)

Feed Solution	Volume Permeating (ml)			Time	Temperature
	Memb. 1	Memb. 2	Memb. 3	(min)	(C)
Pure Water	9.5	10.8	8.4	45	26
Lithium Chloride	21.0	26.5	18.0	105	29
Sodium Chloride	21.4	25.7	17.8	79	27
Potassium Chloride	21.3	25.3	18.0	60	32
Ammonium Chloride	27.6	34.0	24.3	85	31
Magnesium Chloride	24.3	29.0	20.3	90	33
Calcium Chloride	20.3	23.7	16.8	86	32
Aluminum Chloride	23.0	27.3	20.0	75	33
Ferric Chloride	21.7	25.8	18.6	90	32
Sodium Bicarbonate	18.7	23.2	17.0	97	34
Sodium Carbonate	21.0	26.7	19.3	105	35
Sodium Sulfate	24.8	30.5	22.0	111	38
Potassium Sulfate	19.0	23.5	16.6	145	37
Magnesium Sulfate	22.3	28.8	19.7	200	36
Aluminum Sulfate	17.3	21.1	15.0	149	37

Feed Solution	Permeate Conductivity (mS/cm)			Feed Conductivity (mS/cm)	
	Memb. 1	Memb. 2	Memb. 3	Initial	Final
Lithium Chloride	0.89	1.17	1.13	4.79	6.10
Sodium Chloride	1.22	1.53	1.49	6.00	6.23
Potassium Chloride	1.82	2.16	2.14	7.26	8.05
Ammonium Chloride	1.98	2.30	2.25	6.94	8.07
Magnesium Chloride	6.52	7.00	7.04	10.37	11.19
Calcium Chloride	6.60	6.98	7.02	11.00	11.93
Aluminum Chloride	6.12	6.95	6.92	15.58	16.12
Ferric Chloride	9.62	11.06	10.64	19.25	21.00
Sodium Bicarbonate	0.60	0.73	0.73	4.12	5.01
Sodium Carbonate	0.60	0.60	0.77	9.07	10.22
Sodium Sulfate	0.29	0.57	0.54	9.20	10.97
Potassium Sulfate	0.70	0.98	0.92	12.15	11.76
Magnesium Sulfate	2.04	2.60	2.46	6.32	7.15
Aluminum Sulfate	3.29	4.16	4.07	9.53	10.10

Reverse Osmosis Performance Of SPPOH-PES
Composite Membranes Using Different Electrolytes
I.E.C. 1.41 (meq/g)

Feed Solution	Volume Permeating (ml)			Time	Temperature
	Memb. 1	Memb. 2	Memb. 3	(min)	(C)
Pure Water	19.3	19.8	16.2	45	26
Lithium Chloride	45.5	46.0	37.5	105	29
Sodium Chloride	45.0	45.0	37.8	79	27
Potassium Chloride	44.0	44.0	37.0	60	32
Ammonium Chloride	56.5	56.5	47.6	85	31
Magnesium Chloride	49.3	49.1	42.5	90	33
Calcium Chloride	41.0	40.5	35.0	66	32
Aluminum Chloride	45.5	44.0	38.7	75	33
Ferric Chloride	43.6	42.5	37.0	90	32
Sodium Bicarbonate	37.0	38.0	31.0	97	34
Sodium Carbonate	42.0	43.0	35.7	105	35
Sodium Sulfate	50.1	51.0	42.5	111	38
Potassium Sulfate	35.0	36.0	29.0	145	37
Magnesium Sulfate	41.8	45.0	33.0	200	36
Aluminum Sulfate	30.9	34.0	25.0	149	37

Feed Solution	Permeate Conductivity (mS/cm)			Feed Conductivity (mS/cm)	
	Memb. 1	Memb. 2	Memb. 3	Initial	Final
Lithium Chloride	1.11	1.32	1.02	4.79	6.10
Sodium Chloride	1.49	1.70	1.37	6.00	6.23
Potassium Chloride	2.23	2.42	2.07	7.26	8.05
Ammonium Chloride	2.33	2.50	2.22	6.94	8.07
Magnesium Chloride	7.23	7.54	6.98	10.37	11.19
Calcium Chloride	7.22	7.47	7.01	11.00	11.93
Aluminum Chloride	6.08	7.32	5.60	15.58	16.12
Ferric Chloride	11.11	11.40	10.70	19.25	21.00
Sodium Bicarbonate	0.79	0.86	0.71	4.12	5.01
Sodium Carbonate	0.92	1.00	0.79	9.07	10.22
Sodium Sulfate	0.57	0.65	0.45	9.20	10.97
Potassium Sulfate	0.95	1.11	0.75	12.15	11.76
Magnesium Sulfate	2.40	2.98	2.13	6.32	7.15
Aluminum Sulfate	3.54	4.63	3.18	9.53	10.10

Reverse Osmosis Performance Of SPPOH-PES
Composite Membranes Using Different Electrolytes
I.E.C. 1.98 (meq/g)

Feed Solution	Volume Permeating (ml)			Time	Temperature
	Memb. 1	Memb. 2	Memb. 3	(min)	(C)
Pure Water	33.0	38.5	25.0	45	26
Lithium Chloride	79.5	87.5	57.5	105	29
Sodium Chloride	78.5	68.0	58.5	79	27
Potassium Chloride	76.0	87.0	58.0	60	32
Ammonium Chloride	99.2	115.0	78.0	85	31
Magnesium Chloride	88.0	97.7	66.9	90	33
Calcium Chloride	73.5	78.5	55.1	86	32
Aluminum Chloride	82.5	92.5	62.0	75	33
Ferric Chloride	79.0	88.5	60.2	90	32
Sodium Bicarbonate	76.3	88.5	58.8	97	34
Sodium Carbonate	86.5	100.1	66.5	105	35
Sodium Sulfate	102.0	117.0	78.0	111	38
Potassium Sulfate	74.5	84.5	54.6	145	37
Magnesium Sulfate	98.0	113.3	76.0	200	36
Aluminum Sulfate	67.0	73.9	54.0	149	37

Feed Solution	Permeate Conductivity (mS/cm)			Feed Conductivity (mS/cm)	
	Memb. 1	Memb. 2	Memb. 3	Initial	Final
Lithium Chloride	1.49	2.09	1.41	4.79	6.10
Sodium Chloride	1.99	2.58	1.95	6.00	6.23
Potassium Chloride	2.91	3.60	2.83	7.26	8.05
Ammonium Chloride	2.97	3.53	2.90	6.94	8.07
Magnesium Chloride	8.10	8.30	7.61	10.37	11.19
Calcium Chloride	7.99	8.13	7.75	11.00	11.93
Aluminum Chloride	9.43	10.52	10.03	15.58	16.12
Ferric Chloride	12.11	12.75	12.28	19.25	21.00
Sodium Bicarbonate	1.18	1.60	1.14	4.12	5.01
Sodium Carbonate	1.58	2.39	1.42	9.07	10.22
Sodium Sulfate	1.31	2.27	1.16	9.20	10.97
Potassium Sulfate	2.26	3.47	2.02	12.15	11.76
Magnesium Sulfate	3.79	4.22	3.57	6.32	7.15
Aluminum Sulfate	5.73	6.55	5.71	9.53	10.10

Reverse Osmosis Performance of SPPOH-PES
Composite Membranes Using Different Electrolytes
I.E.C. 2.60 (meq/g)

Feed Solution	Volume Permeating (ml)						Time (min)	Temp. C
	Memb 1	Memb 2	Memb 3	Memb 4	Memb 5	Memb 6		
Pure Water	50.0	47.9	58.8	52.2	51.0	48.1	45	25
Lithium Chloride	50.1	48.2	59.7	53.3	50.7	49.0	50	23
Sodium Chloride	55.2	52.3	65.7	58.2	56.9	53.8	45	25
Potassium Chloride	74.0	71.1	87.8	78.2	75.2	71.0	45	27
Ammonium Chloride	79.7	76.5	93.9	82.9	80.1	77.7	50	27
Magnesium Chloride	49.3	48.0	63.3	58.6	52.8	49.2	51	25
Calcium Chloride	54.6	53.4	70.1	65.0	58.5	54.6	50	25
Aluminum Chloride	64.2	62.2	65.8	60.0	56.0	50.2	95	26
Ferric Chloride	65.5	63.4	68.0	61.7	57.5	51.5	95	26
Sodium Bicarbonate	51.1	59.0	73.2	63.8	61.8	59.0	50	26
Sodium Carbonate	58.8	56.7	71.0	62.3	59.8	58.2	55	26
Sodium Sulfate	55.4	52.8	65.8	57.1	56.8	55.1	50	26
Potassium Sulfate	69.0	66.7	81.9	72.0	70.2	68.2	50	25
Magnesium Sulfate	63.1	60.1	73.8	64.9	63.3	61.8	60	26
Aluminum Sulfate	40.0	37.2	45.8	41.1	38.8	39.4	51	26

Feed Solution	Permeate Conductivity (mS/cm)						Feed Cond. (mS/cm)	
	Memb 1	Memb 2	Memb 3	Memb 4	Memb 5	Memb 6	Initial	Final
Lithium Chloride	2.17	2.10	2.19	2.26	2.12	2.28	4.84	5.23
Sodium Chloride	2.75	2.69	2.78	2.85	2.70	2.86	5.36	5.69
Potassium Chloride	3.78	3.69	3.85	3.89	3.74	3.91	6.72	7.20
Ammonium Chloride	3.93	3.86	4.00	4.04	3.91	4.09	6.58	7.16
Magnesium Chloride	7.71	7.61	7.83	7.89	7.64	8.03	9.68	9.78
Calcium Chloride	7.77	7.64	7.97	7.99	7.65	8.06	10.05	10.15
Aluminum Chloride	10.63	9.93	9.60	10.31	9.96	9.87	12.51	12.65
Ferric Chloride	13.08	12.62	13.52	13.71	12.94	14.03	16.25	16.63
Sodium Bicarbonate	1.80	1.74	1.86	1.89	1.78	1.93	4.12	4.50
Sodium Carbonate	2.31	2.24	2.36	2.48	2.23	2.58	8.20	8.61
Sodium Sulfate	2.55	2.42	2.55	2.75	2.39	2.87	8.81	9.75
Potassium Sulfate	3.83	3.66	3.80	4.04	3.61	4.19	10.77	11.90
Magnesium Sulfate	4.64	4.51	4.49	4.52	4.41	4.63	5.64	5.92
Aluminum Sulfate	8.21	8.01	7.91	8.04	7.85	8.17	9.22	9.38

APPENDIX C Intrinsic Viscosity: Experimental Data and Sample Fit.

Intrinsic Viscosity Measurement in Different Chloroform-Methanol Solvent Mixtures
[SPPOH of I.E.C 1.93 (meq/g)]

SPPOH (wt%) In Solution	Solvent Mixture: Methanol		(82% Methanol)		(58% Methanol)		(34% Methanol)	
	Pass Time (s)		Pass Time (s)		Pass Time (s)		Pass Time (s)	
1.000	299	299	291	293	292	284	258	266
0.500	292	292	261	275	258	260	221	222
0.250	265	265	239	238	236	224	195	202
Pure Solvent	198	198	183	183	175	177	156	157

Intrinsic Viscosity is determined by plotting ((T-To)/(To*C)) vs C and linearly extrapolating to C = 0 .
where (C) is the SPPOH concentration in (gram/100ml)
T is the capillary pass time of SPPOH solution of concentration C
To is the capillary pass time of the pure solvent

Sample Fit (below) is for the case of 82 : 18 wt% Methanol : Chloroform Solvent Mixture

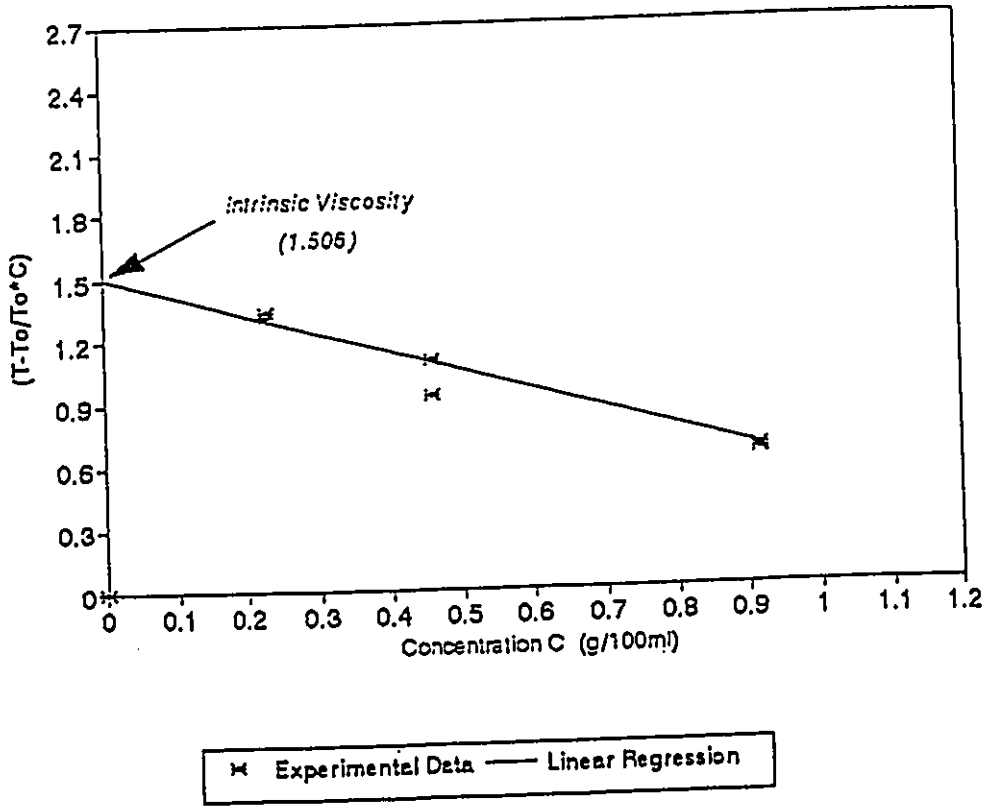

APPENDIX D Sample AFM Section Analysis used to estimate Nodule Size on Surface of Composite Membranes (case below for membrane of I.E.C. 1.93 meq/g using Methanol as Solvent for Coating Solution).

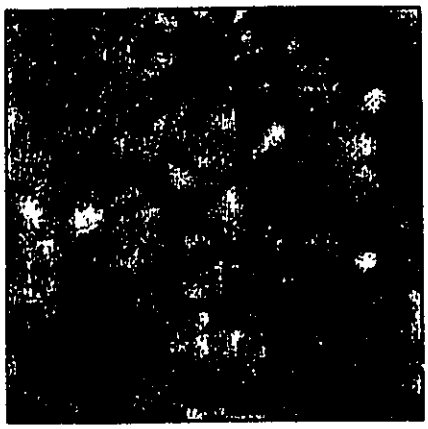

Horiz distance(L)	115.92 nm
Vert distance	0.675 nm
Angle	0.334 deg
Horiz distance	113.29 nm
Vert distance	0.225 nm
Angle	0.114 deg
Horiz distance	**84.309 nm**
Vert distance	**0.600 nm**
Angle	**0.408 deg**
Spectral period	DC
Spectral freq	0 Hz
Spectral amp	**0.116 nm**